TREATMENT OF BIOMASS-DERIVED SYNTHESIS GAS USING COMMERCIAL STEAM REFORMING CATALYSTS AND BIOCHAR

By

LUZ STELLA MARIN

Bachelor of Science in Chemical Engineering
Universidad Simón Bolívar
Caracas, Venezuela
1991

Master of Science in Chemical Engineering
Universidad Simón Bolívar
Caracas, Venezuela
1992

Submitted to the Faculty of the
Graduate College of the
Oklahoma State University
in partial fulfillment of the requirements for
the Degree of
DOCTOR OF PHILOSOPHY
December, 2011

TREATMENT OF BIOMASS-DERIVED SYNTHESIS GAS USING COMMERCIAL STEAM REFORMING CATALYSTS AND BIOCHAR

Dissertation Approved:

Dr. Danielle Bellmer

Dissertation Adviser

Dr. Mark Wilkins

Dr. Ajay Kumar

Dr. Hasan Atiyeh

Dr. Gary Foutch

Outside Committee Member

Dr. Sheryl A. Tucker

Dean of the Graduate College

TABLE OF CONTENTS

Chapter Page

LIST OF TABLES

Table Page

Table Page

LIST OF FIGURES

Figure Page

Figure Page

Figure Page

CHAPTER I

INTRODUCTION

Renewable energy technologies are critical to creating a clean energy future for not only the nation, but the world. Renewable energy comes from natural resources such as biomass. The use of biomass to produce biofuels such as bioethanol or biodiesel can help reduce dependence on foreign oil. Currently, biofuels such as ethanol are mixed with commercial gasoline in various blend ratios. In 2008, about 19% of global energy consumption came from renewable sources, with 13% being from biomass (Renewable Biomass Global Status Report, 2010).

Biomass gasification is a promising route for creating synthesis gas (also called syngas or producer gas) from biomass in a thermochemical conversion process. However, the gas generated in this process contains tars, which are undesirable condensable organic compounds. This gas needs to be cleaned to remove tar and particulates before being used downstream. The efficient removal of tar remains a significant problem when implementing biomass gasification technologies.

At Oklahoma State University, ethanol is produced from biomass through a gasification-fermentation process. Syngas is generated from switchgrass, and the syngas (CO, CO_2 and H_2) feeds a bioreactor where anaerobic bacteria are used to convert the

syngas to ethanol and acetic acid. Gas cleanup is an important issue because tar inhibits the microbial conversion process (Ahmed et al., 2006). Various approaches can be considered for reducing the tar content of the product gas, and catalytic methods show much promise. In particular, steam reforming catalysts have been studied extensively for use in a variety of gas cleanup applications. In addition, previous studies using char, a waste product of gasification, have proven it as a low cost potential material for tar removal (Abu El Rub et al., 2004).

This study deals with the evaluation of several different commercial catalysts for the destruction of the tar generated during biomass gasification. This research also explores the catalytic activity of the biochar generated from gasification of switchgrass.

1.1 Objectives

The main objective of this research is to explore the catalytic destruction of tar formed during biomass gasification using both biochar and commercial steam reforming catalysts.

Specific objectives include:

1 Explore the potential of using our biomass char as a catalyst for tar reduction and compare it with commercial catalysts such as Reformax 250, Hifuel R-110 and NextechA.

2 Evaluate changes in catalyst morphology and performance using standard catalyst characterization techniques.

3 Develop an extent of reaction model to understand the reaction network involved in the steam reforming of toluene.

CHAPTER II

REVIEW OF LITERATURE

Conventional non renewable energy sources such as oil, coal and natural gas are becoming depleted. To partially cover the increasing world energy demand, processes for energy production are focusing on renewable energy sources such as biomass. Biomass gasification has the ability to generate a fuel gas rich in H_2, CO, and CO_2 that can be used for synthesis gas applications, production of biofuels, production of chemicals, fuel cell applications and power generation. However, the destruction of tars present in the fuel gas is a crucial technological barrier for the development and further commercialization of biomass gasification. Improvements in tar destruction will help make the gasification process more cost effective, competitive, dependable and sustainable. This chapter presents an overview of this topic focusing on key aspects related to this research.

2.1 Renewable Energy

Renewable energy comes from natural sources such as geothermal heat, wind, sunlight, and biomass. The use of biomass can reduce dependence on foreign oil or can represent an alternative to cover energy demand in remote areas or parts of the world without available fossil fuels. Even though renewable energy remains a small portion of the world energy distribution, it is growing rapidly.

In recent years, government support mainly in the Western Hemisphere has helped to increase global wind and solar energy contributions (BP Statistical review, 2009). In 2009, global wind and solar generation capacity increased by 31% and 47%, respectively. Growth was led by China and the U.S., which accounted for a combined 62.4% of total growth (BP Statistical review, 2010). Figure 2.1 shows the renewable energy consumption in the United States energy supply in 2008. It can be seen that biomass represents 52% of the renewable energy share.

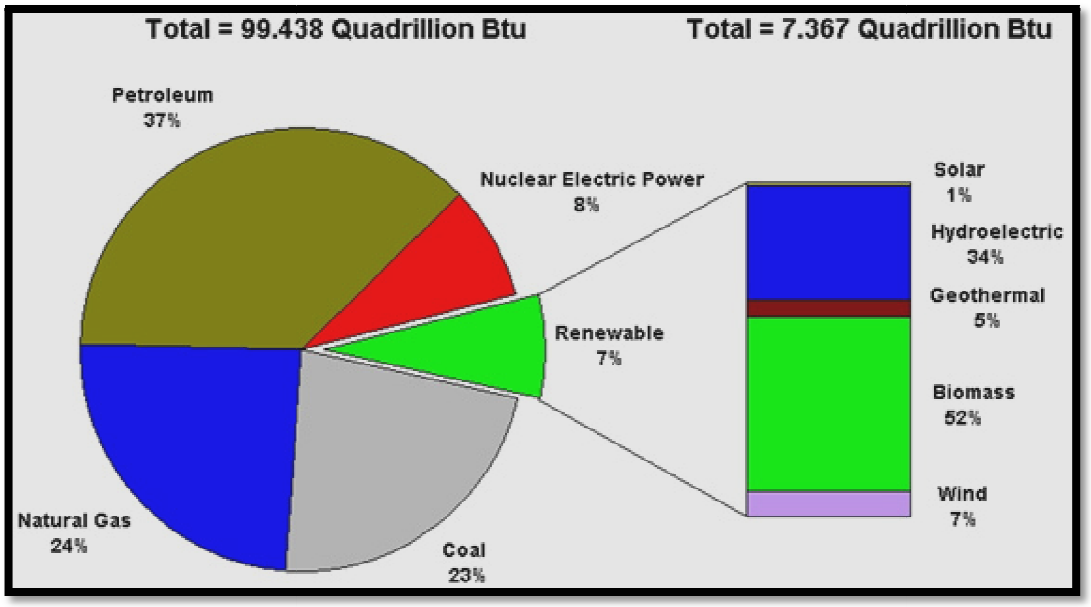

Figure 2.1 Renewable energy consumption in the U. S. supply, 2008. Figure adopted from U.S. Energy Information Administration (2008).

2.1.1 Biofuel

Biofuels are sources of energy that are made from organic matter. Major biofuels include biodiesel, ethanol, and cellulosic ethanol, which is produced from non-edible parts of plants. There are currently private companies working on refining biogasoline

(Renewable Global Status Report, 2010). In the U.S., some of the major companies exploring biofuels include: Pacific Ethanol, ConAgra, Archer-Daniels-Midland Company, and Aventine Renewable Energy Holdings. Liquid biofuel is usually either bioalcohol such as bioethanol or oil such as biodiesel.

Bioethanol is an alcohol made by fermenting the sugar components of plant materials and it is made mostly from sugar and starch crops. However, cellulosic biomass, such as trees and grasses, is also being investigated as a feedstock for ethanol production. Ethanol can be used as a fuel for vehicles mixed with gasoline. Bioethanol is widely used in gasoline in the USA and in other parts of the world (Renewable Global Status Report, 2010).

Biodiesel is made from vegetable oils, animal fats or recycled greases. Biodiesel can be used as a fuel for vehicles in its pure form, but it is usually used as a diesel additive to reduce levels of particulates, carbon monoxide, and hydrocarbons from diesel-powered vehicles. Biodiesel is produced from oils or fats using transesterification and is the most common biofuel in Europe. Biofuels provided 1.8% of the world's transport fuel in 2008 (BP Statistical Review, 2009).

Despite the economic slowdown, the global renewable energy industry has continued to expand rapidly. The United States and China have joined the leading regions such as Europe and Japan, in renewable development. The renewable energy industry is rapidly gaining importance in terms of contribution to economic activity and employment. Global fuel bioethanol production grew 8% to 38 million tons of oil equivalent in 2009 (BP Statistical Review, 2010).

2.2 Biomass

Recently, a considerable effort has been made to find clean and renewable sources of energy. Biomass is one of the most abundant renewable resources known, and it has great potential for energy production.

Biomass is a renewable energy source because through photosynthesis plants capture the sun's energy and when they are degraded this energy is released. In this way, biomass functions as a sort of natural battery for storing solar energy. As long as biomass is produced sustainably, the battery will last indefinitely (Renewable Global Status Report, 2010).

2.2.1 Biomass Gasification

Gasification technologies provide the opportunity to convert renewable biomass feedstock into clean fuel gases or synthesis gases (Corella et al., 1999). The synthesis gas includes mainly hydrogen and carbon monoxide but also contains carbon dioxide, water, methane, and other gaseous hydrocarbons including oxygenated hydrocarbons, tars, char, inorganic constituents and ash.

Biomass gasification is a complex thermochemical process that consists of a number of elementary chemical reactions, beginning with the partial oxidation of a lignocellulosic fuel with a gasifying agent, usually air, oxygen, or steam. One of the advantages of this process is that the feedstock for this process can be any kind of biomass (Kumar et al., 2009).

A generalized reaction describing biomass gasification follows:

$$\text{Biomass} + O_2\,(\text{or } H_2O) \rightarrow CO + CO_2 + H_2O + H_2 + CH_4 + \text{other hydrocarbons}$$

$$\rightarrow \quad \text{tar} + \text{char} + \text{ash}$$

$$\rightarrow HCN + NH_3 + HCl + H_2S + \text{other sulfur gases}$$

(Yung et al., 2009) (2.1)

2.2.2 Gasifiers

Various gasification technologies have been under investigation for converting biomass into a gaseous fuel. These include gasifiers where the biomass is introduced at the top of the reactor and the gasifying medium is either directed co-currently (downdraft) or counter-currently up through the packed bed (updraft). Other gasifier designs incorporate circulating or bubbling fluidized beds (Kumar et al., 2009).

The composition of the gas obtained from a gasifier depends on a number of parameters such as (1) fuel composition, (2) gasifying medium, (3) operating pressure, (4) temperature, (5) moisture content of the fuels, (6) mode of bringing the reactants into contact inside the gasifier, etc. Therefore, it is very difficult to predict the exact composition from a gasifier (Basu, 1996).

All types of gasifiers need to include significant gas conditioning along with the removal of tars and inorganic impurities. The updraft gasifiers generally show the highest tar production while downdraft gasifiers show lower tar levels (Basu, 1996).

Fluidized bed gasifiers show intermediate tar production. The preferred type is the entrained flow gasifier since it shows the lowest tar generation; however, for small scale applications the downdraft gasifier is more common followed by the fluidized bed gasifier (Orio et al., 1997).

2.3 Tar

2.3.1 Definition

Tar is a complex mixture of condensable hydrocarbons and many definitions of biomass tar have been given by several institutions working on biomass gasification**.** However, the current definition for tar is all organic contaminants with a molecular weight larger than benzene (Devi et al., 2002).

2.3.2 Formation

When biomass or organic material is heated, the molecular bonds of the material break, generating tar (BTG report, 1999).The smallest molecules formed are gaseous and the larger molecules are called primary tars. These primary tars can react to secondary tars by further reactions at the same temperature and to tertiary tars at high temperature (Milne, 1998). Tars may form in the range of 400-900 ^{o}C, and this is illustrated by the range of products presented in Table 2.1 developed by Elliot (Elliot, 1988).

Table 2.1 Temperature dependency for tar formation (Adopted from Elliot, 1988).

Compound	**Mixed Oxygenates**	**Phenolics Ethers**	**Alkyl Phenolics**	**Heterocyclic Ethers**	**PAH**	**Larger PAH**
T (^{o}C)	400	500	600	700	800	900

A schematic representation for tar formation can be visualized in Figure 2.2. As can be observed in the figure, during biomass gasification a large number of different compounds can be formed, ranging from small molecules to large and complicated molecules such as aromatic hydrocarbons with several side groups (BTG report, 1999).

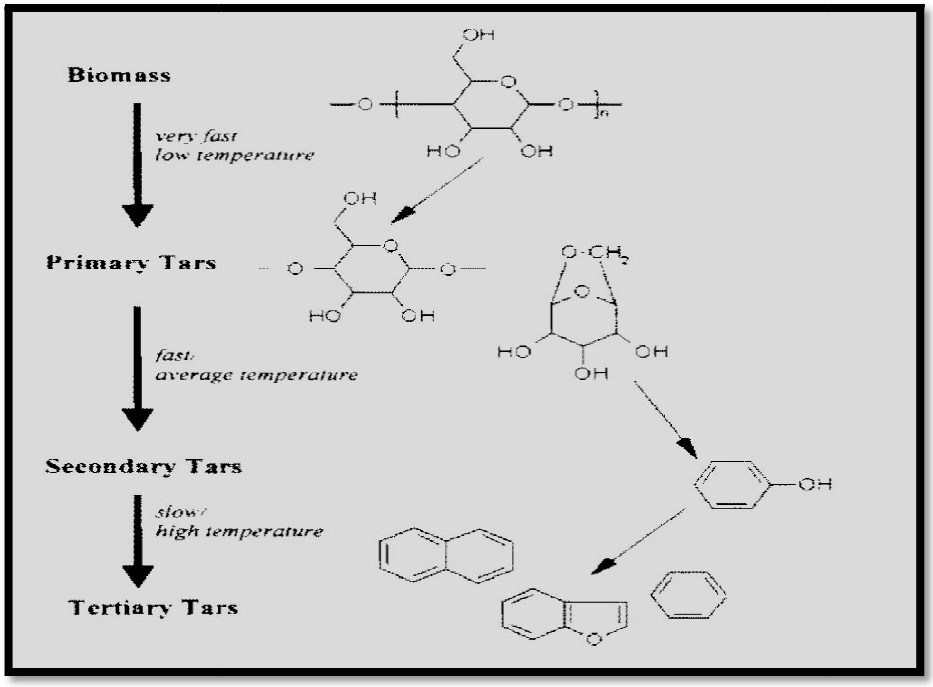

Figure 2.2 Formation of biomass tars (adopted from Milne and Evans, 1998.).

The types of compounds typically found in biomass tar are shown in Figure 2.3. As can be seen in the figure, toluene and naphthalene contribute significantly to tar composition, along with other aromatic hydrocarbons.

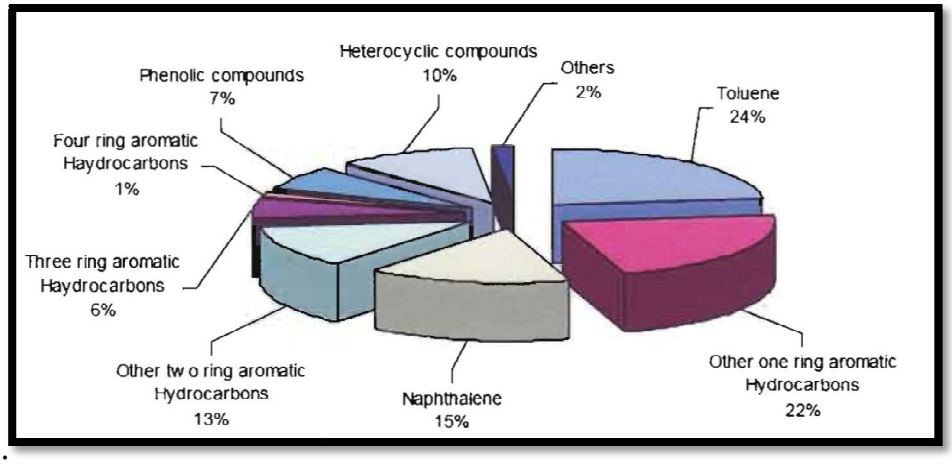

Figure 2.3Typical composition of biomass tar (Adopted from Abu El Rub, 2004).

2.3.3 Tar Model Compounds

Toluene is a stable aromatic compound, and it is a major component of typical tar as shown in Figure 2.3. In addition, it is less harmful than most of the other tar compounds such as naphthalene, phenol. Moreover, high-temperature chemistry of toluene is reasonably well known. For these reasons toluene is a common model tar compound for testing catalysts for biomass tar destruction (Simell et al., 1996; Coll et al., 2001; Orio et al., 1997; Swierczynski et al., 2007; Swierczynski et al., 2008).

2.3.4 Tar Handling Alternatives

Since tar disposal is one of the most critical problems during biomass gasification, a great amount of work concerning tar reduction or reforming has been reported. Traditionally tar removal technologies have been broadly divided into two approaches; treatments inside the gasifier (primary methods) and hot gas cleaning after the gasifier (secondary methods) (Devi et al., 2002). Treatments inside the gasifier are attractive because they may eliminate the need for downstream cleanup. In both the primary and secondary

methods, tar removal is done either by chemical treatment or physical separation. A recent review of literature broadly divided the tar removal technologies into five groups: mechanical methods also called physical processes; self-modification, which deals with the selection of optimal operations parameters; catalytic cracking; thermal cracking; and plasma methods such as Pyroarc, Corona, and Glidarc (Han and Kim, 2008). However, the more common methods to remove tars from producer gas generally involve physical processes, thermal processes or catalytic processes (Zhang et al., 2004).

Physical Processes

Physical processes remove the tar from the producer gas through gas/solid or gas/liquid interactions such as use of filters or wet scrubbers. These methods are effective and relatively easy to maintain, but they do not solve the problem. The tar is not destroyed and it is transferred to another phase, creating an environmental problem regarding the disposal of the filtered material (Zhang et al., 2004).

Thermal Processes

Thermal processes increase the temperature of the producer gas to cracking temperatures, and then the heavy aromatic tar species are broken into lighter and less problematic compounds, such as hydrogen, carbon monoxide and methane. For thermal cracking of tars, it is suggested that temperatures exceed 1100 ^{o}C in order to reduce tars effectively (Abu El Rub et al., 2008). Thermal cracking of tars has been extensively studied because it is a relatively simple process. However, special attention has to be given to the reactor design since high temperatures require the system be constructed of costly alloys. In addition, this is an energy intensive process that requires the use of large amounts of fuel

to achieve the process temperature. In addition, these high temperatures cause a considerable loss of efficiency in the gasification process and have the tendency to form soot (Graham and Bain, 1993).

Self-Modification

This is a primary treatment method that deals with the optimization of the gasification process by paying special attention to gasifier design and selection of operational parameters; the goal is the minimization of tar inside the gasifier. One study found that tar generation in the gasifier decreased when the equivalence ratio (ER) was increased from 0.24 to 0.45 at 800^{o}C; the tar content decreased from a range of (4-18) g/Nm^{3} to (2-7) g/Nm^{3} (Narvaez et al., 1996).

Plasma Methods (PyroArc, Pulsed Corona Discharge, GlidArc)

Plasma can be used for conversion of tars because tars are thermodynamically not stable in a fuel gas containing CO_2 and H_2O. Tars exist because their rate of decomposition is too low at temperatures lower than those needed for thermal cracking. However, exposure to very reactive species (ions, electrons, neutral atoms) can increase the tar decomposition rate to a point that tars can be broken down even at lower temperatures (Neeft, 1996).

There are three types of plasma processes that have been studied for hydrocarbon destruction:

- Pyroarc: this plasma is used to treat pyrolysis/gasification fuel gases. The Pyroarc process was developed by Scanarc Plasma Technologies and Kvaerner

Engineering. This process is a combination of a plasma reactor and thermal cracking of hydrocarbons.

- Pulsed corona discharge: the corona reactor consists of a corona wire in a cylindrical reactor that functions as a counter electrode. This technique has been proven successful for the destruction of toluene and styrene (Smulders et al., 1998). This technique is being developed at Eindhoven University of Technology.

- GlidArc: this technology breaks down heavy compounds into lighter compounds and it has been developed by the University of Orleans (Paris, France). It has been used for several applications such as syngas production from methane, oxidation of N_2O to NO, removal of H_2S and mercaptans, removal of volatile organic hydrocarbons (VOCs) from flue gases(BTG report, 1999).

Catalytic Treatment

Catalytic processes can operate at much lower temperatures (600–800 ^oC) than thermal processes, eliminating the need for expensive alloys for reactor construction and reducing the use of fuel or power compared to thermal processes. This type of process may eliminate the need for cooling the gas as needed for physical processes, which is advantageous because the economics of the process and the thermodynamic efficiency of the gasification process are not compromised. In addition, catalytic cleaning destroys the tar, so there is no need for waste treatment. Finally, chemical reactions of tar may increase the syngas production. Catalytic processes provide a simple and effective means of removing tars.

A number of catalytic processes have been previously investigated. Early on, it was discovered that in situ catalysis, in which the catalysts are placed directly in the gasification reactor is not effective due to rapid catalyst deactivation (Delgado et al., 1999). Hot gas conditioning using current commercially available catalysts offers the best solution for reducing biomass gasification tars. Tars are eliminated, methane can be reformed if desired, and the H_2: CO ratio can be adjusted in a single step. (Devi et al., 2002).

After reviewing all these techniques for removal of tars from producer gas, it becomes clear that one unique effective method for tar destruction does not exist. The choice for one technique or a combination of techniques will be based on operational parameters and particularities of the process itself. Catalytic processes for tar destruction have been selected for our experiment because they are the most suitable option to achieve our goals.

Catalytic tar destruction has been studied for several decades (Mudge, et al., 1985) and a number of reviews have been written on biomass gasification hot gas cleanup (Sutton et al., 2001; Dayton 2002;Devi et al., 2002; Huber 2006; Torres 2007;Yung et al., 2009). An attractive hot gas conditioning method for tar destruction is catalytic steam reforming. This technique offers several advantages:

1) catalyst reactor temperatures can be thermally integrated with the gasifier exit temperature,

2) the composition of the product gas can be catalytically adjusted, and

3) steam can be added to the catalyst reactor to ensure complete reforming of tars (Narvaez et al., 1996).

2.4 Chemical Reactions Network

Several reactions may occur during the steam reforming of this synthetic gas mixture including high temperature reactions of gasification gas, steam reforming or dry reforming of hydrocarbons by CO_2, dealkylation and hydrocracking reactions. Thermal cracking reactions and carbon formation reactions may also take place. Simultaneously, many equilibrium reactions of the main gas components may occur. A summary of these reactions is presented below.

Steam Reforming

Steam reforming of tar leads to production of CO and H_2, enriching gas from biomass gasification in these components. The reaction pathway is described by reactions (2.2) and (2.3). It is an endothermic process and a external source of heat is needed. Steam reforming ideally should be carried out at high temperature, low pressure, and high steam to hydrocarbon ratio in order to achieve maximum conversions (Twigg, 1996).

$$C_nH_m + nH_2O \longrightarrow nCO + (n + m/2)H_2 \text{ (Dermibas, 2002)} \quad (2.2)$$

$$C_nH_m + 2nH_2O \longrightarrow nCO_2 + (2n + m/2)H_2 \text{ (Dermibas, 2002)} \quad (2.3)$$

Dry Reforming

Dry reforming is a process that utilizes carbon dioxide as an oxidant to convert hydrocarbon fuels into syngas. The process is similar to steam reforming in that it is

endothermic; however it usually requires greater energy input for the reaction to proceed. The general reaction scheme for dry (CO_2) reforming is as follows:

$C_nH_m + nCO_2 \longrightarrow 2nCO + (m/2)H_2$ (Devi et al., 2005) (2.4)

Hydrocracking

Toluene may react with hydrogen to produce smaller molecules such as methane

$C_7H_8 + 10H_2 \longrightarrow 7CH_4$ (Simmel et al.,1997) (2.5)

Hydrodealkylation

Hydrodealkylation is a reaction that involves an aromatic compound and hydrogen to generate another aromatic compound

$C_7H_8 + H_2 \longrightarrow C_6H_6 + CH_4$ (Simmel et al., 1997) (2.6)

Steam Hydrodealkylation

Steam hydrodealkylation involves a reaction between an aromatic compound and water to produce an aromatic compound and other gases

$C_7H_8 + H_2O \longrightarrow C_6H_6 + CO + 2\ H_2$ (Simmel et al.,1997) (2.7)

$C_7H_8 + 2H_2O \longrightarrow C_6H_6 + CO_2 + 3\ H_2$ (Simmel et al.,1997) (2.8)

Carbon Formation

Carbon generation may occurs due to the breakdown of toluene

$C_nH_m \longrightarrow nC + (m/2)\ H_2$ (Simmel et al., 1997) (2.9)

Water Gas Shift

The water gas shift (WGS) reaction is an important part of the fuel conversion process because it is possible that a portion of the syngas produced may react with residual CO_2 or H_2O causing a shift in the concentrations of CO and H_2 through the following:

$CO + H_2O \longleftrightarrow CO_2 + H_2$ (Simmel et al.,1997) (2.10)

Methanation

Reactions involving methane that may occur during catalytic treatment are:

$CH_4 + H_2O \longleftrightarrow CO + 3H_2$ (Devi et al., 2005) (2.11)

$C + 2H_2 \longleftrightarrow CH_4$ (Simmel et al.,1997) (2.12)

$CO_2 + 4H_2 \longleftrightarrow CH_4 + 2H_2O$ (Sutton et al., 2001) (2.13)

Boudouard Reaction

The Boudouard reaction is also known as the disproportionation of carbon monoxide into carbon dioxide and graphite or its reverse

$C + CO_2 \longleftrightarrow 2CO$ (Simmel et al., 1997) (2.14)

Water Gas Reactions

Carbon may react with water for additional hydrogen generation

$C + H_2O \longleftrightarrow CO + H_2$ (Simmel et al.,1997) (2.15)

$2H_2O + C \longleftrightarrow CO_2 + 2H_2$ (Simmel et al.,1997) (2.16)

2.5 Catalytic Tar Destruction

An extensive literature review regarding catalytic processes for biomass tar destruction was conducted with the objective of providing an overview of the different catalysts that have been studied and how they have been implemented. The composition of heterogeneous catalysts can be divided into three primary components: an active phase or metal, a promoter which increases activity and/or stability, and a high surface area support that facilitates dispersion of the active phase (Yung et al., 2009). Elements that are being investigated for catalyst conditioning and their performance regarding gas clean up in biomass gasification processes are presented in Figure 2.4.

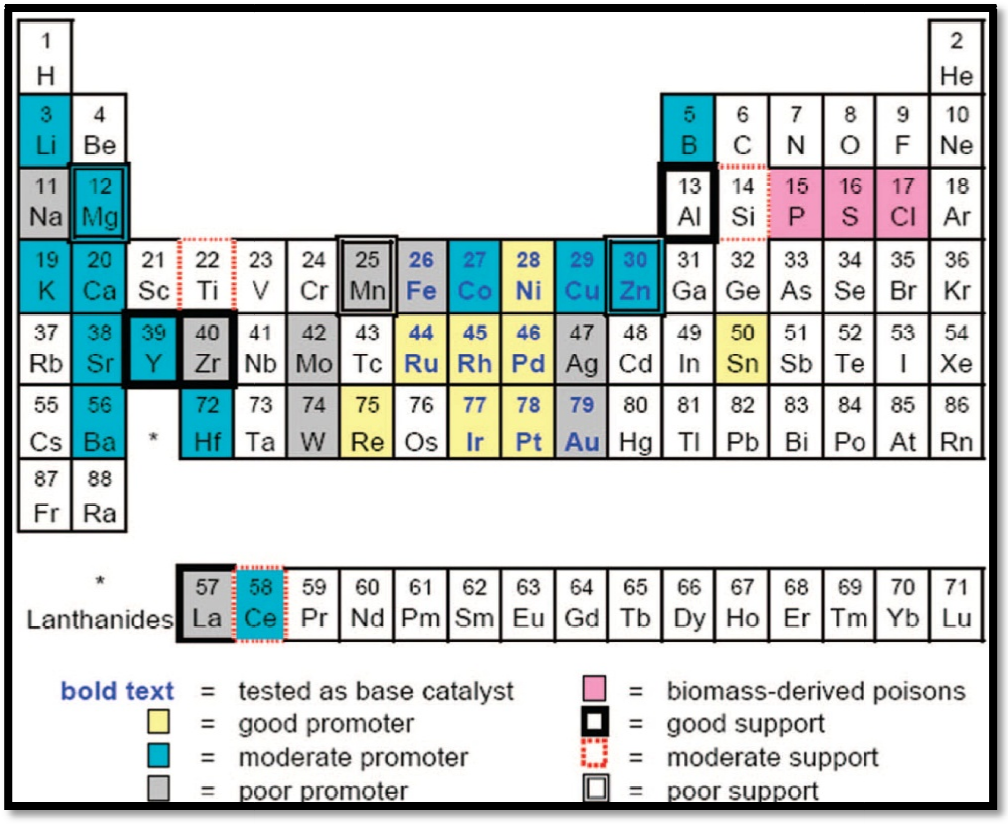

Figure 2.4 Elements studied for catalytic conditioning (Adopted from Yung et al., 2009)

It has been found that three groups of catalyst materials have been applied to tar removal in biomass gasification systems. These catalyst groups are non metallic catalysts, commercial steam reforming catalysts, and optimized catalyst formulations. The properties that determine the technical suitability of a catalyst for tar removal in a gasification process are activity and selectivity (Abu El Rub et al., 2008).

2.5.1 Non Metallic Catalysts

The non-metallic and supported metallic oxide catalysts are usually located in a separate fixed bed reactor, downstream from the gasifier, to reduce the tar content of the gasification product gas; therefore, they are referred to as secondary catalysts. Although the non-metallic catalysts are sometimes used as bed material in fluidized bed gasifiers to affect tar formation, standalone catalytic reactors can be used with any gasification technology and can be independently controlled to maximize the versatility of the hot gas conditioning process. The success of reforming biomass gasification tars with non metallic catalysts has been extensively demonstrated (Corella et al., 1999). The literature associated with these catalysts is reviewed in the next sections.

Dolomites

The most widely studied non-metallic catalysts for biomass gasifier tar conversion are dolomites (calcium and magnesium oxides). CaO and MgO are the most representative basic oxides, with catalytic properties that have been used for pyrolysis of alkenes and aromatics (Taralas et al., 1991), and gasification of oils, coal, and biomass (Corella et al., 1999). The catalytic properties of these materials have also been employed for hot gas cleaning of tars. The activity of CaO is higher than that of MgO. However, catalysts

based on mechanical or natural mixtures of the two oxides exhibit a better performance than CaO The natural mixtures referred to above are obtained by the calcinations of dolomites in which the concentration ratio of the two carbonates is nearly 1:1(Taralas et al., 1991).

Several authors have reported that dolomites only show tar conversion activity after they are calcined. They are the most broadly used nonmetallic catalysts for tar conversion in biomass gasification processes (Devi et al., 2002; Simmel et al., 1999; Taralas., 1991). They are relatively inexpensive and are considered disposable (Sutton et al., 2001). Tar conversion efficiency is high when dolomites are operated at high temperatures (900ºC) with steam. Calcined dolomites are not very robust and quickly undergo attrition in fluidized bed reactors. As a result, calcined dolomite is not an effective primary, or in-bed, catalyst, but it has found use in secondary catalyst beds, particularly in guard beds prior to more active Ni reforming catalyst reactors. The amounts of tar reported for gasifier reactors with in-bed dolomite catalysts vary between 0.5 and more than 5 g/Nm^3 (Devi et al., 2002). The major problem with calcined dolomites is their poor mechanical properties that lead to elutriation (Dayton, 2002). When the calcined dolomite is placed in a secondary reactor, downstream from the gasifier, the bed of dolomite increases the concentration of H_2 and the H_2/CO ratio in the flue gas but has a minor effect on the concentrations of CO_2 and CH_4.

For tar removal, the performance of a calcined dolomite catalyst placed in a secondary unit is determined by the composition of the tars. Phenols and oxygenate compounds decompose readily on the dolomite bed but the polycyclic aromatic hydrocarbons (PAHs) remain in the flue gas (Taralas, 1991). Addition of steam to the secondary reactor also

benefits tar removal. It was found that the levels of tars (treated with steam in a dolomite catalytic reactor) can be lowered to 0.1 g/Nm^3(Simmel et al., 1999).

Olivine

Olivine is a mineral containing magnesium, iron and silica which is a potential in-bed material. Olivine is advantageous in terms of its attrition resistance over that of dolomite. A study conducted by Rapagna showed that olivine has good performance in terms of tar reduction and the activity is comparable to calcined dolomite (Rapagna et al., 1998). They reported more than 90% reduction in average tar content. By contrast, Courson et al., (2000) found that olivine alone does not show any activity for methane reforming. They prepared a Ni-olivine catalyst by impregnation of natural olivine with an excess of nickel salt solution (Courson et al., 2000). The catalyst was then calcined under air for 4 hours at different calcination temperatures of 900-1400^oC. They reported that this Ni-olivine catalyst is active for dry reforming of methane. In addition, Pfeifer et al. (2008) found 75% reduction in tar due to in-bed use of Ni-olivine catalyst (43 % wt) during steam gasification of wood at 850^oC. In a recent investigation, the ability of reducing naphthalene as a model compound was studied by Devi et al. (2005). They found conversions up to 78% and an optimum of ten hours as the calcination period. Olivine has also demonstrated tar conversion activity similar to that of calcined dolomite (Devi et al., 2005). `Olivine is a much more robust material than calcined dolomite and has been applied as a primary catalyst to reduce the output tar levels from fluidized bed biomass gasifiers (Pfeifer et al., 2008). Olivine appears to be an appropriate bed material for fluidized bed gasifiers regardless of other hot gas conditioning methods.

Char

Char is a nonmetallic material. It can be produced by the pyrolysis of coal or biomass. The products of biomass gasification are producer gas, ash and tars. In earlier studies it was noticed that char has good catalytic activity for tar removal (Dogru et al., 2001). For example, in a downdraft gasifier, both fuel and gas flow downward through the reactor, enabling pyrolysis gases to pass through a throated hot bed of char. This can result in cracking the tars into water and non-condensable gases (Wen and Cain, 1984). Other authors like Zanzi found high tar removal in their gasifier by passing the volatiles through a partial oxidation zone followed by a bed of char (Zanzi et al., 1996). They also studied the effect of the rapid pyrolysis conditions on the reactivity of char in gasification and found that the reactivity of char produced in the pyrolysis stage is highly affected by the treatment conditions.

It also has been found that the conversion of tar and pyroligneous liquor over semicoke/charcoal at 950^{o}C resulted in almost complete decomposition into gases of low calorific value (Seshardi et al., 1998). Additionally, the conversion of a coal liquid (tar) over a char-dolomite mixture under different temperatures, pressures, and carrier gases has been studied (Seshardi et al., 1998). An important reduction in the tar content of the producer gas generated in a two-stage gasifier and after passing the gas through a charcoal bed was found in studies conducted by Brandt et al. (2000). Furthermore, in a publication by Abu El Rub et al., (2004) a review of catalysts for tar elimination in biomass gasification processes was made and it was concluded that the biomass char can be a material of high potential for tar reduction in the biomass gasification process. In a different publication by the same group a catalyst comparison between commercial

catalysts and char was based on the activity of the catalyst in a fixed bed reactor. The activity of the catalyst was investigated by the conversion of the model tars naphthalene and phenol into lighter compounds (Abu El Rub et al., 2008).

The source material of char and method of production affect its physical and chemical properties. The char production inside the gasifier can be influenced by manipulating the gasification process parameters such as temperature, particle size, and moisture content (Abu et al., 2004). However, it will be consumed by gasification reactions with steam or CO_2 in the producer gas. The need for a continuous external char supply or withdrawal depends on the balance of char consumption and production in the gasification system (Abu El Rub et al., 2008).

Biomass char properties depend on biomass type and process conditions. While testing char, it is important to consider that char is deactivated by (a) coke formation, which blocks the pores of char and reduces the surface area of the catalyst, and (b) catalyst loss, as char can be gasified by steam and dry reforming (Abu El Rub et al., 2004). It is important to compare the performance of biomass char for tar reduction with other types of active catalysts. The advantage of biomass char for reducing the tar content in producer gas comes from its low cost, since the economics of the overall gasification process are affected by the cost of the catalyst downstream of the biomass gasifier.

2.5.2 Commercial Steam Reforming Nickel Catalysts

A wide variety of Ni-based steam reforming catalysts are commercially available because of their application in the petrochemical industry for naphtha reforming and methane reforming for syngas generation. Nickel-based catalysts have also proven to be very

effective for hot conditioning of biomass gasification product gases (Aznar et al., 1998). Commercial Ni steam reforming catalysts have demonstrated activity for tar destruction with the added advantages of completely reforming methane and water-gas shift activity that allows the H_2:CO ratio of the product gas to be adjusted (Corella et al., 1999). Commercial Ni catalysts are not mechanically robust and are designed primarily for use in fixed bed reactors (Depner and Jess, 1998). Ni catalysts have been most effectively used as secondary catalysts in separate fixed bed reactors downstream from the gasifier. This provides additional process flexibility because the catalyst can be operated independently of the gasifier and its performance optimized. In many processes, a calcined dolomite guard bed will be used to lower the tar levels in the product gas prior to the Ni reforming catalyst. A limitation of Ni catalyst use for hot gas conditioning of biomass gasification product gases is rapid deactivation, which leads to limited catalyst lifetimes (Minowa and Ogi, 1998). Ni catalyst deactivation is caused by several factors. Sulfur, Chlorine, coke, and alkali metals that may be present in gasification product gases act as catalyst poisons (Dayton, 2002). Coke formation on the catalyst surface can be substantial when tar levels in product gases are high.

Catalytic hot gas conditioning will not become a commercial technology unless long catalyst lifetimes can be demonstrated, even for inexpensive, disposable catalysts like calcined dolomite (Devi et al., 2005). Assessment of catalyst lifetimes will allow biomass gasification developers to accurately evaluate the cost of this unit operation. The best currently available tar reforming process consists of a calcined dolomite guard bed followed by a fixed bed Ni catalyst reforming reactor operating at about 800ºC. Selection of the ideal Ni catalyst is somewhat premature. Commercially available steam reforming

catalysts have been demonstrated; however, several of the novel research catalysts appear to have the potential of longer lifetimes that should be verified. This dual bed hot gas conditioning concept has been demonstrated and can be used to condition the product gas from any developing gasification process. For fluidized bed gasifiers, the guard bed could potentially be eliminated if olivine is used as the bed material. A proprietary Ni monolith catalyst has also shown considerable promise for biomass gasification tar destruction and also warrants future consideration (Delgado et al., 1999).

2.5.3 Optimized Catalyst Formulations

Optimized catalyst formulations have been developed based on the commercial success of Ni reforming catalysts. Several studies have explored other catalyst formulations such as Ru and Ce (Asadullah et al.,2001). Asadullah et al. (2002) developed a $Rh/CeO_2/SiO_2$ catalyst for low temperature gasification and observed a complete carbon and tar conversion for cellulose gasification at temperatures between 500-600^oC. Other research groups have focused on developing additional Ni-based catalysts for biomass gasification applications. (Courson et al., 2000; Draelants et al., 2000; Arauzo et al., 1994). These improved catalyst formulations are generally designed to optimize desired catalyst properties.

The effect of catalysts on gasification products is very important. Catalysts not only reduce the tar content, but also improve the gas product quality and conversion efficiency of the gasification process.

The selected catalyst should be effective in the removal of tars, easily regenerated, strong, durable, inexpensive, and resistant to deactivation as a result of carbon fouling and sintering (Sutton et al., 2001).

2.6 Selection of Commercial Catalysts

Over the past years, research regarding catalytic destruction of tars produced during biomass gasification has been extensively conducted using commercial catalysts and specific catalysts developed in research centers and universities. Some of the commercial catalysts that have been studied for this purpose are ICI 46-1 from ICI Katalco, C11 NK from United Catalysts, G1-50 from BASF, R-67 and RKS-1 from Haldor Topsoe.

The three commercial catalysts selected for this study are

A) Hifuel R-110 from Johnson Matthey (London, United Kingdom)

B) Reformax 250 from Sud-Chemie, Inc. (Louisville, KY)

C) NextechA: Cerium Zirconium Oxide – Platinum Catalyst from NexTech Materials, Ltd (Columbus, OH)

In most of the catalysts developed for steam reforming of hydrocarbons, Ni is the main active component. These catalysts have been tested with good results in biomass gasification clean up applications. Catalyst A was selected because it has been successfully used in the steam reforming of light to medium hydrocarbons (Caballero et al., 2000). Catalyst B has been extensively used and its effectiveness is acknowledged for the steam reforming of heavy hydrocarbons such as naphtha (Tsujii et al., 2005).

By contrast, catalyst C is a non-nickel based catalyst that has been used for tar removal applications and looks promising for this research. Comparing the performance of these catalysts in the experimental set up will lead to a recommendation of a suitable catalyst to be implemented in our gasification process to maximize the chemical conversion of tar into synthesis gas.

2.6.1 Hifuel R-110 (from Johnson Matthey)

This catalyst has a similar formulation to ICI Katalco 46-1 which has been extensively studied by several research groups. For example, Caballero et al (2000) found ICI 46-1 highly active and useful for gas cleanup. Gebhard and others (1994) obtained good results with this catalyst and recommended its use in a secondary reactor active for the water gas shift reaction. This catalyst has been tested along with other commercial catalysts and it has shown high conversion levels as reported by several authors (Corella et al., 1999; Garcia et al., 2000;, Coll et al., 2001; Wang et al., 2005; Zhang et al., 2004). In recent years ICI (Imperial Chemical Industry), one of the leading suppliers of catalysts to the ammonia and methanol industries, sold its catalyst business (Synetix), formerly ICI Katalco, to United Kingdom catalyst and precious metals firm Johnson Matthey in London, United Kingdom.

Hifuel R-110, is a nickel on calcium aluminate catalyst for steam reforming of light to medium hydrocarbons. It is a four-holed quadralobe shape: 10½ mm x 13 mm. The recommended operating temperature is 600-900°C, and can be operated with a steam-to-carbon ratio in the range 2.0 to 7.0, according to the manufacturer. Pressure will have minimal effect on approach to equilibrium. It is susceptible to poisons such as sulphur,

chloride, metals and silica. An upstream desulphurization step is recommended that reduces sulphur to < 0.5 ppm. Steaming under full steam or steam-to-carbon 7.0 at 740^{o}C can often remove low levels of poisons, as well as carbon deposits, restoring catalyst activity. The catalyst is supplied in non-reduced form, requiring an activation step prior to use by exposure to dry hydrogen for at least 2 hours at 600°C. Once reduced, the catalyst is pyrophoric and so prior to discharge the catalyst should be exposed to steam and oxidized.

2.6.2 Reformax 250 (from Sud-Chemie)

Reformax 250 (former C11NK) is an industrial catalyst designed for steam reforming of naphtha. This catalyst has been studied for its ability to destroy tars during biomass gasification processes. This catalyst performed very well in experiments conducted by steam reforming of oil produced from waste plastics, and the carbon conversions were very high with low coking ratio (Tsujii et al., 2005). In addition, Pfeifer studied the catalytic tar decomposition downstream from a dual fluidized bed biomass steam gasifier using this catalyst and toluene as model tar compound (Pfeifer et al., 2008). This catalyst has also been extensively studied in research centers such as NREL (National Renewable Energy laboratory), where it was initially tested along with other commercial catalysts for comparison with its proprietary catalysts (Garcia et al., 2000). In a later publication researchers from NREL referred to this catalyst as the best commercial catalyst for tar removal (Bain et al., 2005).

This is a naphtha reforming catalyst used for production of ammonia, hydrogen, methanol, etc., by steam hydrocarbon reforming under varied process conditions for feed stocks of higher hydrocarbon to naphtha (Reformax brochure, 2001).

Reformax250 is nickel oxide on refractory support consisting of oxides of alumina, calcium, magnesia and silica. During manufacture, potash is incorporated in the catalyst to prevent carbon lay down by cracking of hydrocarbons during steam reforming of naphtha.

Reformax250 is produced in 3 grades: standard ReforMax250 with 7% K_2O used for steam reforming of naphtha feed; ReforMax250-02 with 2% K_2O; and ReforMax250-04 with 4% K_2O used for a LPG (liquid petroleum gas) mix of associated gas and higher hydrocarbon feeds. The grade used for this work is standard Reformax 250. This naphtha reforming catalyst is supplied in two forms: Raschig Rings and 5 hole shaped rings. The molecular formula for this catalyst is: Kaolin+Cement+K_2O+MgO+NiO+SiO_2.

Reformax250 is supplied in the nickel oxide form which is relatively active for steam reforming. Hence these catalysts have to be activated by reducing to active metal Nickel by exposure to dry hydrogen for at least 2 hours at 600°C (Reformax brochure).

2.6.3 NextechA: Cerium Zirconium Oxide – Platinum Catalyst (from NexTechMaterials)

Nextech Materials has established a number of highly active catalyst formulations using its proprietary technologies for producing ceria-based support oxides incorporating catalytic metals at high dispersion levels. These catalysts can be used in a wide variety of chemical reactions and have been extensively tested in fuel processing applications.

This company has undergone research in partnership with the Gas Technology Institute for development of effective catalysts for destruction of tar generated in biomass gasification processes (Swartz et al., 2003). The use of a non nickel catalyst, Pt, using 60% cerium oxide as a support has been investigated for the steam reforming of tars produced from cedar wood gasification (Yung et al., 2009).

This catalyst is available in both powder and pellet forms. Standard formats are fine powders, granules and 3x5 mm cylindrical pellets.

This catalyst has a couple of advantages which make it attractive for this application: no activation of catalyst is required, which saves start-up time and money, and it is non-pyrophoric (does not deactivate in presence of oxygen or water).

The recommended operating conditions for this catalyst include an ideal steam to carbon ratio in the range of 2/1 to 3/1, and operating temperatures from 400-800^{o}C. Catalyst regeneration can be accomplished by heating to 500^{o}C in air for a couple of hours.

2.7 Tendency Toward Carbon Formation

Catalyst deactivation is a big problem in steam reforming processes. Carbon deposition may cause blockage of the catalyst active sites (Satterfield, 1991). It is of interest to understand both carbon formation and carbon deactivation and the relationship between those processes.

Usually, the terms carbon and coke are used interchangeably; however, carbon is a product of CO disproportionation and coke is originated by decomposition or condensation of hydrocarbons on metals (Gardner et al., 1981). The formation of carbon

deposits may engage the generation and transformation of various carbon forms such as atomic carbon, amorphous carbon, vermicular carbon, bulk Ni carbide, and graphitic carbon. Three types of coke or carbon species have been observed in a reformer (Sehested, 2006):

-Pyrolytic carbon: formed by exposure of high hydrocarbons to high temperature

-Encapsulating carbon (gum): may be formed during reforming of heavy hydrocarbon feeds with a high content of aromatic compounds

-Whisker carbon: the most destructive form of carbon formed in steam reforming over nickel catalysts. Carbon whiskers grow by the reactions of hydrocarbons or CO at one side of the metal particle.

2.8 Reaction Kinetics

Several institutions working on this subject agreed years ago to use the same reacting network and kinetic analysis to compare their respective results (Devi et al., 2005). The overall tar elimination can be expressed by a simple first-order reaction. Then, working under plug or piston flow conditions the following measurements of activity can be estimated:

a) Conversion

The simplest way to measure activity is in terms of conversion of tar (or a model compound) in a particular condition. The results are expressed in terms of percent (%) conversion of toluene defined as:

$$X\ (\%) = 100x\left(\frac{(Cin-Cout}{Cin}\right) \quad (2.17)$$

where X is the conversion of the model tar compound, C_{in} (gL^{-1}) is the inlet concentration of the model tar compound and C_{out} (gL^{-1}) is the outlet concentration of the model tar compound.

b) Apparent Activation Energy

The apparent rate constant and the apparent activation energy for tar decomposition can be calculated assuming a first order reaction. One major advantage of assuming a first order reaction is that it is easy to evaluate and compare with other references (Corella et al., 1999). The overall rate can be described using the following equation

$$-r_{tar} = k_{app}.C_{tar} \quad (2.18)$$

where r_{tar} is the rate of the model tar conversion, k_{app} is the apparent kinetic constant or pre-exponential factor for overall tar removal, and C_{tar} is the concentration of the tar model compound.

Under plug-flow conditions, the apparent rate constant can be calculated as:

$$k_{app} = \frac{[-\ln(1-X)]}{\tau} \quad (2.19)$$

where τ is the gas residence time defined as

$$\tau = \frac{W}{v_o} \quad (2.20)$$

where W is the weight of the catalyst (kg) and v_o (m^3/s) is the flow rate of the gas mixture at the catalyst bed.

The Arrhenius equation is the most widely used model to express temperature dependence at the rate constant of the reaction rate and can be written as

$$k_{app} = k_o exp\left(\frac{-E}{RT}\right) \quad (2.21)$$

Where E is the apparent activation energy, T is the temperature, R is the universal gas constant k_o is the pre-exponential factor. The kinetics constants for toluene removal for each catalyst can be calculated by

$$ln\left[\frac{-ln(1-X)}{\tau}\right] = lnk_o - \frac{E}{RT} \quad (2.22)$$

The graphic of ln (-(ln ((1-x)/t)) vs. 1/T is a straight line with slope equal to (-E/R) and an intercept equal to k_o.

2.9 Catalyst Characterization

The application of surface analytical techniques is of great value in understanding the performance of a catalyst. However, the results obtained from any of these techniques are often difficult to interpret, especially if only one technique is used by itself.

These analyses permit the correlation of catalyst structure with activity and to understand deactivation processes and sintering. Reduction is the key process that forms the active metallic surface from precursor nickel oxide and it would be useful to understand how Ni

crystallites form and change (Ni crystals can sinter with temperature). This can be accomplished through catalyst characterization.

Structural changes in the catalysts during the tests will be described by means of catalyst characterization. A combination of characterization techniques will be used in order to provide detailed information about the surface structure. Surface analysis techniques that are of interest in this research are described.

BET

The BET theory first established by Stephen Brunauer, Paul High Emmett, and - Edward Teller set the basis to establish a common technique for measuring the surface area of a material based on the physical adsorption of molecules of a gas on the surface of a solid. This theory expanded the Langmuir theory to multilayer adsorption and it is based on the following hypothesis: a) gas molecules physically absorb on a solid in layers, b) there is no interaction between each absorption layer and c) the Langmuir theory can be applied to each layer. To perform this analysis the solid surface should be clean. This means that physisorbed material should be removed before any adsorption measurement can be done (Devi et al., 2005).

FTIR

Infrared spectroscopy such as Fourier Transform infrared provides specific information about chemical bonding and molecular structure. Fourier Transform Infra Red analysis has been used to obtain information regarding the structure of the coke on the spent catalysts (Pieck et al, 1992; Ibarra et al., 1995). In addition, this technique has been used

for biochar characterization (Ozcimen et al., 2010). The measure of radiation absorption as a function o frequency produces a spectrum that can be used to identify functional groups and compounds. This method is used to determine the functional groups present in the char sample.

TGA

Thermogravimetric analysis is a useful technique to follow microscopic weight change during the analysis so a profile of weight change vs. temperature is recorded and the weight temperature profile is used for determination of coke amount on spent catalysts. TGA provides straightforward information regarding the weight of material that is being gasified from the catalyst (Dou et al., 2003).

SEM

Scanning Electron Microscope has been used to study the morphology of catalyst surface (Devi et al., 2002). In addition, the localization, nature and structure of coke deposits can be examined with electron microscopy (Zhang et al., 2004). The type of carbon produced by our feedstock can be identified as pyrolytic, encapsulated or whisker carbon by means of scanning electron microscopy. Typically, electron microscopy alone does not provide much information, and is generally used in combination with related spectroscopic measurements.

XPS

X- ray Photoelectron Spectroscopy (XPS) has been used to gain information regarding catalyst surface since the peaks are related to surface concentration (Devi et al., 2005;

Pleths, et al., 2001). In addition, this characterization method can be used on catalytic system regardless of its crystallinity (Poncelet et al., 2005). XPS may detect unreacted regions on a catalyst surface (Beccat et al., 1999) and the structure of the total coke deposits can be determined by XPS (Konya et al., 2004).

TPR

Temperature Programmed Reduction is a powerful tool to evaluate the reduction conditions of a catalyst (Courson et al., 2000). Temperature programmed reduction is used to characterize metal oxides dispersed on a support; this technique offers quantitative information of the reducibility of the oxide's surface.

2.10 Extent of Reaction Method

More than fifty years ago Prigogine and Defay introduced the concept of reaction coordinates for a batch reaction (Friedly, 1991). Years later this concept became useful in many chemistry and chemical engineering applications (Froment and Bischoff, 1979; Smith and Van Ness, 1996). Several authors have pointed out the underlying basis in linear algebra for the utility of the reaction coordinate in various applications. The extent of reaction may be referred to as a macroscopic reaction coordinate, which varies as the reaction proceeds (Canagaratna, 2000).

In a system where several independent reactions occur simultaneoulsy, let subscript j be the reaction index , and let ε_j be the reaction coordinate associated with each reaction. Then, for a system with r independent reactions and n compounds; the general expression to describe the relationship between the number of moles of a compound at any point, the

reaction coordinate and the initial number of moles of compound i can be calculated by the following expression (Foutch G. And Johanes A. , 2000)

$$N_i = N_{io} + \sum_j \nu_j \varepsilon_j \qquad (2.23)$$

where

ε= reaction coordinate

i = species involved (i = 1, 2, …n)

j= reactions involved (j = I, II, …… r)

ν= stoichiometric coefficient (positive for products; negative for reactants)

N_i = Number of moles at any stage of specie i

N_{io} = Initial number of moles of specie i

This system of linear equations is algebraically equivalent to the matrix equation

$$AX = B \qquad (2.24)$$

where

A = matrix of stoichiometric coefficients

X = vector of unknowns, in this case ε values

B = vector of known constants, in this case N_i - N_{io}

Then, the values for the extent of reaction which are the solution of the system can be calculated in Excel by:

$$\varepsilon = A^{-1} \cdot B \tag{2.25}$$

The extent of reaction values can be used to determine which reactions are dominant in a system of reactions.

CHAPTER III

EXPERIMENTAL COMPARISON OF BIOCHAR AND COMMERCIAL CATALYSTS FOR TAR REMOVAL

Abstract

The destruction of tars is a crucial technological barrier for the development and further commercialization of biomass gasification. It is known that the decomposition of tar compounds using catalysts is a suitable solution to this problem. Biochar, which is generated during gasification, is also a potential catalyst for tar destruction. Biochar and three commercial steam reforming catalysts were evaluated for tar removal using toluene as a model tar compound. Two of the commercial catalysts were nickel based (Reformax 250 and Hifuel R-110) and one was platinum based (NextechA). The biochar was generated during switchgrass gasification in a down draft gasifier at the OSU thermochemical conversion facility. Tar destruction experiments were performed in a bench scale fixed bed reactor between 600 and 800^{o}C under atmospheric pressure using a synthetic gas mixture with similar composition to the syngas generated from switchgrass gasification. Toluene conversion results showed that the biochar performance was comparable to the commercial catalysts and Reformax was the most active of the tested catalysts. The activation energy of toluene steam reforming over these catalytic materials was found to be 50.26 kJ/mol for Reformax 250; 51.18 kJ/mol for Hifuel R-110; 59.44

kJ/mol for NextechA and 61.59 kJ/mol for biochar. Catalyst characterization by SEM, XPS, TGA, and FTIR was also conducted on the used catalysts. According to the XPS spectra, graphitic carbon was found on all catalysts and according to TGA results Hifuel R-110 is the catalyst with the highest tendency toward coke formation, followed by biochar.

3.1 Introduction

Conventional non renewable energy sources such as oil, coal, and natural gas are becoming depleted. To cover the world energy demand, processes for energy production are focusing on renewable energy sources like biomass. Biomass gasification has the ability to generate a syngas rich in H_2, CO, and CO_2 that can be used for synthesis gas applications, production of chemicals, fuel cell applications and power generation. One of the advantages of using biomass gasification is that the feedstock for this process can be any kind of biomass (Kumar et al., 2009). However, the destruction of tars present in the syngas is an important obstacle that needs to be overcome for the development and further commercialization of biomass gasification so that this process can be cost effective, competitive, dependable and sustainable.

Tar disposal is one of the most important problems during biomass gasification, and a great amount of work concerning tar reduction or reforming has been reported. Traditionally tar removal technologies have been broadly divided into two approaches: treatments inside the gasifier (primary methods) and hot gas cleaning after the gasifier (secondary methods) (Devi et al., 2002). Treatments inside the gasifier are interesting because they may eliminate the need for downstream cleanup. In both the primary and

secondary methods, tar removal is done either by chemical treatment or physical separation. A number of catalytic processes have been previously investigated. Early on, it was discovered that in situ catalysis, in which the catalysts are placed directly in the gasification reactor, is not effective due to rapid catalyst deactivation (Delgado et al., 1999). Catalytic processes may eliminate the need for cooling the gas as needed for physical processes, which is advantageous because the economics of the process and the thermodynamic efficiency of the gasification process are not compromised. Catalytic tar destruction has been studied for a long time and various reviews have been written on biomass gasification hot gas cleanup (Dayton, 2002; Devi et al., 2002; Huber 2006; Torres 2007; Yung et al., 2009).

Earlier research using char as a catalyst has found it to be a promising material for tar removal (Ankita et al., 2010; Abu El Rub et al., 2008). In addition, previous research has shown promising results for tar removal by using char supported nickel catalysts (Wang et al., 2005). The use of biomass char for tar removal purposes could be combined with the gasification process since char is a waste product from the gasification process itself. This type of arrangement would have a positive impact on the economics of the project due to reduced catalyst investment. The goal of this work was to compare the use of biochar to several commercial catalysts for tar destruction in a biomass gasification system.

3.2 Methods

3.2.1 Catalyst Details

A description of the catalysts selected for this study is presented in Table 3.1. The selected commercial catalysts have been tested with good results in biomass gasification clean up applications in the petrochemical and refining industry, especially in the steam reforming of hydrocarbons. The biochar used as a catalyst in this research was generated by gasification of switchgrass in a down draft gasifier operating at atmospheric pressure at the Oklahoma State University thermochemical conversion facility.

Table 3.1 Description of catalysts used in this study.

Catalyst	Type	Manufacturer	Composition	Form	Density (g/cm^3)
Reformax 250	Nickel steam reforming	Sud-Chemie	Kaolin(20-40)%; Portland cement(20-30)%; NiO (15-30)%; MgO (10-20)%; K_2O (3-4)%; silica quartz (0.5-4)%	Pellets	0.95
Hifuel R-110	Nickel steam reforming	Johnson Mathey	NiO (15-40) on ceramic support	Rings	0.951
NextechA	Optimized formulation	Nextech Materials	Zirconium doped Ceria (support) Platinum (2%wt)	Powder	6.6
Biochar	Non-metallic	OSU	See Table 3.4	Powder	0.194

Table 3.2 presents the mineral content of the biochar, as determined by ICP (inductive coupled plasma) in the soils laboratory at Oklahoma State University. Tables 3.3 and 3.4 show the proximate and ultimate analysis of biochar, respectively. The proximate and ultimate analyses were performed by Midwest Micro Laboratories (Indianapolis, IN).

Table 3.2 Mineral content of biochar generated from switchgrass at OSU.

Element	**Weight %**
P	0.23%
Ca	4.86%
K	0.90%
Mg	0.61%
Na	0.31%
S	0.08%
Fe	2240 ppm
Zn	43.8 ppm
Cu	13.7 ppm
Mn	326 ppm

Table 3.3 Proximate analysis of biochar generated from switchgrass at OSU.

Material	Volatile Matter (%)	Fixed Carbon (%)	Ash (%)
Biochar	18.85	63.65	17.5

Table 3.4 Ultimate analysis of biochar generated from switchgrass at OSU.

Element	C	H	N	S	O
(wt. %)	87.43	1.49	0.74	0.08	10.26

3.2.2 Experimental Set up

The selected catalysts were evaluated for steam reforming activity in a high temperature reactor system that provides real time steam reforming kinetic data. Toluene was selected as the model tar compound because it represents a stable aromatic compound which is present in tar and it is less harmful than most of the other tar compounds.

The experimental setup consisted of a laboratory scale fixed-bed tube reactor working at atmospheric pressure. The reactor was placed inside a tube furnace (Thermcraft Incorporated, Winston Salem, North Carolina) equipped with a temperature controller (Thermcraft Incorporated, Winston Salem, North Carolina). The quartz tube reactor had an inner diameter of 0.01 m. and a length of 0.88m. A schematic representation of the experimental setup is given in Figure 3.1.

The reactor is fed with a synthetic gas mixture with a composition similar to the producer gas generated when gasifying switchgrass using air as the gasifying agent in the fluidized

bed gasification process. The exact gas composition of this synthetic gas mixture is presented in Table 3.5.

The reaction zone consists of the catalyst bed, supported by quartz wool. A K-type thermocouple is kept inside a thermowell which is set in the middle of the catalyst bed to ensure that the reactions occur at the desired temperature (Mudinoor, 2006). The position of the bed has been determined according to the temperature profile over the reactor and the temperature across the catalyst bed can be considered constant during each experiment.

Table 3.5 Composition of synthetic gas mixture.

Compound	**Composition (mole %)**
Hydrogen	5.15
Methane	7.49
Carbon Dioxide	16.79
Carbon Monoxide	19.30
Nitrogen	Balance

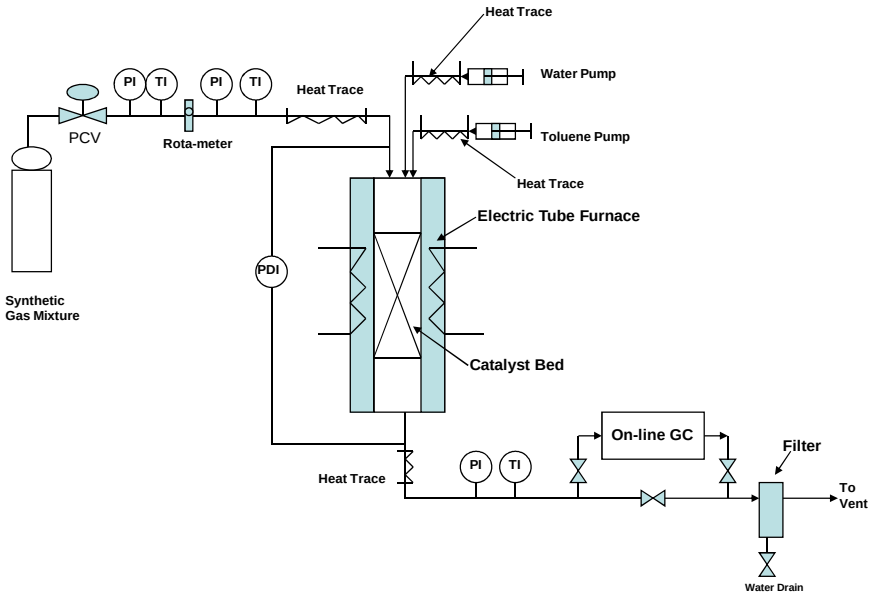

Figure 3.1 Schematic representation of experimental set up for catalyst testing.

The liquid reactants (water and toluene) were introduced to the system through syringe pumps (KD Scientific, Holliston, Massachusetts, model 780100 for toluene and model 780200 for water). These reactants were vaporized before mixing with the gas stream. The pipes were heated to 250^{o}C using heat tape (Omega, Stanford, Connecticut) in order to avoid condensation of water and toluene. A detailed experimental procedure including catalyst testing protocol is presented in Appendix A-1.

3.2.3 Sampling and Analytical Methods

The gaseous effluent was analyzed by means of an on-line gas chromatograph (HP 5889, Houston, Texas) equipped with a 250 micro liter loop housed in a six-port valve. This valve system was heated to 200^{o}C . The analysis was performed with two columns in

series: an HP Plot Q column from Agilent Technologies (0.53mm ID, 30m length) and a Molsieve column also from Agilent Technologies (0.53mm ID, 30m length). The GC had two detectors: a TCD (thermal conductivity detector) and a FID (flame ionization detector).

Another six-port valve was utilized to isolate carbon dioxide, water and toluene from the molsieve column. Hydrogen, carbon monoxide, methane, and nitrogen were separated on the molsieve column. Carbon dioxide, toluene and water were separated on the Plot Q column. Methane and toluene were detected by the FID while the other gases were detected by the TCD. Toluene conversion as a function of time on stream was used to quantitatively evaluate catalyst reforming performance. The carrier gas flow rate was set at 5 mL min−1; the flow through the vent was set at 50 mL/ min; the reference gas flow rate was set at 20 mL/ min; the air and hydrogen gas flow rates to the FID were set at 240 and 60 mL/min, respectively. Argon was used as the carrier gas and its flow rate was set at 5 mL/ min. A sample was analyzed every 21 minutes.

3.2.4 Experimental Parameters

Since the composition of the synthetic gas mixture is associated with the data for air gasification of switchgrass in the pilot scale fluidized bed gasifier, the toluene and gas mixture flow rates were based on that data when using a scaling factor of 0.1%. The gas flow rate used for experimentation was 0.0283 m^3/h. The steam to carbon ratio was set at 2, based on experimentation and manufacturer recommendation. Experiments were conducted at atmospheric pressure in a temperature range of 600-800^oC in the catalyst

bed. A summary of the important operational parameters for catalyst testing is presented in Table 3.6

Table 3.6 Operational parameters for toluene conversion experiments.

Parameter	Value
Temperature (^{o}C)	600-800
Pressure (Pa)	101325
Gas flow rate (m^3/h)	0.0283
Toluene flow rate (mL/h)	2.0
Water flow rate (mL/h)	24
Steam/Carbon ratio	2
Mass of catalyst (g)	0.15
Mass of char (g)	0.3
Mass of support (sand) (g)	0.75

3.2.5 Initial Experiments

Initial concentrations of compounds with no catalyst loading

Experiments to determine initial concentration values for all of the compounds under analysis were conducted with no catalyst loading. The results of the initial concentration experiments at three different temperatures are presented in Table 3.7. Values represent an average of three runs at each temperature, and for each value the standard deviation is <5%.

Note that water is not included in the table since water passes through the GC without being quantified. Water measurements were made manually at the end of each experiment by collecting the water in liquid phase retained in the water trap at the exit line. Water in the gas phase was calculated using psychrometrics.

Table 3.7 Initial concentration values at three different temperatures

Temperature (^{o}C)	Methane (g/l)	Toluene (g/l)	Carbon Dioxide (g/l)	Hydrogen (g/l)	Nitrogen (g/l)	Carbon Monoxide (g/l)
600	0.01993	0.02204	0.1197	0.001603	0.2104	0.0855
700	0.01895	0.02005	0.1266	0.001687	0.2327	0.0911
800	0.02172	0.02661	0.1261	0.001818	0.2142	0.0855

Constant temperature zone

Since the catalyst bed needs to be placed at a point where the temperature remains constant over time, an experiment to identify the reactor constant temperature zone was conducted by placing the catalyst bed at different locations along the reactor. That zone was found when the difference between the temperature measured by the thermocouple at the catalyst bed and the temperature indicated by the reactor temperature controller was minimal. The constant temperature zone was found at 0.622m from the top of the reactor.

Catalyst pretreatment

Before using the Nickel steam reforming catalysts (Reformax 250, Hifuel R110) for experimentation it was necessary to conduct reduction and activation of the catalysts and to reduce their particle sizes. The platinum catalyst did not need any pretreatment since it could be used as received from the manufacturer.

Reformax 250 and Hifuel R 110 were received from the manufacturer in the form of pellets and rings, respectively. Their size was reduced by using a mortar and pestle to obtain a fine powder. This fine powder was sieved using two sieves which have mesh numbers 270 and 70 to obtain a particle size between 53-212µm. The powder that passed through mesh 70 and was left on mesh 270 was recovered and used for testing. The char used for these experiments underwent the same size reduction treatment to obtain a similar particle size.

Both nickel catalysts used in this work, Reformax 250 and Hifuel R 110, have nickel oxide as the active phase. They require a reduction step before being used to release nickel to activate the catalyst. This process is described by the following reaction:

$$NiO + H_2 \longrightarrow Ni + H_20 \qquad (3.1)$$

Catalysts were reduced in situ in a hydrogen environment for two hours at 650^{o}C according to manufacturer recommendations. The hydrogen flow rate was set at 150 ml/min. The catalysts were used immediately after the activation step. In the case of char, nitrogen gas was passed over the char for 30 minutes at reaction temperature before beginning experimentation.

3.2.6 Mass Balance

Since the composition of the synthetic gas mixture is known and this can be considered an ideal gas, the total number of moles can be calculated by the ideal gas law:

$$n = \frac{PV}{RT} \tag{3.2}$$

where

P = pressure (Pa), T = temperature (K), V= volumetric flow rate (m^3/h), R = universal gas constant (8.3144kJ/kmolK) and n = number of moles entering the system (mol/h).

The number of moles of each compound entering the system in each experiment can be calculated, along with the number of grams per hour per compound entering the system.

The total number of moles leaving the system was determined based on the assumption that nitrogen is an inert (gas tracer technique) and using gas chromatograph composition results.

$$Total\ number\ of\ moles\ exiting\ per\ run = \frac{Ni}{\frac{\%Ne}{100}} \tag{3.3}$$

where

N_i = mol/h of nitrogen at inlet

$\%N_e$ = mol percent of nitrogen at exit per run.

Carbon Balance

A carbon balance was performed by calculating grams of carbon entering the system by

$$C_i = \sum n_i a_i \quad (3.4)$$

where C_i = grams of carbon entering the system, n_i = number of mol of carbon in each compound containing carbon at the inlet (CO, CO_2, CH_4, C_7H_8) and a_i = number of atoms of carbon in each compound containing carbon at the inlet (CO=1, CO_2=1,CH_4=1, C_7H_8=7)

Carbon exiting the system was calculated by

$$Ce = \frac{21}{60} \sum Ne \quad (3.5)$$

$$\textit{Total grams of carbon exiting the system per compound} = 12(Ce)\,(ai) \quad (3.6)$$

where Ce = moles of carbon exiting the system, Ne = number of mol/h of carbon in each compound containing carbon at the exit (CO, CO_2, CH_4, C_7H_8). Each online measurement is taken every 21 minutes, so the 21/60 converts minutes to hours. An example of a mass balance and a carbon balance is presented in Appendix A- 2.

3.2.7 Kinetic Studies

Kinetic measurements are based on the assumption of one single reaction for the toluene elimination and working under plug or piston flow conditions.

Conversion

The conversion of model tar can be expressed in terms of conversion of toluene as

$$X\,(\%) = 100\left(\frac{(Cin - Cout)}{Cin}\right) \quad (3.7)$$

where X is the conversion of toluene, C_{in} is the inlet concentration of toluene (g/l) (found in Table 3.7) and C_{out} is the outlet concentration of toluene (g/l).

Apparent Activation Energy

Assuming a first order reaction in toluene, the overall rate can be described using the following equation:

$$-r_{tar} = k_{app} C_{tar} \tag{3.8}$$

where r_{tar} is the rate of the model tar conversion, k_{app} is the apparent kinetic constant, and C_{tar} is the concentration of the tar model compound

Under plug-flow conditions, the apparent rate constant can be calculated as:

$$k_{app} = \frac{[-\ln (1-X)]}{\tau} \tag{3.9}$$

where τ is the gas residence time defined as

$$\tau = \frac{W}{v_o} \tag{3.10}$$

where W is the weight of the catalyst and v_o is the gas flow rate of the gas mixture at the catalyst bed.

The reaction rate constant kapp changes according to the Arrhenius equation as

$$k_{app}(T) = k_o exp\left(-E/RT\right) \tag{3.11}$$

where E is the apparent activation energy, T is the temperature, k_o is the pre-exponential factor and R is the universal gas constant.

Measurements of toluene conversion were made at different times on stream for the same test. The apparent kinetic constant (k_{app}) was calculated for three different experiments and an average value of $k_{aap}$was used for the determination of activation energy.

3.2.8 Statistical Analysis

Since the goal is to compare the toluene conversion achieved using four catalyst materials (Reformax 250, Hifuel R-110, NextechA, and biochar) and molar composition of four gas compounds (H_2, CO, CH_4, CO_2) per catalyst; an analysis of variance (ANOVA) was conducted to determine if the variable under consideration (toluene conversion or molar concentration) for a catalyst was statistically different from the other catalysts. Since the experiments were conducted at three different temperatures a temperature comparison was also performed. This analysis was conducted in Excel using the ANOVA function at 0.05 level of significance. Twelve online measurements were taken in each experiment.

3.2.9 Testing Catalysts in Series

Previous studies have been successfully conducted for char in combination with nickel based catalysts (Ankita et al., 2010). The same experimental set up described previously was used to test biochar in series with one of the commercial catalysts (NextechA) to determine the catalytic performance of char in combination with a platinum based catalyst. The tube reactor was loaded with these two catalysts in series using three different loading options. Two of the options explored are illustrated in Figure 3.2. In

option A, the tube reactor was loaded with 2 beds, separated by an empty space between the two beds, with each one supported by quartz wool. In this arrangement the two catalyst beds were not in contact. In option B the tube reactor was loaded with the same 2 catalyst beds, but they were in direct contact with each other. In option C (not presented in Figure 3.2) the two catalysts were mixed homogeneously and tested as one catalyst bed. The catalyst loads remained the same as reported in Table 3.6.

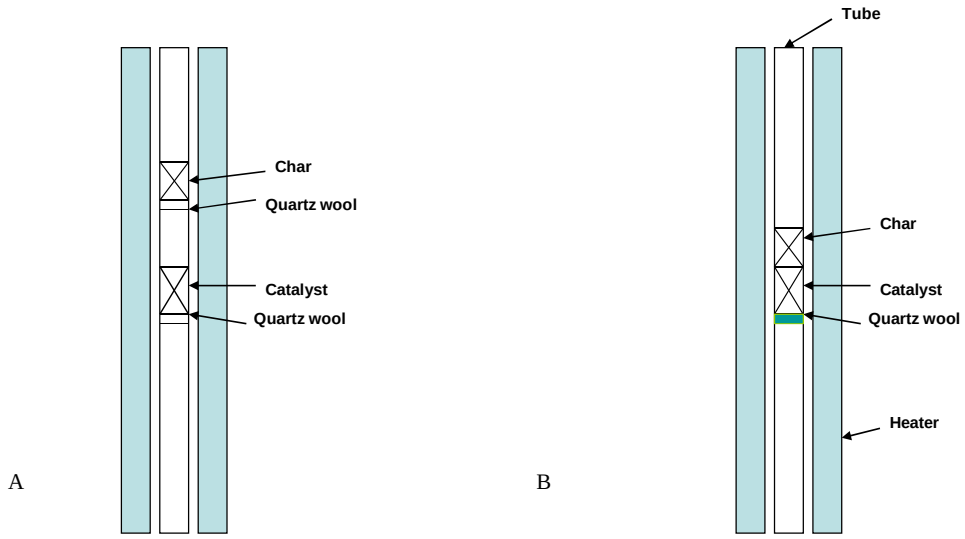

Figure 3.2 Options for loading catalysts in series.

3.2.10 Catalyst Characterization

Various techniques were used for catalyst characterization to analyze chemical and physical properties of the four catalyst materials.

BET

Surface area measurements were obtained using an Autosorb-1C model No. AS1-CT-11 by Quantachrome Instruments (Boynton Beach, Florida). Measurements of adsorption and desorption isotherms for characterization of surface area were conducted. Before performing analysis, the samples, 500 milligrams in all cases were degassed overnight at 200^{o}C. This analysis was conducted in the OSU Bioenergy laboratory.

FTIR

Fourier Transform Infra Red (FTIR) spectra were acquired on a Nicolet 6700 FTIR (Houston, Texas) using a sample size of 5mg. Analysis of the spectra to determine structure of the coke and functional groups present on catalyst materials was conducted using the FTIR Thermo Scientific OMNIC-Spectra software.

XPS

X-ray Photoelectron Spectroscopy (XPS) was used to study the sample surface and XPS spectra were acquired using PerkinElmer equipment (Waltham, Massachusetts). The samples were prepared and identified on a stainless steel ribbon with each sample occupying an area of approximately 7 mm^2. Before turning on the x-ray source, samples

were exposed to high vacuum for two hours. In order to conduct XPS analysis the ultra-vacuum needed to be below 10^{-8} torr (Beccat et al., 1999).

TGA

Thermogravimetric analysis (TGA) was carried out using a Versatherm high sensitivity model 771-0070 (Fisher Scientific). TGA data was obtained by using thermal analyst data acquisition software. Catalyst samples of 25 mg were used and were heated from room temperature to 800^{o}C at a rate of 10^{o}C/min. The sample size in the case of char was 9mg, as suggested by previous researchers due to char volatile nature (Drogu et al., 2002). Thermo-gravimetric analysis is used for determination of the amount of coke deposited on spent catalysts.

TPR

Temperature Programmed Reduction (TPR) was conducted on an Autosorb-1C by Quantachrome Instruments. Two hundred milligrams of catalyst was placed between two pieces of quartz wool in a U-shaped quartz cell. The reducing gas mixture (5% hydrogen in nitrogen) was fed to the cell and heated from room temperature to 700^{o}C at a rate of 20 ^{o}C/min.

SEM

Scanning Electron Microscopy (SEM) images were obtained using a Jeol JMS 6360 scanning electron microscope (Tokyo, Japan). The catalyst surface was coated with a gold layer before the samples were placed in the multi specimen holder which can hold up to four samples at a time. Different magnifications were used at 20KV.

3.3 Results

3.3.1 Toluene Conversion at Different Temperatures

Steam reforming of toluene over three commercial catalysts and biochar as a function of temperature was studied. Figures 3.3, 3.4 and 3.5 show conversion of toluene vs. time on stream for each of the catalysts tested at temperatures of 600, 700, and 800 ^{o}C, respectively. It can be observed that all catalysts are active in converting toluene, with the nickel based catalysts performing the best, followed by the platinum based catalyst and then biochar. It was also observed that the conversion for each catalyst increased with an increase in temperature.

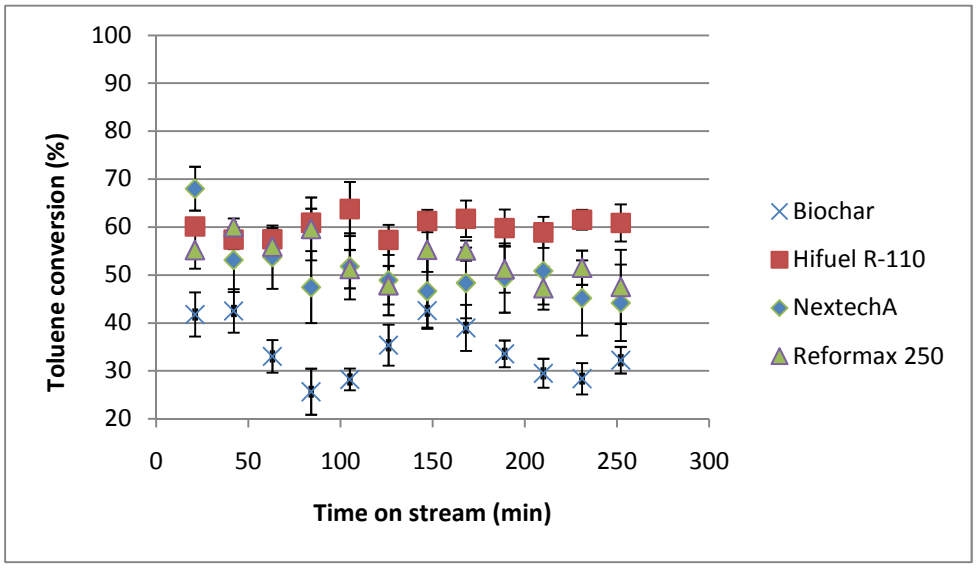

Figure 3.3 Toluene conversion vs. time on stream for commercial catalysts and biochar. Experimental conditions were T = 600 $^{\circ}$C, weight of catalyst = 0.15 g, weight of char= 0.3 g; steam to carbon ratio = 2. Error bars represent standard deviation, n = 3 for each point.

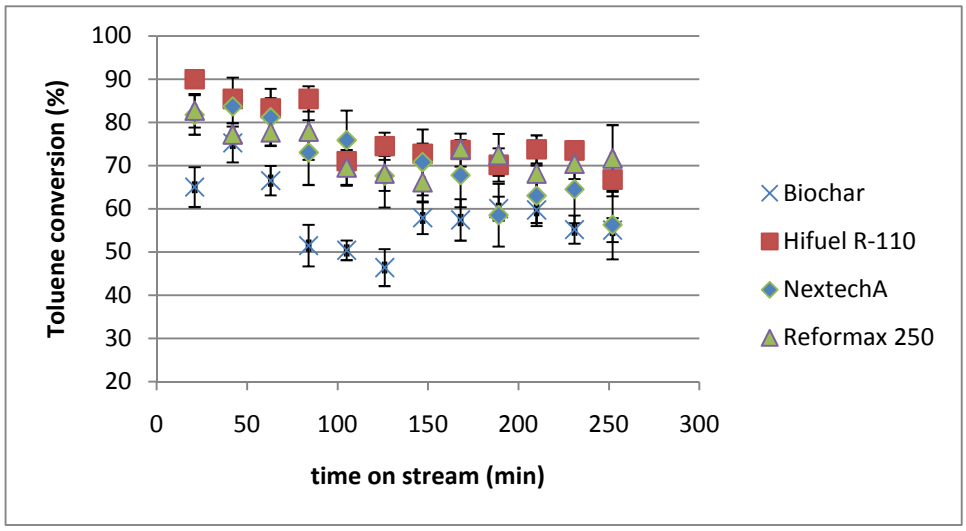

Figure 3.4 Toluene conversion vs. time on stream for commercial catalysts and biochar. Experimental conditions were T = 700 ˚C, weight of catalyst = 0.15 g, weight of char= 0.3 g, steam to carbon ratio = 2. Error bars represent standard deviation, n = 3 for each point.

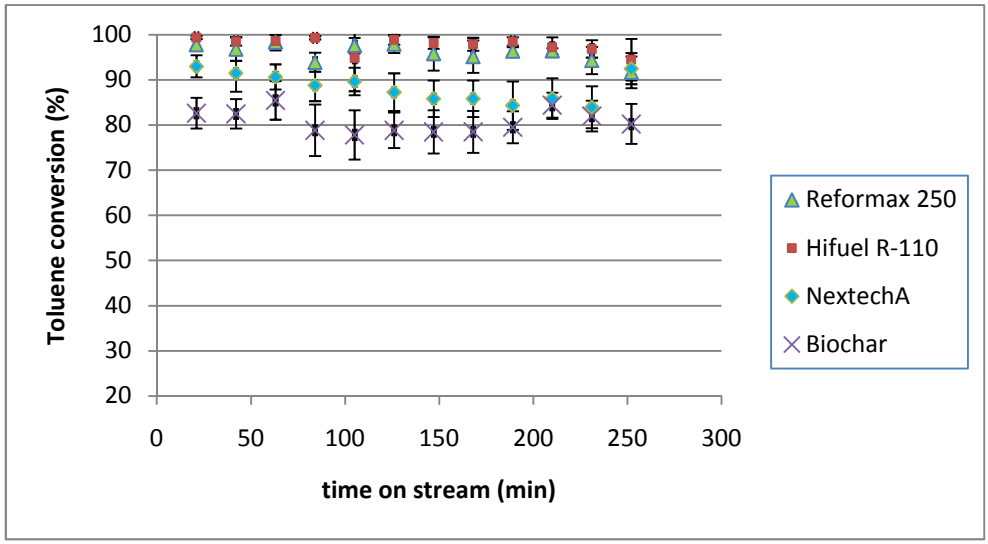

Figure 3.5 Toluene conversion vs. time on stream for commercial catalysts and biochar. Experimental conditions were T = 800 ˚C, weight of catalyst = 0.15 g, weight of char= 0.3 g, steam to carbon ratio = 2. Error bars represent standard deviation, n = 3 for each point.

An analysis of variance (ANOVA) was conducted to determine whether the toluene conversion was significantly different among the catalysts. For the analysis, the 12 measurements at time points 21-252 minutes were averaged for each catalyst. Table 3.8 shows the mean toluene conversion for each of the catalysts at each of the three temperatures tested. At a significance level of α=.05, it was determined that there was no significant difference between the three commercial catalysts, but the char was significantly different from the other three. Biochar showed potential for tar removal at the experimental conditions used, but even at twice the mass of the other catalysts, the char was not as efficient in converting toluene as the three commercial catalysts. Statistical analysis also showed a significant difference in conversion at each of the three temperatures tested for all four catalysts (α=.05).

Table 3.8 Mean toluene conversion and significant differences for tested catalysts. Experimental conditions were T = 600-800 $^{\circ}$C, weight of catalyst = 0.15 g, weight of biochar=0.3 g, steam to carbon ratio = 2. Mean value for n=3.

Catalyst	**Mean Toluene Conversion* (%) at T = 600 $^{\circ}$C**	**Mean Toluene Conversion* (%) at T = 700 $^{\circ}$C**	**Mean Toluene Conversion* (%) at T = 800 $^{\circ}$C**
Biochar	34.32[a]	58.37[a]	80.75[a]
NextechA	50.64[b]	70.32[b]	88.25[b]
Reformax 250	53.13[b]	72.99[b]	95.97[c]
Hifuel R-110	60.08[b]	76.67[b]	97.70[c]

*Means followed by the same letter within a column are not significantly different (α=0.05)

The Arrhenius dependency for all tested catalysts is presented in Figure 3.6. Using the Arrhenius equation, the values for the apparent activation energy (E_{app}) were calculated and are shown in Table 3.9. Residence time calculations and individual activation energy plots for each catalyst can be found in Appendix A-3.

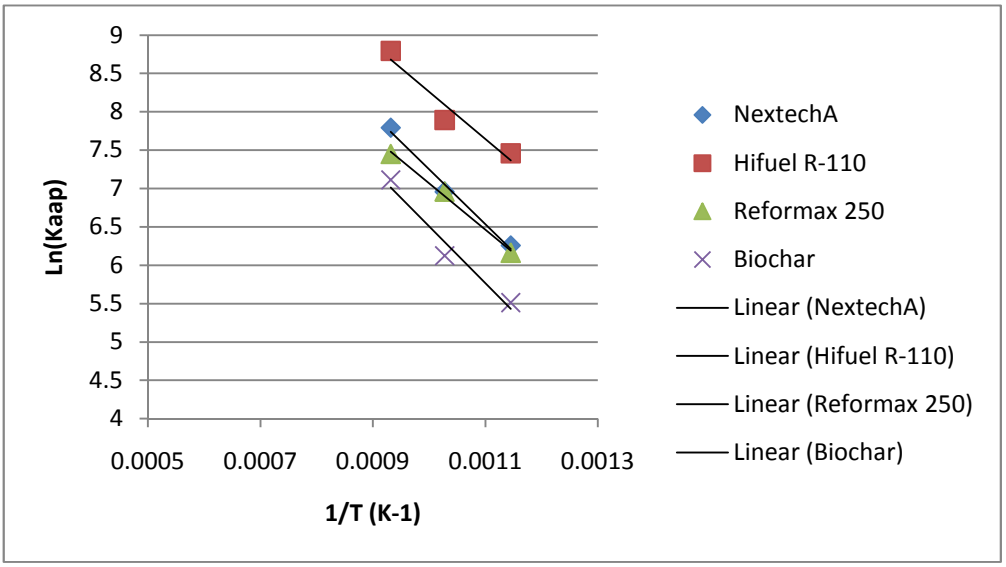

Figure 3.6 Arrhenius dependency for four catalysts tested.

Table 3.9 Activation energy results for commercial catalysts and biochar.

Catalyst	Apparent Activation Energy (kJ/mol)
Reformax 250 (Sud-Chemie)	50.60
Hifuel R-110 (Johnson Mathey)	51.18
NexTechA (Nextech Materials)	59.44
Biochar	61.59

These values are in agreement with previously reported activation energy values. Activation energy values of 61 kJ/mol have been reported for commercial biomass char (Abu et al., 2008) and in studies of biochar from pine bark, an activation energy value of 81.6 kJ/mol was reported (Ankita et al., 2010). Activation energy values of 50 kJ/mol have been reported for steam reforming catalysts (Corella et al., 1999). For the platinum catalyst, activation energies in the range of 66-75 kJ/mol have been reported for the water gas shift reaction (Swartz et al., 2003).

Since the activity of a catalyst increases when the apparent activation energy decreases, these results indicate that the nickel steam reforming catalysts are more active for this application.

3.3.2 Effect on Other Gas Components

The effect of catalysts on gasification products is very important. Catalysts not only reduce the tar content, but also affect the distribution of the other gas components in the system. This behavior can be explained by the reactions involved in toluene steam reforming. A summary of the potential reactions follows:

Steam reforming

$$C_7H_8 + 7H_2O \longrightarrow 7CO + 11H_2 \qquad \text{(Dermibas, 2002)} \qquad (3.12)$$

$$C_7H_8 + 14H_2O \longrightarrow 7CO_2 + 18H_2 \qquad \text{(Dermibas, 2002)} \qquad (3.13)$$

Methanation

$$CH_4 + H_2O \longleftrightarrow CO + 3H_2 \qquad \text{(Devi et al., 2005)} \qquad (3.14)$$

Dry reforming

$C_7H_8 + 7CO_2 \longrightarrow 14CO + 8H_2$ (Devi et al., 2005) (3.15)

Water gas shift reaction

$CO + H_2O \longleftrightarrow CO_2 + H_2$ (Simmel et al.,1997) (3.16)

Boudouard reaction

$C + CO_2 \longleftrightarrow 2CO$ (Simmel et al., 1997) (3.17)

Carbon formation

$C_nH_m \longrightarrow nC + (m/2)\ H_2$ (Simmel et al., 1997) (3.18)

Hydrogen

For all tested catalysts, hydrogen generation increased with temperature. Plots showing hydrogen concentration at 600, 700, and 800^oC for all catalysts are presented in Figures 3.7, 3.8, and 3.9. It can be seen that hydrogen generation is higher when Hifuel is used as the catalyst, followed by biochar. However, NextechA and Reformax also promote hydrogen generation. The generation of hydrogen in this process is a positive outcome since it increases the value of the syngas to be used for biofuel production.

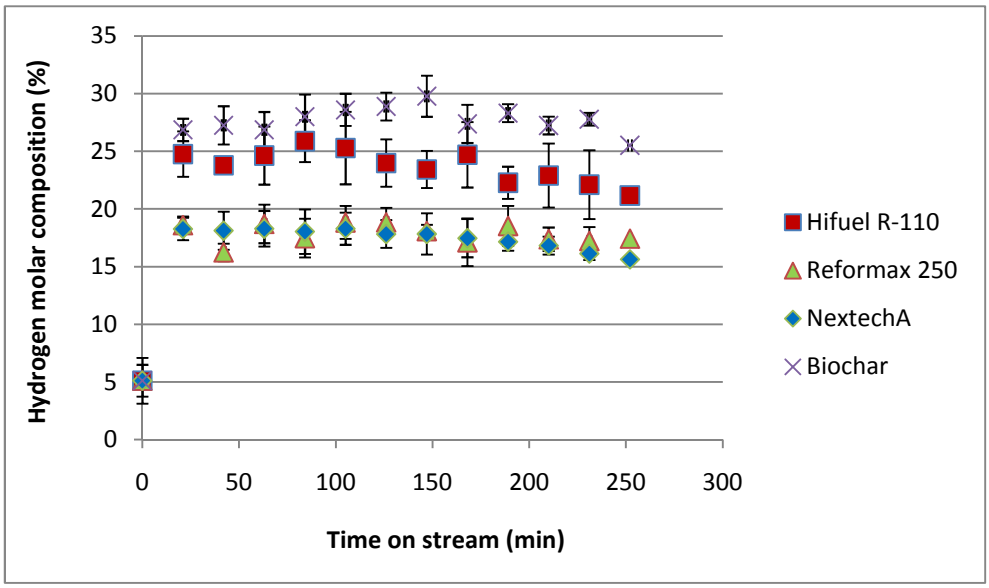

Figure 3.7 Mole percent of hydrogen for tested catalysts. Experimental conditions were T = 600 ˚C, weight of catalyst = 0.15 g, weight of char= 0.3 g, steam to carbon ratio = 2, n = 3 for each catalyst. Error bars show standard deviation.

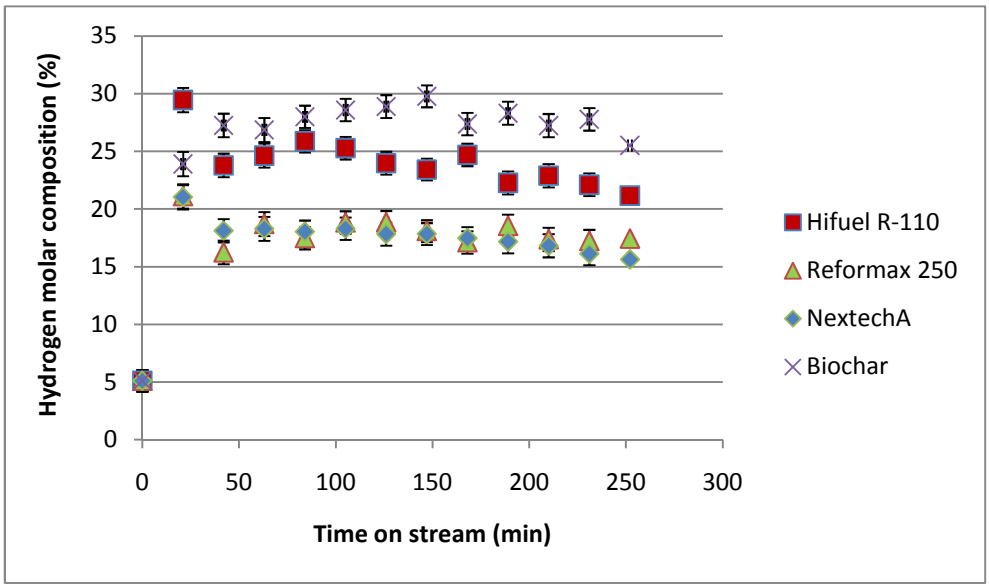

Figure 3.8 Mole percent of hydrogen for tested catalysts. Experimental conditions were T = 700 ˚C, weight of catalyst = 0.15 g, weight of char= 0.3 g, steam to carbon ratio = 2, n = 3 for each catalyst. Error bars show standard deviation.

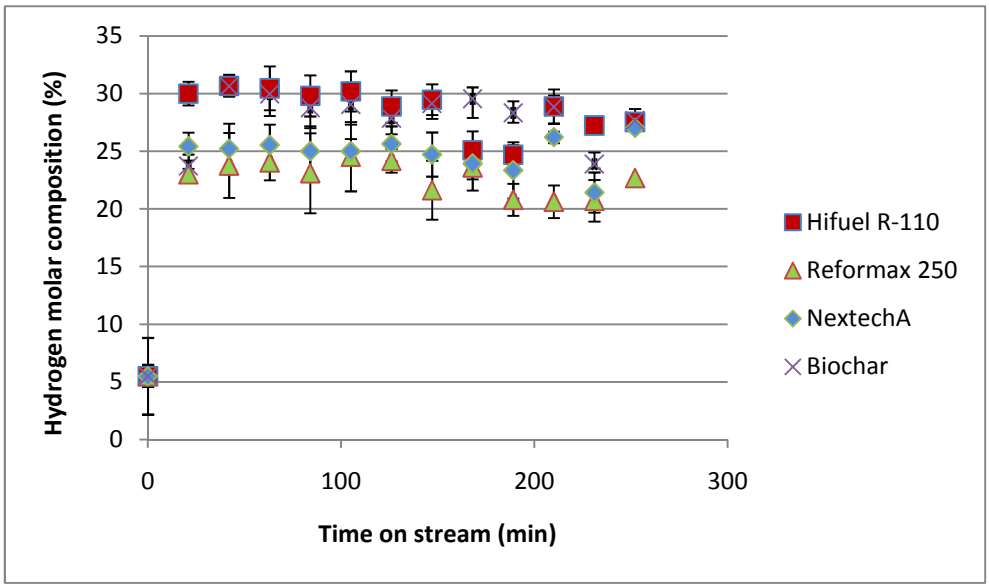

Figure 3.9 Mole percent of hydrogen for tested catalysts. Experimental conditions were T = 800 ˚C, weight of catalyst = 0.15 g, weight of char= 0.3 g, steam to carbon ratio = 2, n = 3 for each catalyst. Error bars show standard deviation.

An analysis of variance (ANOVA) was conducted to determine whether hydrogen generation was significantly different among the catalysts. Results are presented in Table 3.10. A comparison among catalysts indicates that there is not a significant difference among the catalysts at 800^{o}C, but at 700^{o}C Hifuel produces significantly more hydrdogen than the other catalysts, and at 600^{o}C, hydrogen production from Hifuel and biochar is significantly higher than the other two catalysts. A temperature comparison for each catalyst (also in Table 3.10) shows a few significant differences, but no common trend related to hydrogen production as a function of temperature.

Table 3.10 Mean hydrogen production and significant differences for tested catalysts. Experimental conditions were T = 600-800°C, weight of commercial catalyst = 0.15 g, weight of char= 0.3 g, steam to carbon ratio = 2. Mean value for n=3.

Catalyst	Mean Hydrogen Molar Composition (%) at T = 600 °C	Mean Hydrogen Molar Composition (%) at T = 700 °C	Mean Hydrogen Molar Composition (%) at T = 800 °C
Biochar	$25.99^{a,f}$	$22.07^{c,g}$	$26.38^{e,f}$
NextechA	$16.57^{b,n}$	$19.67^{c,i}$	$23.37^{e,j}$
Reformax 250	$16.92^{b,k}$	$17.15^{c,k}$	$21.39^{e,l}$
Hifuel R-110	$22.33^{a,m}$	$26.26^{d,n}$	$26.79^{e,n}$

*Means followed by the same letter within a column (catalyst comparison) or row (temperature comparison) are not significantly different (α=0.05)

Carbon Monoxide

Unlike hydrogen, the overall concentration of carbon monoxide dropped when comparing outlet to inlet. The concentration of carbon monoxide over the experiment length is presented in Figures 3.10 , 3.11, and 3.12 for the four catalysts tested at three different temperatures.

Analysis of variance (ANOVA) was conducted to determine whether carbon monoxide levels for each of the catalysts was significantly different and results are presented in Table 3.11. The use of biochar consistently resulted in the highest levels of carbon monoxide, and at 600°C, biochar was significantly higher than the other three catalysts. NextechA consistently resulted in lower levels of carbon monoxide than the other catalysts.

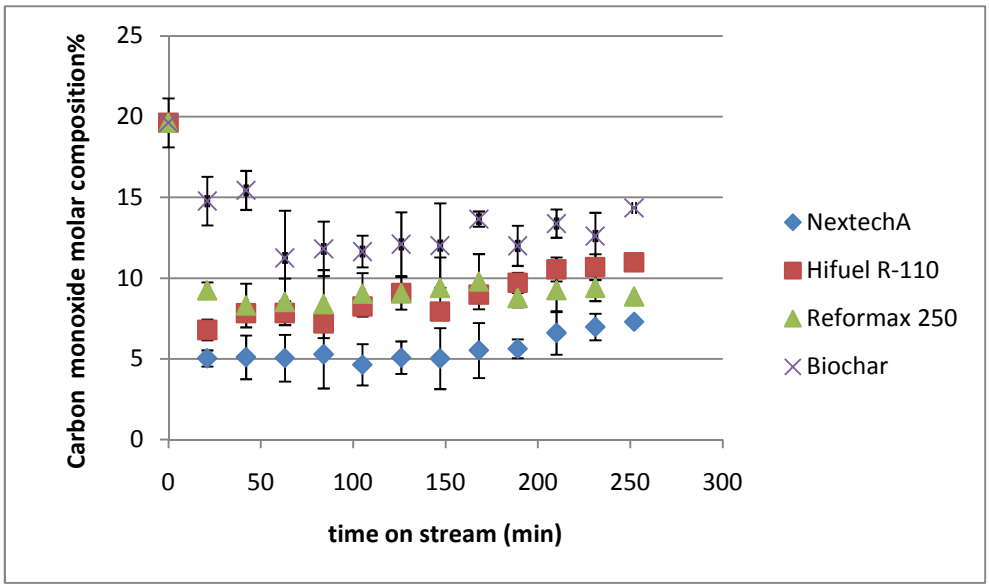

Figure 3.10 Mole percent of carbon monoxide for tested catalysts. Experimental conditions were T = 600 ◦C, weight of catalyst = 0.15g, weight of char= 0.3 g, steam to carbon ratio = 2, n = 3 for each catalyst. Error bars show standard deviation.

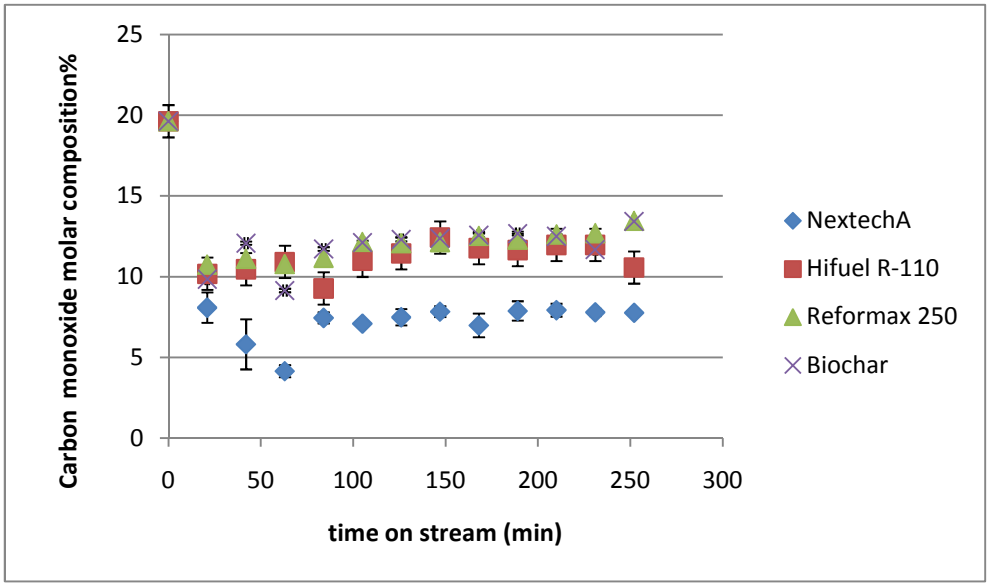

Figure 3.11 Mole percent of carbon monoxide for tested catalysts. Experimental conditions were T = 700 ◦C, weight of catalyst = 0.15g, weight of char= 0.3 g, steam to carbon ratio = 2, n = 3 for each catalyst. Error bars show standard deviation.

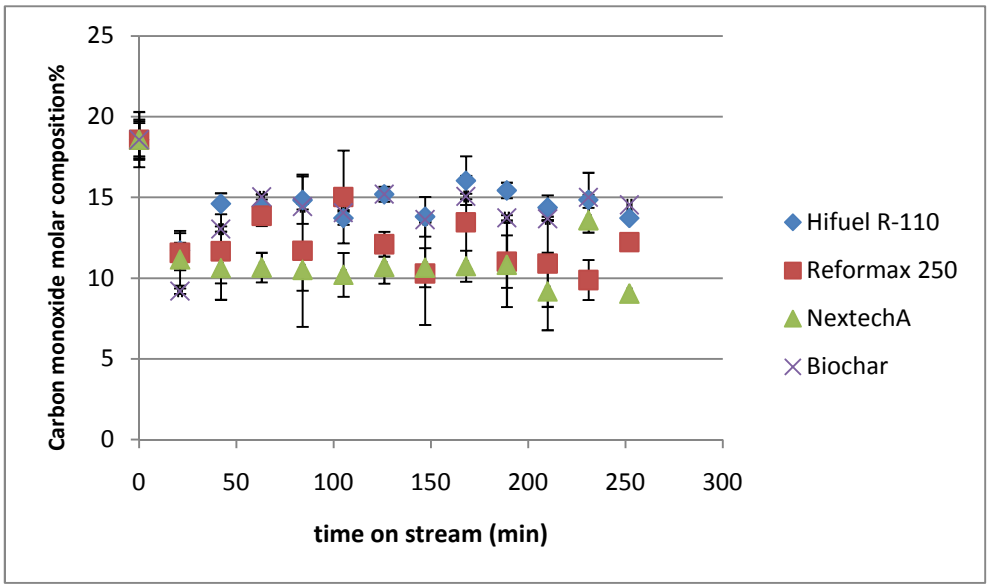

Figure 3.12 Mole percent of carbon monoxide for tested catalysts. Experimental conditions were T = 800 ◦C, weight of catalyst = 0.15g, weight of char= 0.3 g, steam to carbon ratio = 2, n = 3 for each catalyst. Error bars show standard deviation.

Table 3.11 Mean carbon monoxide production and significant differences for tested catalysts. Experimental conditions were T = 600-800˚C, weight of commercial catalyst = 0.15 g, weight of char= 0.3 g, steam to carbon ratio = 2. Mean value for n=3.

Catalyst	Mean Carbon Monoxide Molar Composition (%) at T = 600 ˚C	Mean Carbon Monoxide Molar Composition (%) at T = 700 ˚C	Mean Carbon Monoxide Molar Composition (%) at T = 800 ˚C
Biochar	$13.44^{a,g}$	$12.46^{c,g}$	$14.24^{e,f,h}$
NextechA	$6.68^{b,i}$	$8.14^{d,i}$	$11.27^{e,j}$
Reformax 250	$9.82^{b,k}$	$12.57^{c,l}$	$12.49^{e,f,l}$
Hifuel R-110	$9.65^{b,m}$	$11.79^{c,m}$	$14.71^{f,n}$

*Means followed by the same letter within a column (catalyst comparison) or row (temperature comparison) are not significantly different (α=0.05)

Other Compounds

Methane and carbon dioxide are also products of this experiment. Figures 3.13 to 3.15 and 3.16 to 3.18 show the mole percentages obtained for CH_4 and CO_2, respectively, for all catalysts tested at 600,700, and 800^{o}C. ANOVA results for mole percent of methane for catalysts tested are presented in Table 3.12. and the same results for carbon dioxide are shown in Table 3.13.

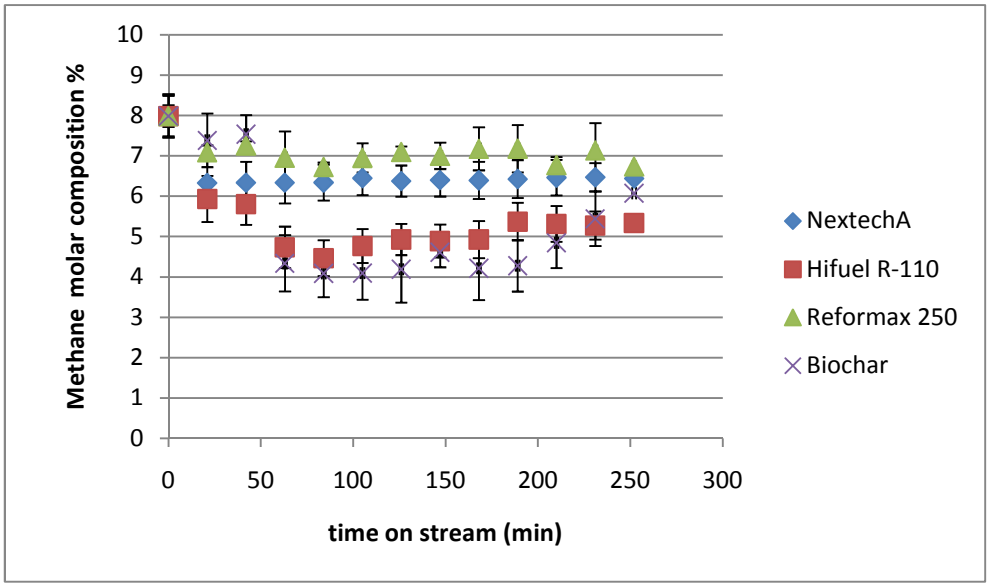

Figure 3.13 Mole percent of methane for tested catalysts. Experimental conditions were T = 600 ◦C, weight of catalyst = 0.15g, weight of char= 0.3 g, steam to carbon ratio = 2, n = 3 for each catalyst. Error bars show standard deviation.

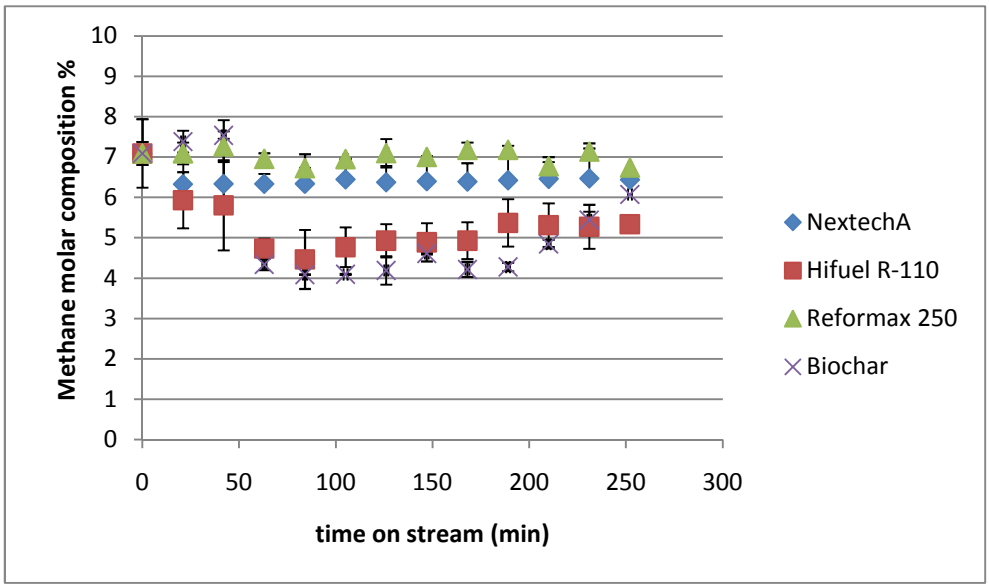

Figure 3.14 Mole percent of methane for tested catalysts. Experimental conditions were T = 700 ◦C, weight of catalyst = 0.15g, weight of char= 0.3 g, steam to carbon ratio = 2, n = 3 for each catalyst. Error bars show standard deviation.

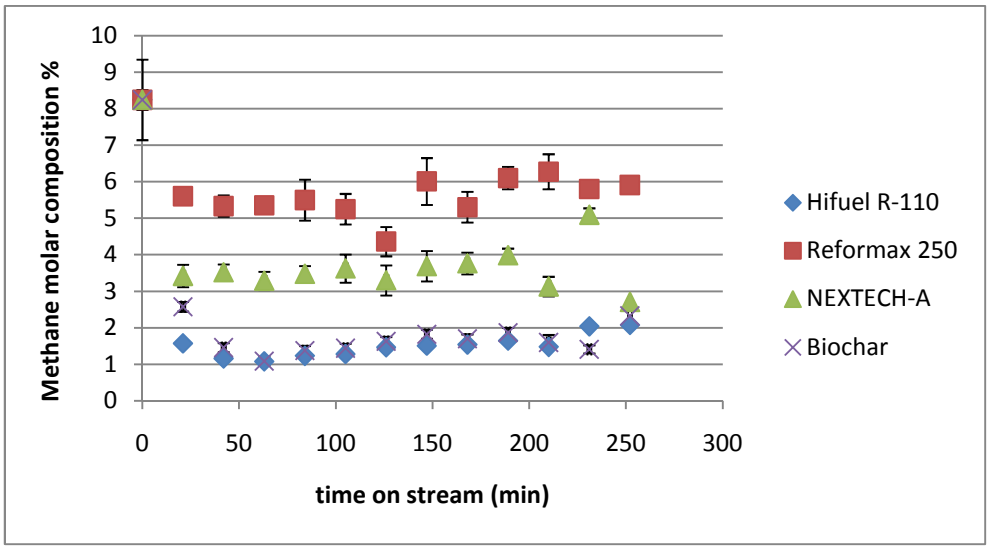

Figure 3.15 Mole percent of methane for tested catalysts. Experimental conditions were T = 800 ◦C, weight of catalyst = 0.15g, weight of char= 0.3 g, steam to carbon ratio = 2, n = 3 for each catalyst. Error bars show standard deviation.

Table 3.12 Mean methane production and significant differences for tested catalysts. Experimental conditions were T = 600-800°C, weight of commercial catalyst = 0.15 g, weight of char= 0.3 g, steam to carbon ratio = 2. Mean value for n=3

Catalyst	Mean Methane Molar Composition (%) at T = 600 °C	Mean Methane Molar Composition (%) at T = 700 °C	Mean Methane Molar Composition (%) at T = 800 °C
Biochar	5.31[a,e]	5.25[b,e]	2.03[c,f]
NextechA	6.52[a,g]	6.45[b,g]	2.19[c,h]
Reformax 250	7.08[a,i]	7.01[b,i]	3.94[c,j]
Hifuel R-110	5.36[a,k]	5.29[b,k]	5.77[d,k]

*Means followed by the same letter within a column (catalyst comparison) or row (temperature comparison) are not significantly different (α=0.05)

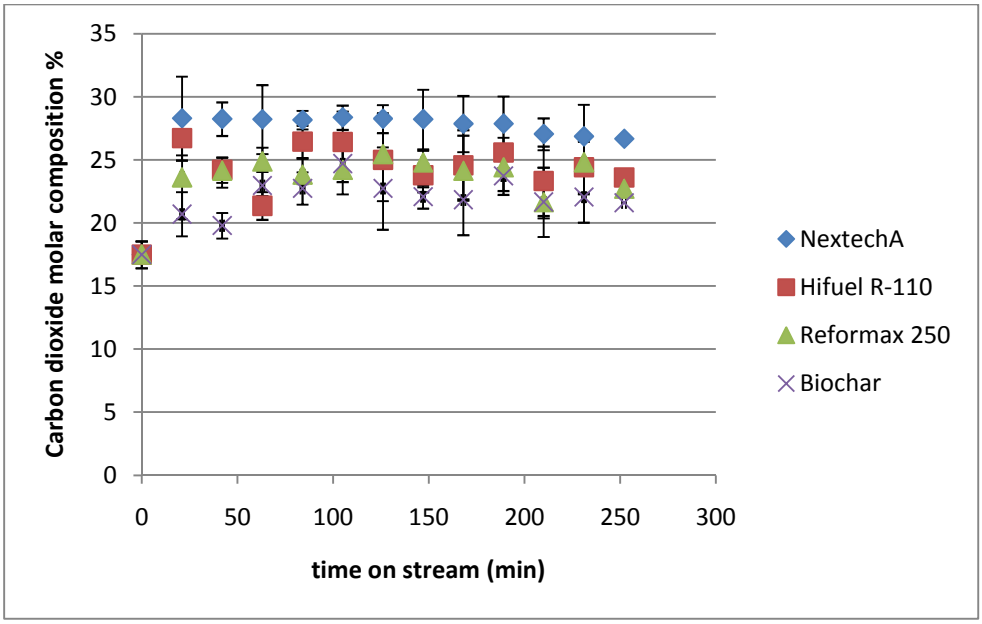

Figure 3.16 Mole percent of carbon dioxide for tested catalysts. Experimental conditions were T = 600 °C, weight of catalyst = 0.15g, weight of char= 0.3 g, steam to carbon ratio = 2, n = 3 for each catalyst. Error bars show standard deviation.

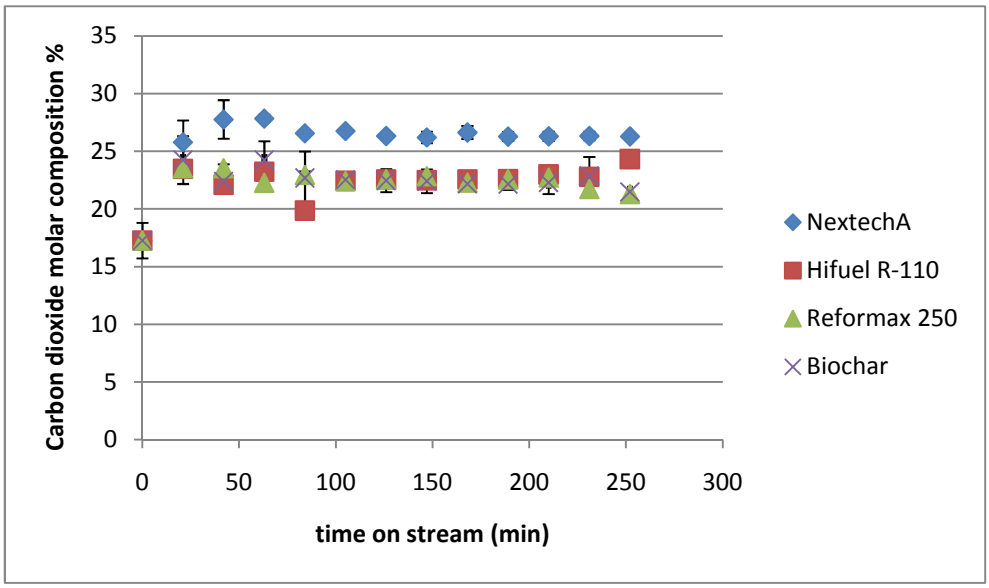

Figure 3.17 Mole percent of carbon dioxide for tested catalysts. Experimental conditions were T = 700 ˚C, weight of catalyst = 0.15g, weight of char= 0.3 g, steam to carbon ratio = 2, n = 3 for each catalyst. Error bars show standard deviation.

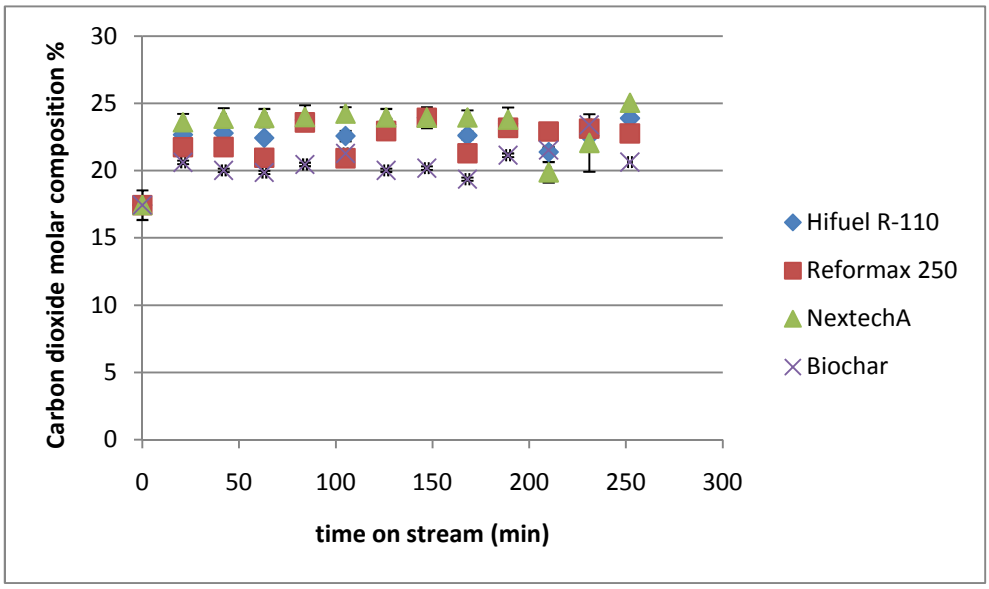

Figure 3.18 Mole percent of carbon dioxide for tested catalysts. Experimental conditions were T = 800 ˚C, weight of catalyst = 0.15g, weight of char= 0.3 g, steam to carbon ratio = 2, n = 3 for each catalyst. Error bars show standard deviation.

Table 3.13 Mean carbon dioxide production and significant differences for tested catalysts. Experimental conditions were T = 600-800°C, weight of commercial catalyst = 0.15 g, weight of char= 0.3 g, steam to carbon ratio = 2. Mean value for n=3

Catalyst	Mean Carbon Dioxide Molar Composition (%) at T = 600 °C	Mean Carbon Dioxide Molar Composition (%) at T = 700 °C	Mean Carbon Dioxide Molar Composition (%) at T = 800 °C
Biochar	22.22[a,e]	22.25[c,e]	20.46[d,e]
NextechA	27.83[b,f]	25.87[c,g]	23.044[d,g]
Reformax 250	24.05[a,h]	22.15[c,i]	22.04[d,i]
Hifuel R-110	24.61[a,j]	22.20[c,k]	22.54[d,k]

*Means followed by the same letter within a column (catalyst comparison) or row (temperature comparison) are not significantly different (α=0.05)

As can be seen from Tables 3.12 and 3.13, there were only two significant differences in the amounts of methane and carbon dioxide obtained at each of the three temperatures with the four different catalysts. NextechA produced significantly higher levels of CO_2 at 600°C, and Hifuel produced significantly higher levels of methane at 800°C.

It is of interest to look at all gases produced during the course of an experiment. Figure 3.19 shows the mole percentage distribution over the length of the experiment for methane and carbon dioxide along with hydrogen and carbon monoxide when Hifuel was used as a catalyst at 800°C. Hifuel R-110 promoted the highest generation of hydrogen and carbon monoxide in the outlet gas at 800°C. All of the catalysts generate a great amount of carbon dioxide and methane. However, the minimum amount of methane is generated when using Hifuel R-110 as a catalyst.

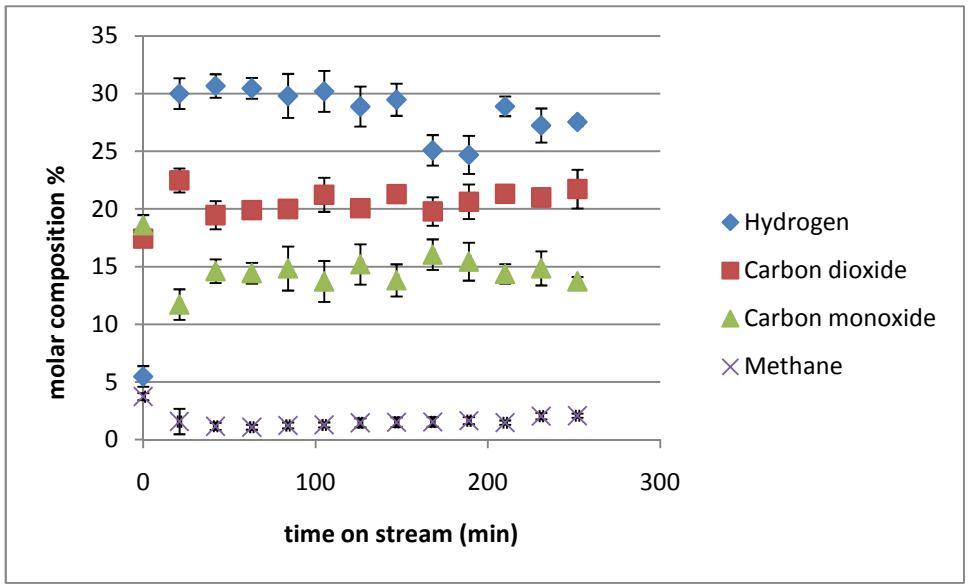

Figure 3.19 Mole percent of CO, CO_2, H_2, CH_4 for Hifuel R-110. Experimental conditions were T =800°C, weight of catalyst = 0.15 g, steam to carbon ratio = 2, n = 3. Error bars show standard deviation.

Mass Balance Verification

A mass balance verification was conducted. An example of mass balance results for an experiment using NextechA is presented in Figure 3.20. The figure shows total grams entering and exiting for each of seven different compounds measured. See Appendix A-2 for details regarding the mass balance calculations.

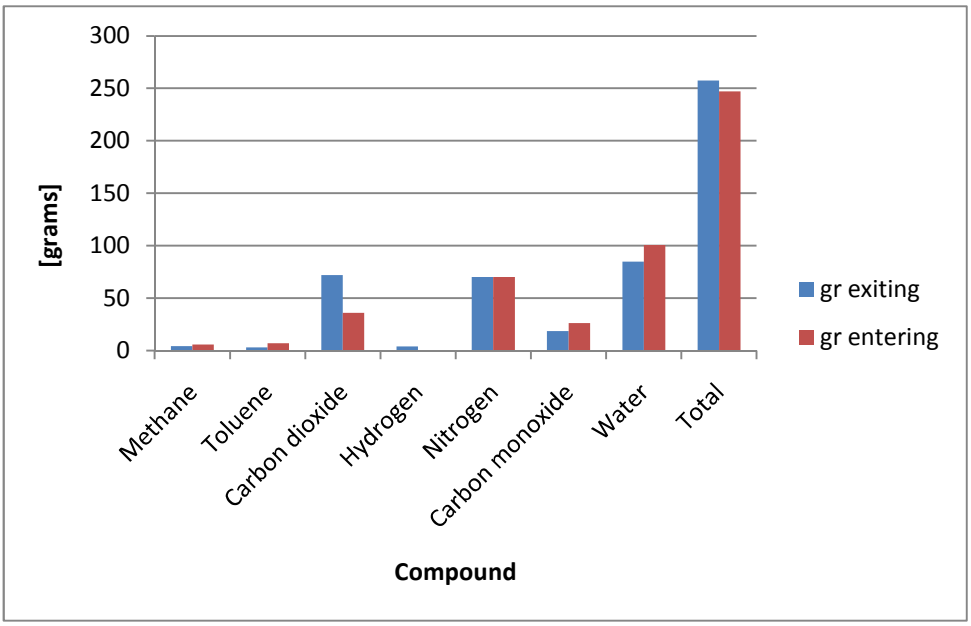

Figure 3.20 Mass balance for an experiment using NextechA showing grams entering and grams exiting for 7 compounds. Experimental conditions were T =800 °C, weight of catalyst = 0.15 g, steam to carbon ratio = 2.

3.3.3 Testing Catalysts in Series

Figure 3.21 shows the performance of biochar and NextechA tested in series using the three options discussed in section 3.2.9 at 700°C. In option A the two catalysts are separated by an air space, in option B the two catalyst beds are in direct contact, and in option C the two catalysts are homogeneously mixed.

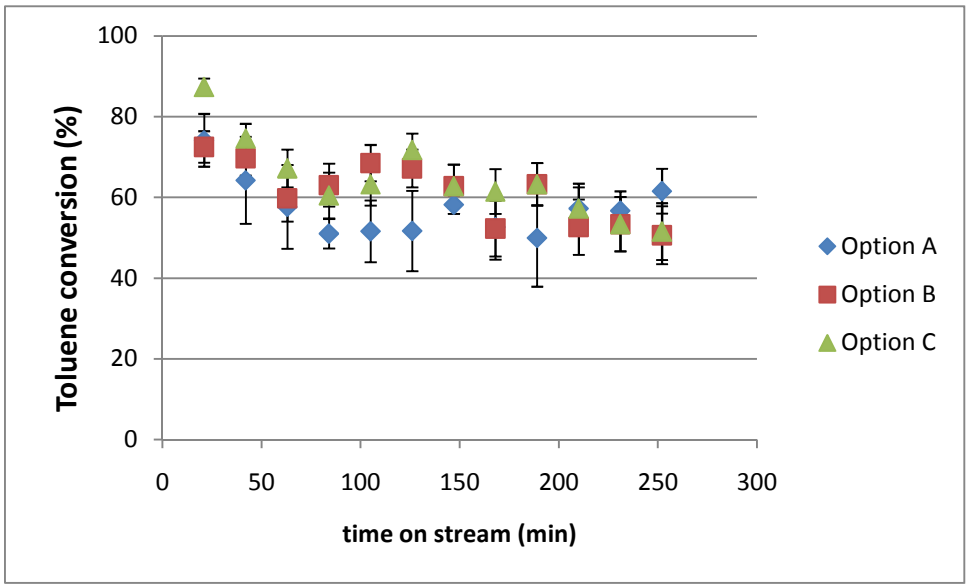

Figure 3.21 Conversion of toluene vs. time on stream for testing of catalysts in series. Experimental conditions were T = 700 ◦C, weight of catalyst = 0.15 g , weight of char = 0.30 g, steam to carbon ratio = 2. Error bars represent standard deviation, n = 3 for each point.

From this figure it can be seen that the testing of the two materials at 700^{o}C in three different arrangements have similar performance. ANOVA was conducted to determine if the conversion of toluene obtained from different arrangements of catalysts tested in series was statistically different. As shown in Table 3.14, they were not found to be significantly different (α=.05), but there does appear to be a trend that increasing contact between the two catalysts increases the toluene conversion.

Table 3.14 Observed significant differences in toluene conversion percent for catalysts in series. Experimental conditions were T = 700°C, weight of catalyst = 0.15 g , weight of char = 0.30 g, steam to carbon ratio = 2, n=3.

Catalyst	Toluene Mean Conversion* (%)
Two catalyst beds separated (Option A)	57.22[a]
Two catalyst beds in contact (Option B)	61.31[a]
Catalysts mixed (Option C)	64.53[a]

*Means followed by the same letter are not statistically different (α=0.05)

3.3.4 Catalyst Characterization

Samples of the catalysts were examined using a variety of characterization techniques, including TPR, BET, XPS, TGA, SEM, and FTIR.

TPR

Temperature Programmed Reduction (TPR) was conducted on fresh samples of the nickel catalysts after size reduction treatment in order to verify that the reduction temperature for these materials was the same as that recommended by manufacturers. TPR plots for Reformax 250 and Hifuel R-110 can be found in Appendix A-4. The reduction peaks for Reformax and Hifuel R-110 can be observed at 650°C and 670°C, respectively. These results are in agreement with the reduction temperature recommended by each respective manufacturer.

BET

The specific surface area of the fresh and used catalysts was determined by nitrogen adsorption using the BET method on a Quantasorb instrument (Quantachrome, USA). Results of BET analysis of catalyst samples are presented in Table 3.15. Biochar surface area is notably larger than the commercial catalysts. For all four catalysts there is a drastic reduction of surface area after use regardless of fresh catalyst surface area. It is typical that catalysts undergo a decrease in BET surface area after reaction, probably due to carbon deposition on the catalyst surface (Djaidja et al., 2006).

Table 3.15 BET results for fresh and used catalysts (tested at 800 ^{o}C).

Catalyst	**Fresh Catalyst Surface Area (m^2/g)**	**Used Catalyst (at 800^{o}C) Surface Area (m^2/g)**
Reformax 250	22.39	2.24
Hifuel R110	21.28	2.33
NextechA	66.67	5.47
Biochar	221.7	10.27
Catalyst Mix (NextechA and Biochar)	159.0	9.26*

*catalyst mix was tested at 700^{o}C

XPS

X-ray Photoelectron Spectroscopy (XPS) was conducted on fresh and used commercial catalyst samples. Figure 3.22 shows the XPS spectra for fresh and used Reformax 250. The spectrum shows the intensity of the photoelectrons versus the binding energy of the electrons (Konya et al., 2004). From Figure 3.22 it can be seen that the carbon peak is higher for the used sample. Figure 3.23 shows an expanded view of the carbon region of the XPS spectrum for this catalyst. Table 3.16 shows the binding energy obtained for each used catalyst, which is an indication of the type of coke deposited on the used catalysts. In Figure 3.23b it can be seen that the carbon peak corresponds to 284 ev of binding energy, which corresponds to a graphitic carbon. Similar results were found for all three commercial catalysts.

Table 3.16 Type of coke deposited on used catalysts based on XPS spectra.

Used Catalyst	Binding energy (ev)	Type of coke deposited
Reformax 250	284	Graphitic
Hifuel R110	284	Graphitic
NextechA	285	Graphitic

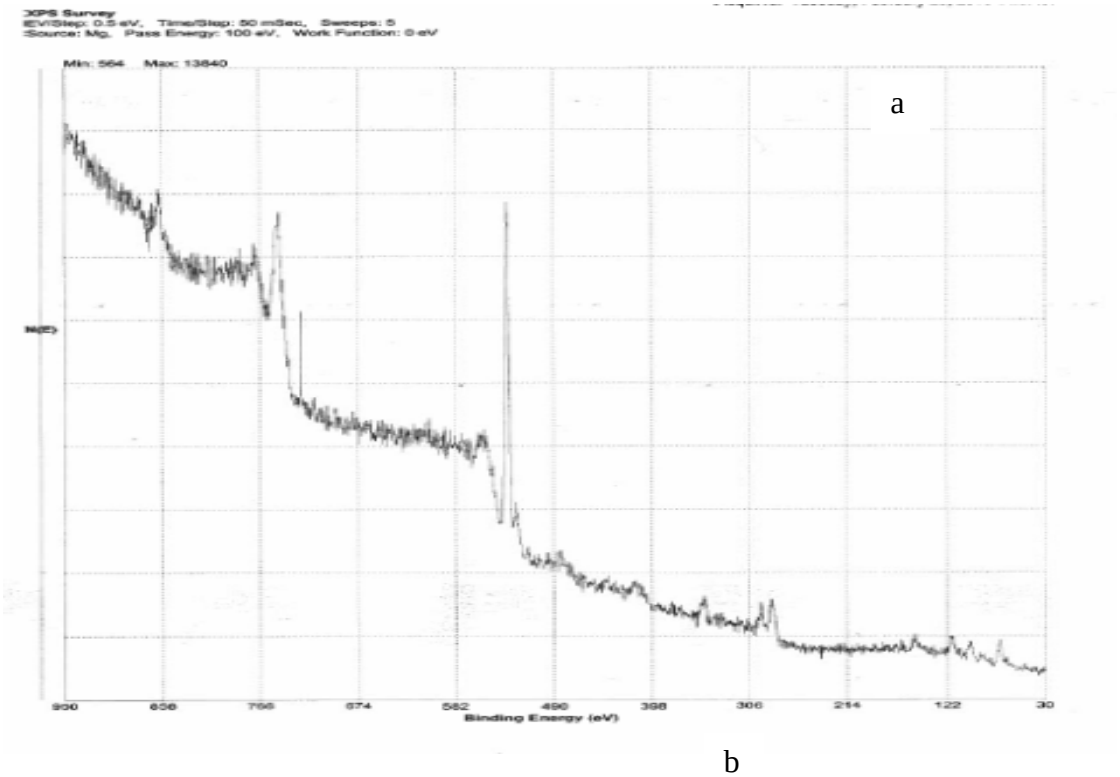

b

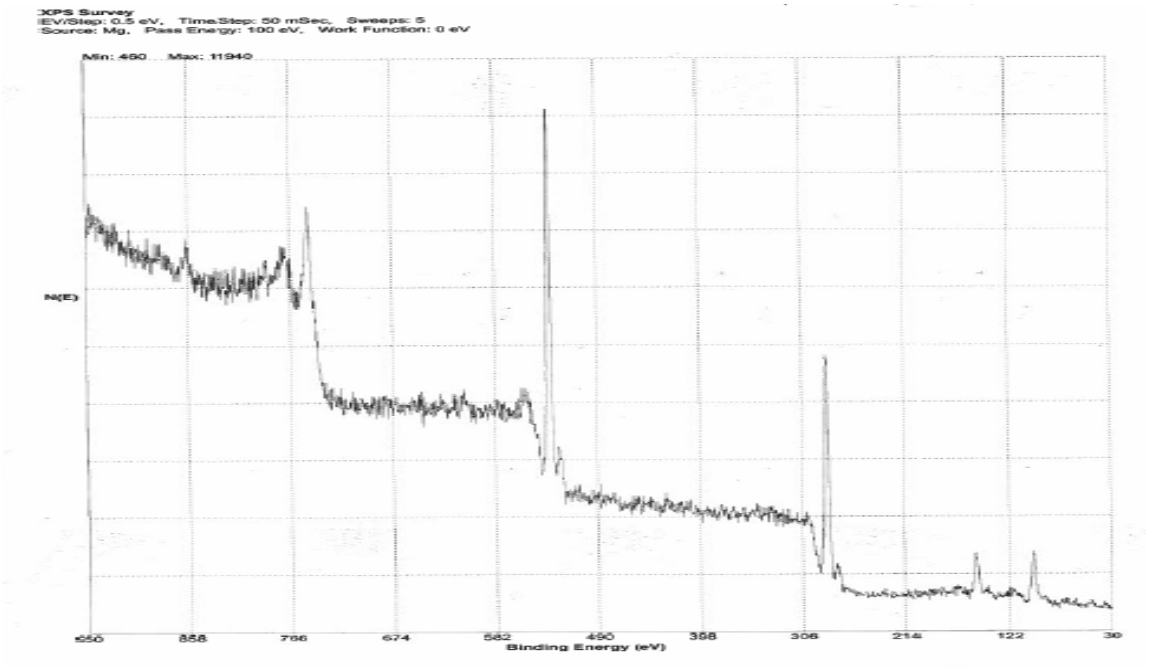

Figure 3.22 XPS spectra for a) fresh and b) used Reformax 250 catalyst tested at 700^{o}C.

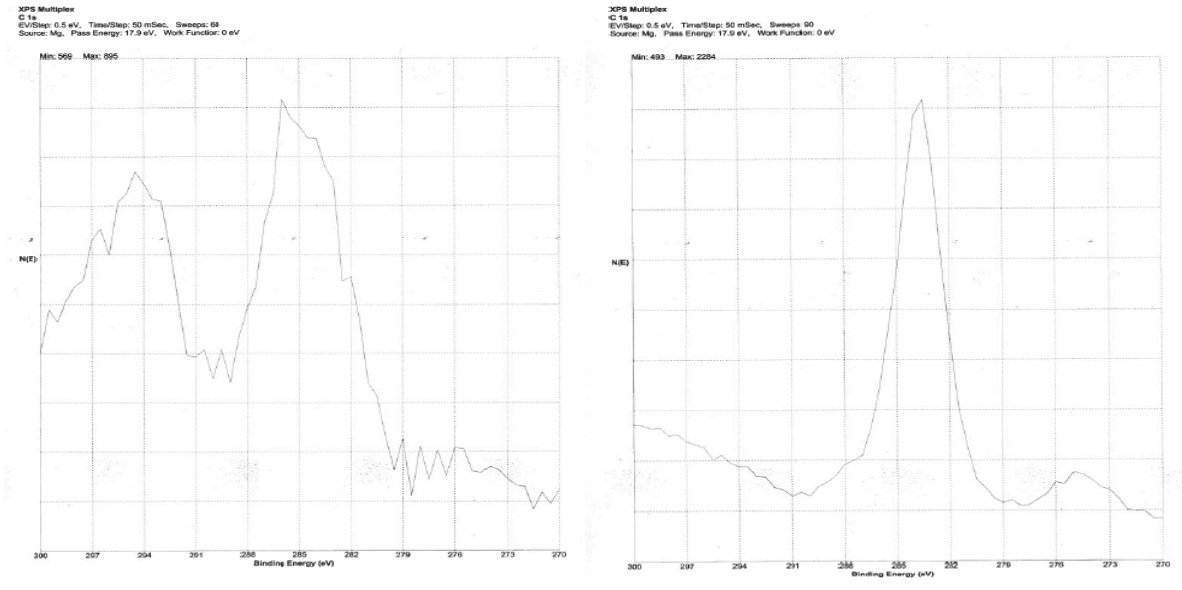

a) b)

Figure 3.23 XPS spectra of carbon region for a) fresh and b) used Reformax 250 catalyst tested at 700^{o}C.

TGA

Thermogravimetric analysis (TGA) measures the variation in weight of the catalyst sample as a function of temperature. Figure 3.24 shows TGA curves for the four used catalysts at 800^{o}C and Figure 3.25 presents a comparison of TGA curves for fresh char, used char at 700^{o}C and used catalyst mix (char and NextechA catalyst) at 700^{o}C. It is clear that overall, char is the catalyst that lost the most weight during thermogravimetric analysis, indicating that it would have the highest tendency toward coke formation. When we compare fresh char with used char it is evident that fresh char lost more weight than used char probably because there is more volatile compounds present in the fresh char sample. Of the commercial catalysts, Hifuel R110 lost more weight during testing than

the other two catalysts, and NextechA and Reformax lost very little weight, indicating very little coke formation.

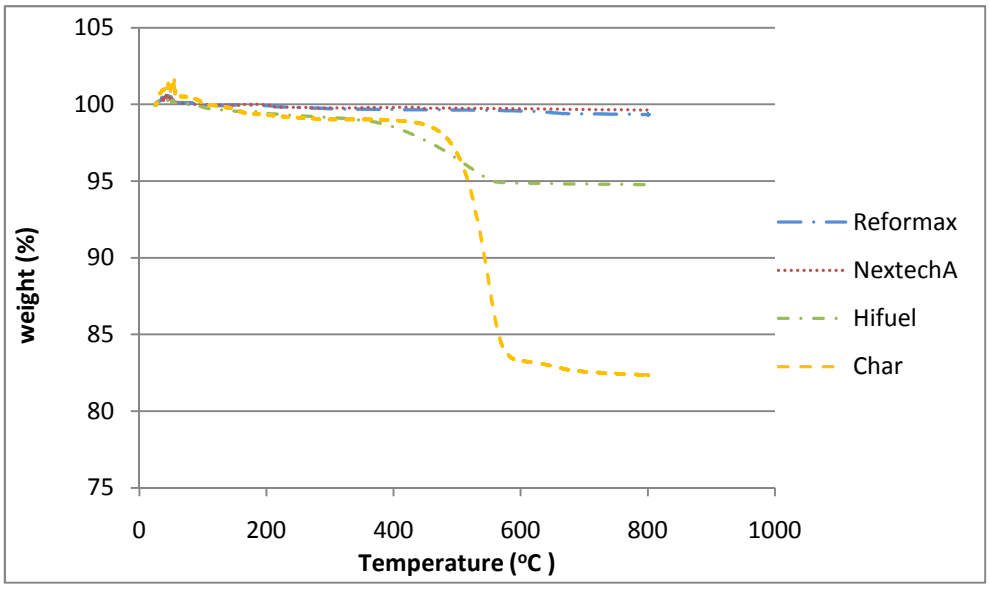

Figure 3.24 TGA curves for used catalysts at 800°C.

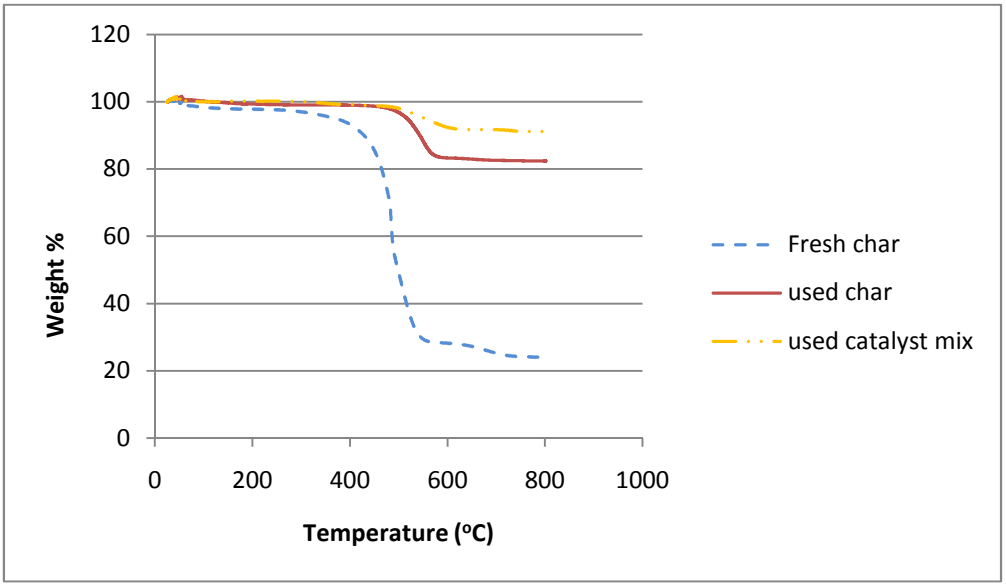

Figure 3.25 TGA curves for fresh char, used char and used catalyst mixture (char + NextechA) at 700°C.

SEM

A series of scanning electron microscopy (SEM) image analyses were performed on fresh and used catalyst samples after the steam reforming experiments. Figure 3.26a shows a SEM picture of fresh Reformax and Figure 3.26b shows a picture of used Reformax. In Figure 3.26b coke deposits (cake like) can be observed on the catalyst surface (Zhang et al., 2004). In addition, on the surface of the fresh catalyst (Figure 3.26a) particle agglomerations can be seen, which is an indication of high surface area. The surface of the used catalyst (Figure 3.26 b) has a smooth appearance, which is an indication of low surface area. These results are in agreement with the BET results reported earlier.

Figure 3.26c is a picture of the same used catalyst at different magnification where pyrolitic carbon can be observed along with coke deposits on the catalyst surface. It is known that graphitic carbon can be present in the form of pyrolitic carbon or nanotubes. This finding supports the results of the XPS spectra, showing graphitic carbon.

Images of the platinum catalyst (NextechA) are shown in Figure 3.27. Part a is fresh catalyst, and part b is used catalyst at 800^{o}C. The SEM image in Figure 3.27b looks brighter and this could be an indication of a graphite deposit because graphite is conductive to the electron beam possibly causing bright areas (Lei et al., 2001).

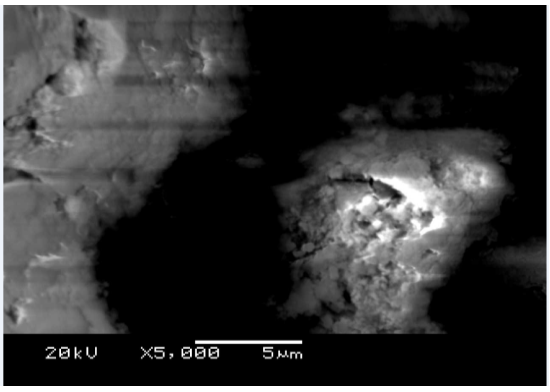

a

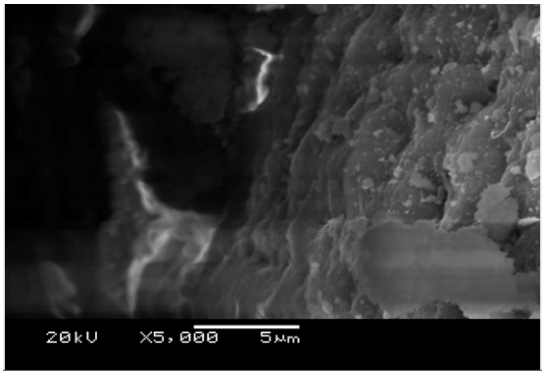

b

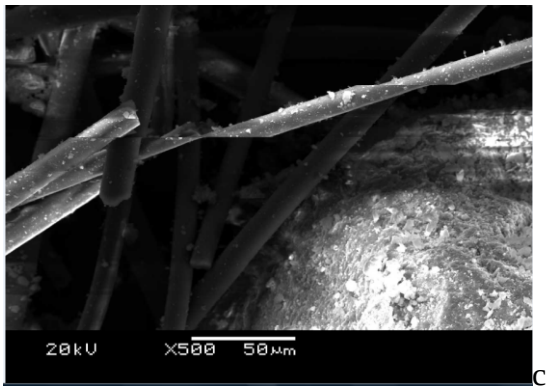

c

Figure 3.26 SEM images for Reformax 250 catalyst at 800^{o}C. Part a is fresh catalyst, part b is used catalyst and part c is used catalyst at lower magnification.

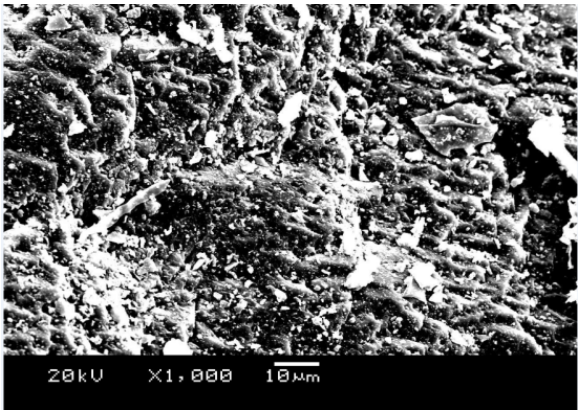

a

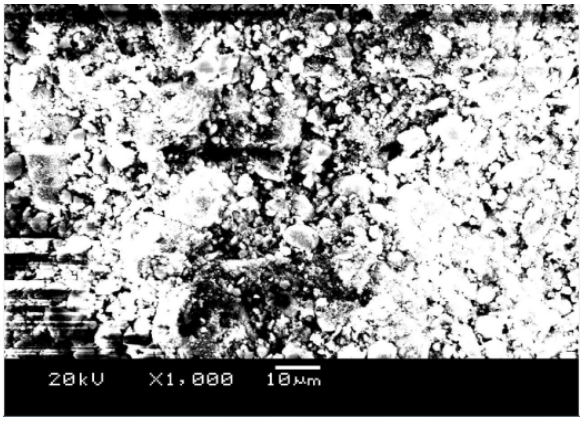

b

Figure 3.27 SEM images for a) fresh and b) used NextechA catalyst at 800^{o}C.

In addition, comparing Figures 3.27 a and b, it is observed that their surface characteristics are different. The surface of the fresh catalyst (part a) seems to contain high crystallinity with plate sheet layers that have some pore structure; these characteristics are indicators of high surface area. On the contrary, Figure 3.27 b shows a collapsed structure with no crystallinity, which is equivalent to low surface area. These results are in agreement with the BET results reported in Table 3.15.

Figure 3.28 shows SEM images of fresh biochar (a and c) and used biochar (b and d). The char, after reaction, may have lost part of the carbon. In the fresh samples, the bright

areas are possibly associated with carbon deposits present on the char sample before use, while in the used char some graphitic carbon zones can be presumed. Cake like zones suggesting coke deposits on the catalyst surface after reaction are not observed in the SEM images for biochar.

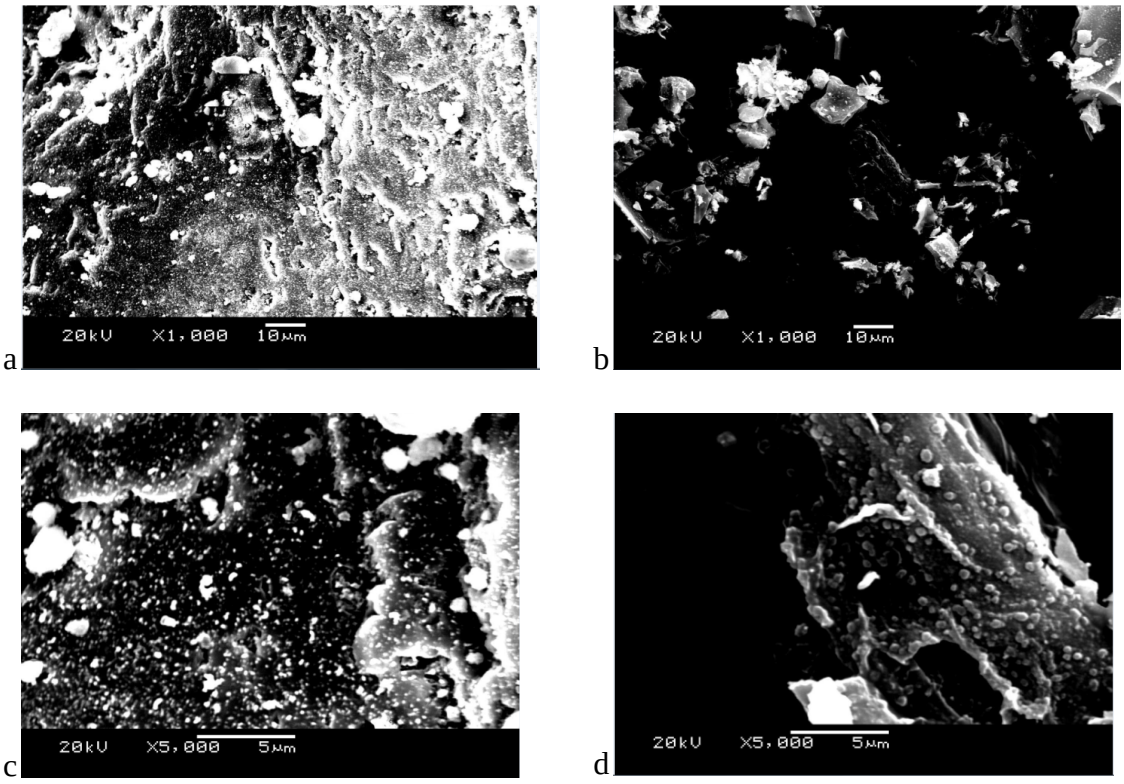

Figure 3.28. SEM images for fresh char (a and c); and used char (b and d).

Figure 3.29 shows SEM images for the mixed catalyst sample containing char and NextechA. Part a is the fresh mixture and part b is the used catalyst mix. The used sample appears to have a smoother surface in addition to oval structures that represent particle agglomeration, which is common in used catalysts.

Overall, SEM images verified the presence of graphitic carbon on the surfaces of used catalysts along with coke deposits on commercial catalysts. SEM images showed

differences between fresh and used catalysts which suggest lower surface area in used catalysts; this is consistent with BET results.

a 

b 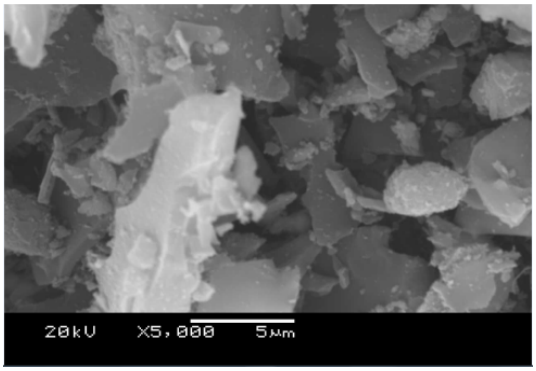

Figure 3.29 SEM images for a) fresh and b) used catalyst mixture (char and NextechA).

FTIR

This method is used to find out the functional groups present in the four tested catalysts (fresh and used samples). This especially useful to characterize the char used in this research which is generated from swithchgrass gasification. The functional groups identified from the FTIR spectrum of the catalyst samples are reported in Table 3.17. It can be seen that the used catalysts have similar functional groups which correspond to carbon deposited on each catalyst surface. Figure 3.30 shows the interferogram for fresh char. Interferograms for the remaining catalysts can be found in Appendix A-4.

Table 3.17 Functional groups present on catalyst samples determined by FTIR.

Commercial Catalyst	Wave numbers (cm-1)	Functional Groups	Reference
Hifuel R-110	1577 1112	Aromatic C=C ring stretching Aromatic CO stretching	(Pieck et al., 1992) Ozcimenet al., 2010)
Nextech-A	1112 1577	Aromatic CO stretching Aromatic C=C ring stretching	Ozcimen et al., 2010) (Pieck et al., 1992)
Reformax 250	1590 897	Aromatic C=C ring stretching Aromatic ring	(Ozcimen et al., 2010) Ozcimen et al., 2005)
Fresh biochar	1577 1160 1373 3342	Aromatic C=C stretching Aromatic CO stretching Aliphatic CH3 deformation -OH stretching	(Pieck et al., 1992) (Ozcimen et al., 2010) (Ozcimen et al., 2010) Ozcimen et al., 2010)

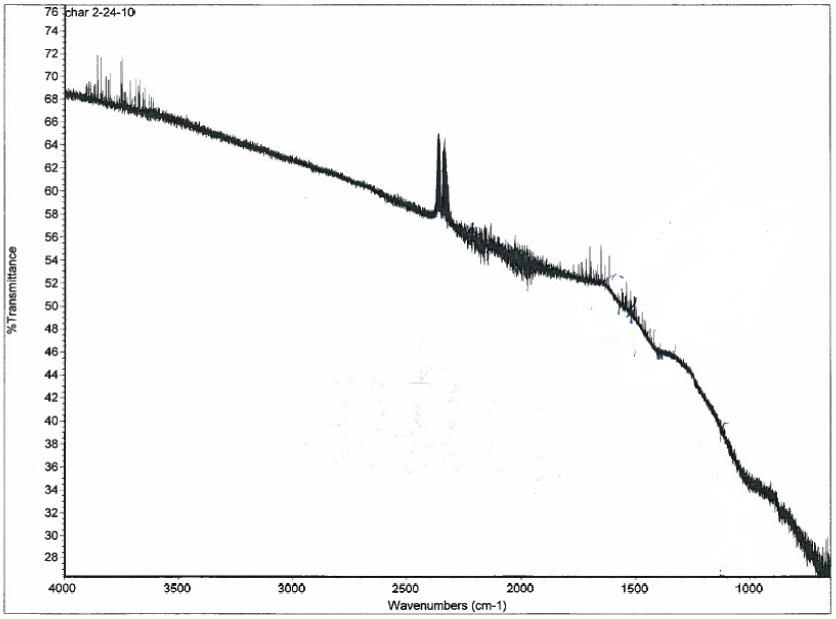

Figure 3.30 Interferogram for fresh char

3.3 Conclusions

Major conclusions from this work are summarized below.

Commercial Catalyst Comparison

The three tested commercial catalysts have similar activity for tar removal. Nickel based catalysts generally performed better for toluene conversion than the platinum based catalyst.

Biochar as a Catalyst

Char as a catalyst was observed to be suitable for toluene destruction although its activity was lower than the commercial catalysts. When twice the mass of catalyst was used for char at 800^{o}C, char conversion of toluene was 84% that of Reformax 250. Char has a significant cost advantage over the other catalysts. Even though it may not be as efficient

as Reformax or Hifuel, it is a low cost option to reduce the presence of tar in the synthesis gas.

Activation Energies

The activation energies of toluene steam reforming over these catalytic materials were found to be 50.26 kJ/mol for Reformax 250; 51.18 kJ/mol for Hifuel R-110; 59.44 kJ/mol for NextechA and 61.59 kJ/mol for biochar. These values are in agreement with values reported in the literature for similar commercial catalysts and char.

Catalyst Property Changes

According to the XPS spectra, graphitic carbon was found on all catalysts. This was verified by SEM results. Reformax and NextechA have a medium tendency to coke formation while Hifuel has the highest tendency to coke formation based on thermogravimetric analysis (TGA).

Overall Conclusions

Based on high toluene conversion, low coke deposition, and ease of regeneration Reformax 250 is the recommended commercial catalyst for this application.

CHAPTER IV

USE OF THE EXTENT OF REACTION COORDINATE METHOD DURING CATALYTIC STEAM REFORMING OF TOLUENE

Abstract

During steam reforming of toluene, an array of different reactions may be occurring. The goal of this work was to model the reaction network in an attempt to determine which reactions tend to dominate during the steam reforming process. Four different catalyst materials were tested during steam reforming of toluene, including one platinum based (NextechA) and two nickel based (Reformax 250 and Hifuel R-110) commercial catalysts and biochar generated during gasification of switchgrass. The resulting product distributions were then used with a molar extent of reaction model to determine the relative importance of different reactions in the reaction network.

For the commercial catalysts, the extent of reaction model worked well for determining the distribution of products, but for the biochar the extent of reaction values were often erratic. Reformax 250 and Hifuel R-110 showed the larger extents of reaction for steam reforming, and the extent of reaction for steam reforming increased with temperature. The methanation reaction was highly sensitive to temperature, and extent of reaction values were positive at 600 ^{o}C and negative at 700 and 800 ^{o}C. Extent of reaction values for the carbon formation reactions were very small and were independent of temperature.

4.1 Introduction

Biomass gasification can be used to convert a renewable biomass into synthesis gas, which can then be used for biofuel production, production of chemicals, fuel cell applications and power generation. However, the destruction or conversion of tars produced during gasification is a crucial technological barrier for the development and further commercialization of biomass gasification. It is known that the decomposition of tar compounds using catalysts is a suitable solution to this problem.

An attractive hot gas conditioning method for tar destruction is catalytic steam reforming. This technique offers several advantages: catalyst reactor temperatures can be thermally integrated with the gasifier exit temperature, the composition of the product gas can be catalytically adjusted, and steam can be added to the catalytic reactor to ensure complete reforming of tars (Devi et al., 2002). During steam reforming, a number of different reactions may take place which transform the tars into lighter compounds.

More than fifty years ago Prigogine and Defay introduced the concept of reaction coordinates for a batch reaction (Friedly, 1991). Years later this concept became of use in chemistry and chemical engineering, and several authors have pointed out the utility of the reaction coordinate system (Froment and Bischoff, 1979; Smith and Van Ness, 1996). The extent of reaction may be referred to as a "macroscopic reaction coordinate", which varies as the reactions take place (Canagaratna, 2000). In this method, the relationship between the number of moles of a compound at any point, the initial number of moles of a specific compound, and the extent of various reactions occurring can be found. The concept of extent of reaction has also been used in many chemical process applications (Mann, 2009; Doraiswamy, 2001; O'Rear, 1989).

In this work, the molar extent of reaction method was applied to the steam reforming of toluene. The goal was to determine the relative importance of different reactions in the reaction network involved in the steam reforming process.

4.2 Methods

4.2.1 Catalytic Steam Reforming Experiments

Biochar along with three commercial steam reforming catalysts were evaluated for tar removal using toluene as a model tar compound. Two of the commercial catalysts were nickel based (Reformax 250 and Hifuel R-110) and one was platinum based (NextechA). The biochar was generated during switchgrass gasification in a down draft gasifier at the OSU thermochemical conversion facility. Tar destruction experiments were performed in a bench scale fixed bed reactor that provides real time steam reforming kinetic data for the selected model tar compound. The reactor was operated between 600 and 800^{o}C under atmospheric pressure using a synthetic gas mixture with similar composition to the synthesis gas generated from switchgrass gasification. For more details regarding setup and operating conditions, see Chapter 3.

4.2.2 Reaction Network

Several reactions may occur during the steam reforming of the synthetic gas mixture including steam reforming or dry reforming of hydrocarbons by CO_2, dealkylation, and hydrocracking reactions. Thermal cracking reactions and carbon formation reactions may also take place. Simultaneously, many conversion and equilibrium reactions of the main gas components may occur. A summary of these reactions is presented below.

Steam reforming

$C_7H_8 + 7H_2O \longrightarrow 7CO + 11H_2$ (Dermibas, 2002) (4.1)

$C_7H_8 + 14H_2O \longrightarrow 7CO_2 + 18H_2$ (Dermibas, 2002) (4.2)

Dry reforming

$C_7H_8 + 7CO_2 \longrightarrow 14CO + 4H_2$ (Devi et al., 2005) (4.3)

Carbon formation

$C_7H_8 \longrightarrow 7C + 4H_2$ (Simmel et al., 1997) (4.4)

Hydrocracking

$C_7H_8 + 10H_2 \longrightarrow 7CH_4$ (Simmel et al.,1997) (4.5)

Water gas shift reaction

$CO + H_2O \longleftrightarrow CO_2 + H_2$ (Simmel et al.,1997) (4.6)

Methanation reactions

$CO + 3H_2 \longleftrightarrow CH_4 + H_2O$ (Devi et al., 2005) (4.7)

$CO_2 + 4H_2 \longleftrightarrow CH_4 + 2H_2O$ (Sutton et al., 2001) (4.8)

$2H_2 + 2CO \longleftrightarrow CH_4 + CO_2$ (Devi et al., 2005) (4.9)

Hydrogasification reaction

$C + 2H_2 \longleftrightarrow CH_4$ (Simmel et al.,1997) (4.10)

Water gas reactions

$C + H_2O \longleftrightarrow CO + H_2$ (Simmel et al.,1997) (4.11)

$2H_2O + C \longleftrightarrow CO_2 + 2H_2$ (Simmel et al.,1997) (4.12).

Boudouard reaction

$C + CO_2 \longleftrightarrow 2CO$ (Simmel et al., 1997) (4.13)

The final products can be seen as the outcome of the competition between these reactions.

4.2.3 Molar Extent of Reaction Method

In a system where several independent reactions occur simultaneoulsy, the molar extent of reaction method can be used to determine the relative importance of different reactions. For a system with r independent reactions and n compounds the general expression to describe the relationship between the number of moles of a compound at any point, the reaction coordinate, and the initial number of moles of compound i can be calculated by the following equation (Foutch and Johannes,2000):

$$N_i = N_{io} + \sum_j \nu_{ij} \varepsilon_j \quad (4.14)$$

where

ε_j = reaction coordinate associated with each reaction

i = species involved (i = 1, 2 …n)

j = reaction involved (j = I, II … r)

ν_{ij} = stoichiometric coefficient (positive for products; negative for reactants)

N_i = Number of moles at any stage of specie i

N_{io} = Initial number of moles of specie i

4.2.4 Application to Toluene Conversion

In the analysis of chemical reaction systems where several compounds are involved, special care must be taken in the selection of the equations to be used in the extent of reaction model to ensure that a set of independent stoichiometric equations is used. Chemical reactions are independent if the stoichiometric equation of any one of these reactions cannot be obtained by adding and/or subtracting multiples of the stoichiometric equations of the others (Felder, 1999). By examining the 13 stoichiometric equations presented previously (equations 4.1-4.13) several cases of dependency can be found. A few examples are:

(4.2) + (4.3) = (4.1);

(4.12) + (4.13) = (4.11);

(4.9) + (4.8) = (4.7);

(4.6) + (4.7) = (4.9)

For the toluene conversion model, the species considered are: CO, CO_2, H_2O, C_7H_8, H_2, C and CH_4. These seven species contain a total of 3 elements: C, H and O. Since the

number of independent stoichiometric equations which can be solved is equal to the total number of species involved minus the number of elements present in those reactions (Herz, 1999), the set of independent stochiometric equations possible for this system is four (7 species minus 3 elements).

Even though there are several possible sets of reactions that can meet the mathematical requirements for the independent stoichiometric concept, knowledge of the toluene conversion process suggests that the potential set of reactions should include one steam reforming or dry reforming reaction for conversion of toluene, one reaction for carbon formation, the water gas shift reaction and at least one reaction that involves methane.

The following five different sets of reactions were created based on those criteria:

Set 1: Reactions 4.1, 4.4, 4.6 and 4.7

Set 2: Reactions 4.2, 4.4, 4.6 and 4.7

Set 3: Reactions: 4.1, 4.6, 4.7 and 4.13

Set 4: Reactions: 4.2, 4.6, 4.7 and 4.13

Set 5: Reactions: 4.3, 4.4, 4.6 and 4.7

For a given set of reactions, the extent of reaction (ε_j) was calculated for each of the four catalysts tested (three commercial catalysts and biochar). As an illustration let us apply the extent of reaction method, equation (4.14), to set number one and find the matrix of stoichiometric coefficients.

The four equations involved are:

$$C_7H_8 + 7H_2O \longrightarrow 7CO + 11H_2 \quad (4.1)$$

$$C_7H_8 \longrightarrow 7C + 4H_2 \quad (4.4)$$

$$CO + H_2O \longrightarrow CO_2 + H_2 \quad (4.6)$$

$$CO + 3H_2 \longleftrightarrow CH_4 + H_2O \quad (4.7)$$

The four species to be used in the analysis are C_7H_8, C, CH_4, and CO. Writing equation (4.14) for each compound, a system of 4 linear equations can be obtained:

$$A = \begin{array}{r|cccc} & \varepsilon_1 & \varepsilon_2 & \varepsilon_3 & \varepsilon_4 \\ C_7H_8 & -1 & -1 & 0 & 0 \\ C & 0 & 7 & 0 & 0 \\ CH_4 & 0 & 0 & 0 & 1 \\ CO & 7 & 0 & -1 & -1 \end{array}$$

.

This system of linear equations is algebraically equivalent to the matrix equation

$$AX = B \quad (4.15)$$

where

A = matrix of stoichiometric coefficients

X = vector of unknowns, in this case ε values

B = vector of known constants, in this case $N_i - N_{io}$

The values for the extent of reaction can then be calculated in Excel by:

$$\varepsilon = A^{-1} * B \qquad (4.16)$$

where

A^{-1}=

ε_1	ε_2	ε_3	ε_4
-1	-0.143	0	0
0	0.143	0	0
-7	-1	-1	-1
7	0	1	0

Values for B (N_i-N_{io}) come from experimental data. The number of moles of compound i at any stage were obtained by performing mass balance calculations on experimental data. Final numbers of moles per compound were calculated for three different experiments (3 replications) at each temperature (600, 700, and 800^{o}C). Measures of toluene conversion were made at different times on stream during an experiment. For each experimental treatment, an average value of final number of moles per compound at a time of 168 minutes was used for the determination of extent of reactions.

The values of initial number of moles per compound which are common to all experiments are reported in Table 4.1.

Table 4.1 Initial molar flow rate for each compound

Compound	**CO_2**	**CO**	**C_7H_8**	**H_2**	**CH_4**	**H_2O**	**C**
N_{io} (mol h^{-1})	0.1958	0.2249	0.0187	0.0595	0.0876	1.3296	0.0

As an illustration of the method using Hifuel R-110 catalyst at 800^{o}C, the difference between the final number of moles and initial number of moles for all compounds at time 168 minutes using this catalyst are shown in Table 4.2.

Table 4.2 ($N_i - N_{io}$) for Hifuel R-110 at 800^{o}C.

	Compound						
	CO_2	**CO**	**C_7H_8**	**H_2**	**CH_4**	**H_2O**	**C**
$N_i - N_{io}$ ($molh^{-1}$)	0.0602	0.0081	-0.0174	0.1623	-0.0621	-0.2349	0.000972

Then, for this example (using equation set 1) the extent of reaction values calculated by applying equation (4.16) are:

$\varepsilon_1 = 0.0174$

$\varepsilon_2 = 0.0001$

$\varepsilon_3 = 0.1739$

$\varepsilon_4 = -0.0621$

where ε_1, ε_2, ε_3 and ε_4 are the extent of reactions for steam reforming, hydrocracking, water gas shift and methanation at 800^{o}C, respectively.

This method was applied to all four tested catalysts at each of three temperatures (600, 700, and 800^{o}C) and for each of the five sets of equations explained above.

Once the extent of reaction for each one of the reactions in the set is calculated, equation (4.14) can be applied to the three remaining compounds, H_2O, H_2 and CO_2, to calculate the difference (N_i-N_{io}) for each one of these compounds. This calculated result can then be compared with the experimental results obtained from the mass balance, and serves as a validation tool. For example, for hydrogen, which is present in all of the reactions for set one, the expected change in hydrogen concentration can be found from the following expression using the calculated values for ε_1, ε_2, ε_3, ε_4:

$$N_{H2} - N_{H2o} = 11\varepsilon_1 + 4\varepsilon_2 + \varepsilon_3 - 3\varepsilon_4 \qquad (4.17)$$

This calculated result for H_2 can be compared to the experimental results for change in H_2 concentration.

4.2.5 Gibbs Free Energy

The extent of reaction concept tries to match multiple reactions that comply with the material balance for that set and it provides a possible overall model, but it does not show the chemical reaction path or whether a given chemical change is thermodynamically possible under the operational conditions. In order to complement the information given by the extent of reaction, the Gibbs free energy was also calculated for the set of main reactions chosen.

Gibbs free energy serves as the master variable that determines whether a chemical reaction is thermodynamically probable. The experiments in this work were performed at atmospheric pressure and temperatures between 600 and 800^{o}C, so it is of interest to determine whether some of the reactions are thermodynamically favorable at this set of conditions. The concept of Gibbs free energy is useful for this application when comparing the variation of the free energy between products and reactants. If the free energy of the reactants is greater than that of the products, the reaction will take place spontaneously. On the other hand, if the free energy of the products exceeds that of the reactants, then the reaction will tend to proceed in the reverse direction. The relationship between the change in Gibbs free energy and entropy is shown in the following expression:

$$\Delta G = \Delta H - T\Delta S \tag{4.18}$$

where:

ΔG = change in Gibbs free energy between products and reactants at 1 atm (kJ)

ΔH = change in enthalpy between products and reactants at 1 atm (kJ)

T = reaction temperature (K)

ΔS = change in entropy between products and reactants at 1 atm (kJ/K)

Using the equation shown above, we can develop a new expression which shows the changes in Gibbs free energy as a function of the system temperature and standard conditions (1 atm and 298.15 K). The relation between changes in the free energy from

products to reactants, temperature of the system and standard conditions can be written according the expression shown below (Smith Van Ness, 1996):

$$\frac{\Delta G^O}{RT} = \frac{\Delta G_O^O - \Delta H_O^O}{RT_O} + \frac{\Delta H_O^O}{RT} + \frac{1}{T}\int_{T_O}^{T} \frac{\Delta C_p^o}{R} dT - \int_{T_o}^{T} \frac{\Delta C_p^o}{R} \frac{dT}{T} \quad (4.19)$$

where:

ΔG^o= standard Gibbs free energy change of reaction at reference pressure (J/mol)

ΔH^o= standard enthalpy change of reaction at reference pressure (J/mol)

ΔG_o^o= standard Gibbs free energy change of reaction at reference pressure and temperature (J/mol)

ΔH_o^o= standard enthalpy change of reaction at reference pressure and temperature (J/mol)

T = reaction temperature (K)

T_o = reference temperature (298 K)

R = universal gas constant (J/molK)

C_p^o = standard heat capacity at constant pressure (J/molK)

The expression above does not show the effect of pressure, but this is not important for this application since our system is operated at reference pressure (1 atm). The above expression plus specific correlations to find values for C_p are taken from Smith Van Ness (1996). The expression used for C_p is:

$$\frac{\Delta C_p^{ig}}{R} = A + BT + CT^2 + DT^{-2} \quad (4.20)$$

where T= temperature (K); A, B, C, D are coefficients for each component; and ig stands for ideal gas (Smith Van Ness, 1996).

Using the equations above, the change in Gibbs free energy for each reaction shown in the previous section was determined.

4.3 Results

4.3.1 Extent of Reactions

The extent of reaction was calculated using each of the five sets of reactions shown previously for each of four different catalysts at each of three different temperatures.

Steam Reforming and Dry Reforming

Table 4.3 shows the extent of reaction values calculated for all tested catalysts for steam reforming and/or dry reforming (equations 4.1, 4.2 or 4.3) using each of the five sets of equations at three different temperatures. It can be seen from the table that the calculated extent of reaction shows very little dependence on the set of reactions chosen; the extent of reaction is nearly constant at a given temperature, regardless of which set is chosen. For example, the extent of reaction is between 0.0113-0.0114 for Reformax at 600 ^{o}C for all five sets. This pattern was similar for all four catalyst materials tested. These reactions are especially important for the conversion of toluene since steam reforming and/or dry reforming is the main reaction that allows the destruction and subsequent conversion of toluene into syngas.

Table 4.3 Extent of reaction values for steam and dry reforming reactions (Equation 4.1, 4.2, or 4.3) for tested catalysts with five different sets of equations at three different temperatures.

		Extent of Reaction, ε (mol/h)				
Catalyst	**Temperature (^oC)**	**Set 1**	**Set 2**	**Set 3**	**Set 4**	**Set 5**
Reformax 250	600	0.01131	0.01131	0.01140	0.01140	0.01131
	700	0.01489	0.01489	0.015	0.015	0.01489
	800	0.01728	0.01728	0.0174	0.0174	0.01728
Hifuel R110	600	0.01066	0.01066	0.01080	0.01080	0.01066
	700	0.013764	0.01376	0.0139	0.0139	0.01376
	800	0.017261	0.01726	0.0174	0.0174	0.01726
NextechA	600	0.00692	0.00692	0.00700	0.00700	0.00692
	700	0.01106	0.01106	0.0112	0.0112	0.01106
	800	0.00986	0.009861	0.0100	0.0100	0.00986
Biochar	600	0.00742	0.00742	0.00770	0.00770	0.00742
	700	0.01061	0.01061	0.0109	0.0109	0.01061
	800	0.00058	0.00058	0.0009	0.0009	0.000589

Another important point from Table 4.3 is that the steam and/or dry reforming reactions represent a majority of the toluene conversion which is occurring, while other reactions, such as the carbon formation reaction (included in sets 1, 2 and 5) represent a very small contribution (less than 1%) in the conversion of toluene. For instance, at 600 ^{o}C with Reformax 250 the difference between inlet and outlet toluene is 0.0114 mol/hr. Based on the extent of reaction values calculated for the steam reforming/dry reforming and carbon formation reactions at these conditions, only 0.000088 mol/hr of toluene react through the carbon formation reaction (shown in Table 4.6) representing only 0.77% of the toluene conversion, while 0.0113 mol/hr of toluene reacts through the steam reforming or dry reforming reaction, which represents 99.23% of the toluene conversion.

The steam reforming and dry reforming extent of reaction also shows a clear dependence on temperature. Figure 4.1 shows an important increase in the extent of reaction with temperature. This is expected, since steam reforming reactions are known to be a strong function of temperature. Interestingly, the extent of reaction for Nextech and Biochar did not increase when going from 700 to 800 ^{o}C.

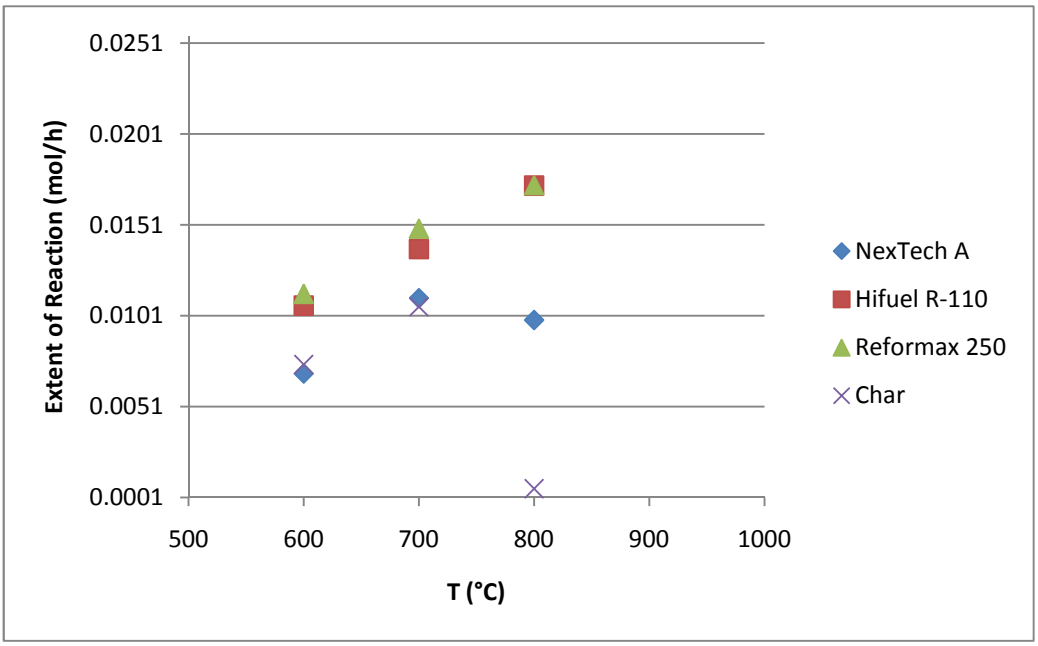

Figure 4.1 Extent of reaction vs. temperature for tested catalysts for reaction 4.1 in set one.

Figure 4.1 also shows the variation in the extent of reaction values between catalysts. In general, the larger the extent of reaction for the steam reforming and/or dry reforming reaction, the better the catalyst performs for that specific application. It appears that Reformax and Hifuel show the best performance for toluene conversion within the range of operation of this system. This finding is true regardless of the set of reactions chosen.

Water Gas Shift

Table 4.4 shows the extent of reaction values for the water gas shift reaction for tested catalysts at three different temperatures for all five sets of reactions. For the water gas shift reaction, the calculated extent of reaction shows a high dependence on the set of reactions chosen. In fact, it is highly dependent on the steam or dry reforming reaction used in the respective set. Dry reforming does not require water to proceed, so the extent

of reaction for set 5 is the highest value. On the other hand, if the set of reactions includes steam reforming (reaction 4.2) the extent of reaction for the water gas shift has the minimum value. This pattern is evident in Table 4.4.

The water gas shift extent of reaction shows a mild temperature dependence. Figure 4.2 shows the relationship between the extent of reaction, temperature and catalyst for the water gas shift reaction using reaction set 2. As can be seen from the figure, in most cases the extent of reaction values decrease with increasing temperature; except in the case of set 5 (with dry reforming) there is a slight increase with temperature. The decrease in extent of reaction with temperature suggests that the water gas shift reaction is less favorable at higher temperatures.

Table 4.4 Extent of reaction values for all five reaction sets at different temperatures for the water gas shift reaction (Equation 4.6).

		Extent of Reaction, ε (mol/h)				
Catalyst	**Temperature (°C)**	**Set 1**	**Set 2**	**Set 3**	**Set 4**	**Set 5**
Reformax 250	600	0.1518	0.07260	0.1512	0.07137	0.2309
	700	0.1657	0.0613	0.1648	0.05983	0.2698
	800	0.1629	0.0419	0.1622	0.0404	0.2839
Hifuel R110	600	0.19161	0.11700	0.19062	0.1150	0.2662
	700	0.1708	0.0745	0.1698	0.07259	0.2672
	800	0.1748	0.054	0.1739	0.0521	0.2957
NextechA	600	0.2080	0.15960	0.2074	0.1585	0.2565
	700	0.1995	0.1221	0.1986	0.1202	0.2769
	800	0.1571	0.0881	0.1562	0.086156	0.2262
Biochar	600	0.09662	0.04470	0.09464	0.04074	0.1485
	700	0.1337	0.0594	0.13174	0.05544	0.20804
	800	0.01412	0.01	0.01194	0.00564	0.01824

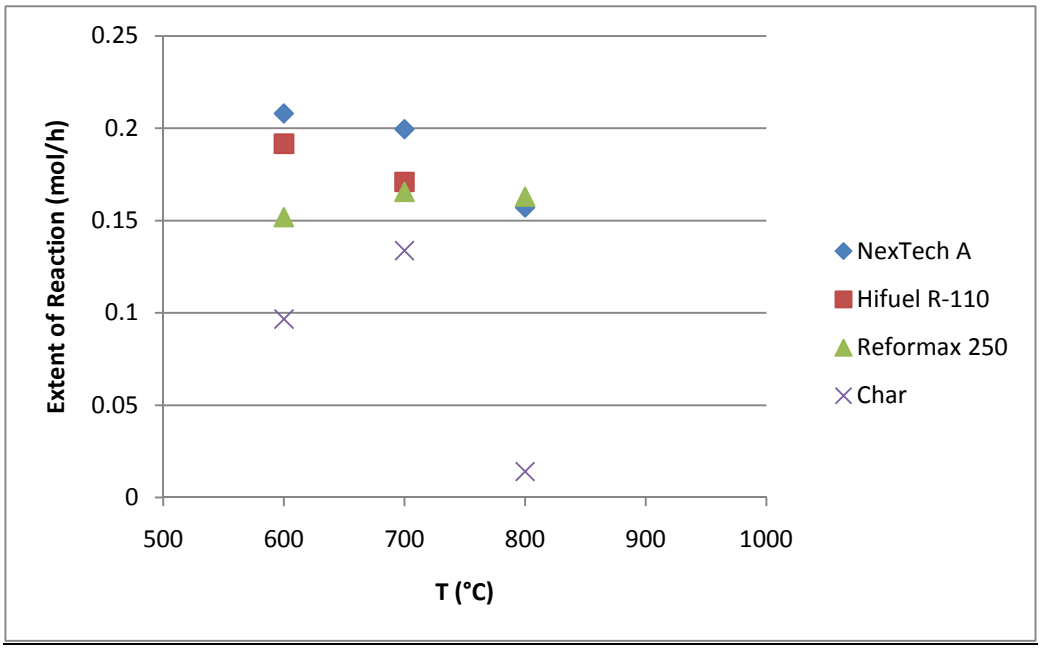

Figure 4.2 Extent of reaction vs. temperature for tested catalysts for the water gas shift reaction (equation 4.6) using reaction set two.

Methanation

Table 4.5 shows the calculated extent of reaction values for the methanation reaction (equation 4.7) for tested catalysts at 600, 700 and 800 ^{o}C for all five sets of reactions. The extent of the reaction is independent of the set of reactions chosen, as all values are identical for the five different reaction sets. The values also exhibit a dependence on temperature, and in many cases it appears that the reverse of this equilibrium reaction is occurring , generating a negative sign for the extent of reaction at those conditions.

Table 4.5 Extent of reaction values for tested catalysts for all five sets of reactions at different temperatures for the methanation reaction (equation 4.7).

		Extent of Reaction, ε (mol/h)				
Catalyst	**Temperature (°C)**	**Set 1**	**Set 2**	**Set 3**	**Set 4**	**Set 5**
Reformax 250	600	0.01610	0.01610	0.01610	0.01610	0.01610
	700	-0.0128	-0.0128	-0.0128	-0.0128	-0.0128
	800	0.0046	0.0046	0.0046	0.0046	0.0046
Hifuel R110	600	-0.00580	-0.00580	-0.00580	-0.00580	-0.00580
	700	-0.047	-0.047	-0.047	-0.047	-0.047
	800	-0.0621	-0.0621	-0.0621	-0.0621	-0.0621
NextechA	600	0.00390	0.00390	0.00390	0.00390	0.00390
	700	-0.0074	-0.0074	-0.0074	-0.0074	-0.0074
	800	-0.0213	-0.0213	-0.0213	-0.0213	-0.0213
Biochar	600	-0.05450	-0.05450	-0.05450	-0.05450	-0.05450
	700	-0.0437	-0.0437	-0.0437	-0.0437	-0.0437
	800	-0.0542	-0.0542	-0.0542	-0.0542	-0.0542

Figure 4.3 shows the dependence of the methanation reaction on temperature for reaction set one. The three commercial catalysts show a consistent decrease in extent of reaction with temperature. Char appears to behave very differently than the other catalysts. One possible reason for this behavior is that char may be releasing volatile compounds during the course of the experiment.

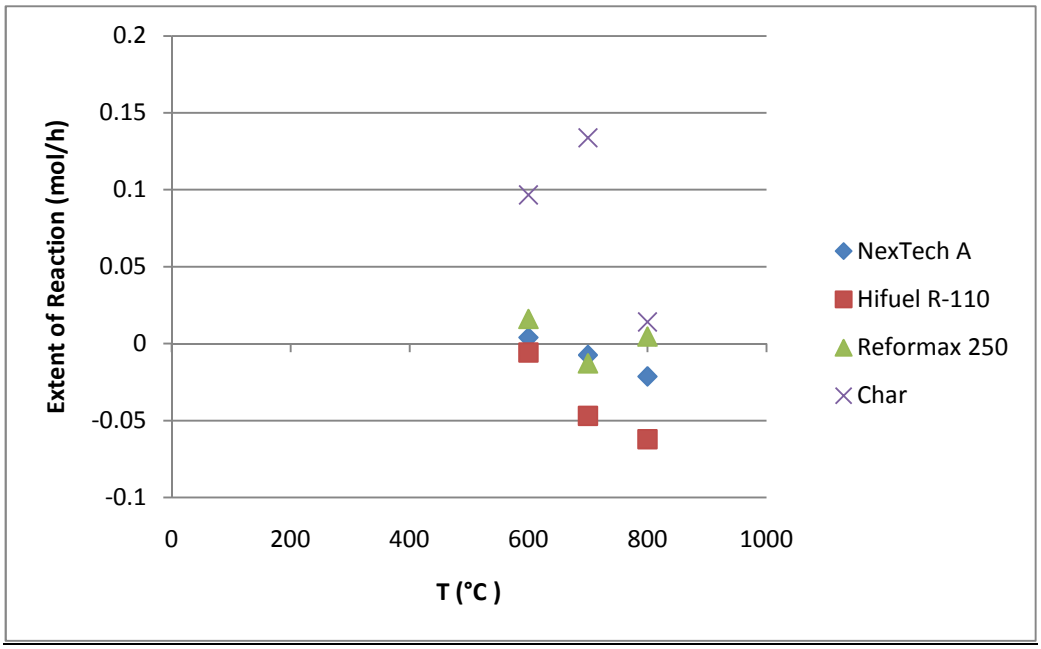

Figure 4.3 Extent of reaction vs. temperature for tested catalysts for the methanation reaction (equation 4.7) using reaction set one.

Carbon Formation and Boudouard Reaction

For the reactions involving carbon formation (equation 4.4 or 4.13), the calculated extent of reaction shows a strong dependence on the set of reactions chosen. This observation was similar for all tested catalyst materials. Table 4.6 shows the calculated extent of reaction values at 600, 700 and 800 ^{o}C for all five sets of reactions. The values for the reactions involving carbon are small in comparison to the other reactions considered, since the amount of carbon formed is small. The extent of reaction values for carbon formation show very little dependence on temperature. As can be seen in Figure 4.4, the slope of the line with temperature is nearly horizontal.

Table 4.6 Extent of reaction values for tested catalysts for all five sets and different temperatures for the carbon formation reaction (equation 4.4 or 4.13)

		Extent of Reaction, ε (mol/h)				
Catalyst	**Temperature (°C)**	**Set 1**	**Set 2**	**Set 3**	**Set 4**	**Set 5**
Reformax 250	600	0.000088	0.000088	0.000615	0.000615	0.000088
	700	0.000105	0.000105	0.000734	0.000734	0.000105
	800	0.000111	0.000111	0.000774	0.000774	0.000111
Hifuel R110	600	0.000142	0.000142	0.000992	0.000992	0.000142
	700	0.000136	0.000136	0.000952	0.000952	0.000136
	800	0.000139	0.000139	0.000972	0.000972	0.000139
NextechA	600	0.000082	0.000082	0.000575	0.000575	0.000082
	700	0.000136	0.000136	0.000952	0.000952	0.000136
	800	0.000139	0.000139	0.000972	0.000972	0.000139
Biochar	600	0.000283	0.000283	0.00770	0.001980	0.000283
	700	0.000283	0.000283	0.00198	0.00198	0.000283
	800	0.000311	0.000311	0.0009	0.00218	0.000311

.

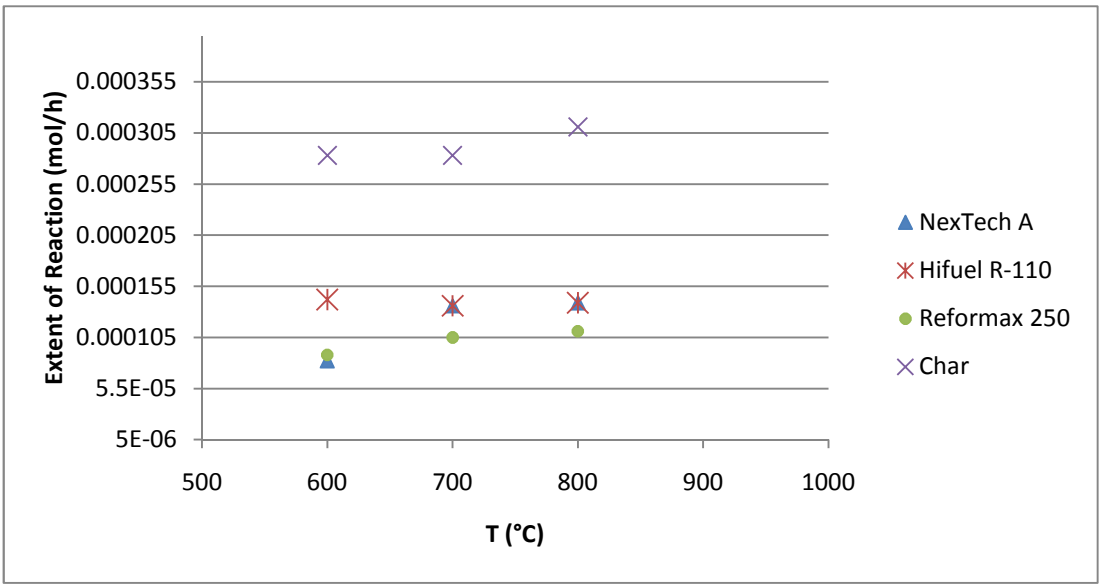

Figure 4.4 Extent of reaction vs. temperature for tested catalysts for the carbon formation reaction (equation 4.4) using reaction set one.

4.3.2 Mass Balance Verification

The accuracy of the model for the set of independent stochiometric equations and extent of reaction values for the four reactions was tested using the three independent species that were not included in the model: H_2O, CO_2 and H_2. The change in concentration of these three species (as measured experimentally) was compared to the same value calculated using the extent of reaction values. The mass balance calculated values vary with temperature and catalyst; however there is not much difference based on the chosen set of reactions. Mass balance verification results for reaction set one for tested catalysts at 600^{o}C, 700^{o}C and 800^{o}C is shown in Table 4.7. The table shows the model calculated results, the experimental results, and the percent difference. The percent difference values show a large amount of variation, and are generally much higher for biochar, indicating that the model was less accurate for biochar. The best match between experimental and

calculated values occurs with Hifuel at 700^{o}C with differences ranging between 4 and 19 percent. The same data for the remaining four reaction sets is shown in Appendix A.5.

Table 4.7 Mass balance verification showing model calculated results (Cal), experimental results (Exp) and the percent difference (% Diff) for reaction set one for tested catalysts at three different temperatures.

		600 °C			700 °C			800 °C		
Catalyst	**Compound**	**Cal**	**Exp**	**% Diff**	**Cal**	**Exp**	**% Diff**	**Cal**	**Exp**	**% Diff**
Reformax 250	**H_2O**	-0.21	-0.24	10.81	-0.28	-0.28	0.72	-0.28	-0.21	32.90
	CO_2	0.15	0.10	47.65	0.17	0.12	39.48	0.16	0.20	16.58
	H_2	0.23	0.17	33.96	0.37	0.17	111.5	0.34	0.30	12.39
Hifuel R110	**H_2O**	-0.27	-0.24	15.16	-0.31	-0.30	4.28	-0.36	-0.23	52.30
	CO_2	0.19	0.22	11.37	0.17	0.18	6.69	0.17	0.06	190.4
	H_2	0.33	0.38	13.45	0.46	0.39	18.89	0.55	0.16	239.8
NextechA	**H_2O**	-0.25	-0.19	34.55	-0.28	-0.23	25.89	-0.25	-0.21	19.03
	CO_2	0.21	0.22	6.59	0.20	0.20	0.48	0.16	0.19	17.00
	H_2	0.27	0.22	24.49	0.34	0.26	32.66	0.33	0.30	10.20
Biochar	**H_2O**	-0.20	-0.26	21.91	-0.25	-0.30	16.61	-0.07	-0.30	75.82
	CO_2	0.10	0.01	866.2	0.13	0.17	22.57	0.01	0.15	90.52
	H_2	0.34	-0.01	6956	0.38	0.37	3.75	0.18	0.49	62.37

4.3.3 Gibbs Free Energy

Figure 4.5 shows the change in Gibbs free energy for the steam reforming and dry reforming reactions. It is evident that the change in Gibbs free energy is negative within

the range of temperatures between 600 and 800 ^{o}C, indicating that these reactions are thermodynamically favorable. In addition, the reaction that has the lowest value (highest negative value) is the steam reforming based on equation 4.2. Therefore, from a thermodynamic standpoint, this is the most probable reaction for the conversion of toluene in the system. The values for all three reactions become more negative with temperature, and at 800 ^{o}C, they are all nearly identical.

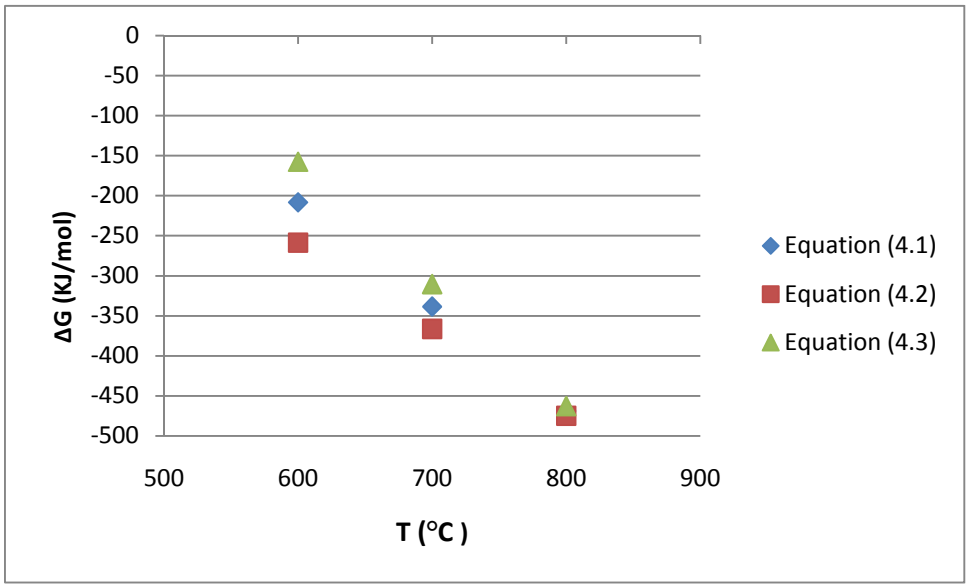

Figure 4.5 Gibbs free energy for steam reforming and dry reforming reactions (equations 4.1, 4.2 and 4.3).

Figure 4.6 shows the change in Gibbs free energy for the water gas shift reaction. These values become less negative with an increase in temperature, but the change of Gibbs free energy remains negative between 600 and 800 ^{o}C, indicating that the reaction is thermodynamically favorable within this temperature range. At temperatures slightly over 800 ^{o}C, the change in Gibbs free energy becomes positive for this reaction.

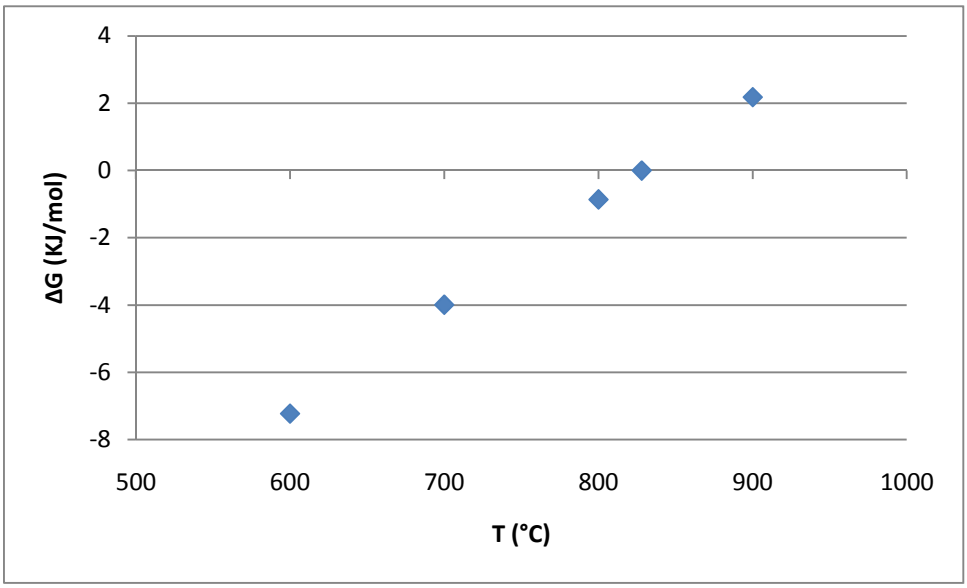

Figure 4.6. Gibbs free energy for the water gas shift reaction (equation 4.6).

Figure 4.7 shows the change in Gibbs free energy for the methanation reaction. Interestingly, the change in Gibbs free energy becomes positive at temperatures over 620 ^{o}C, meaning that at 600 ^{o}C the reaction is thermodynamically favorable, but at 700 ^{o}C the reaction will proceed from right to left (see equation 4.7). This finding is consistent with the values of extent of reaction calculated in the previous section, where most values for the methanation reaction at 600 ^{o}C were positive, but at 700 ^{o}C and 800 ^{o}C they became negative.

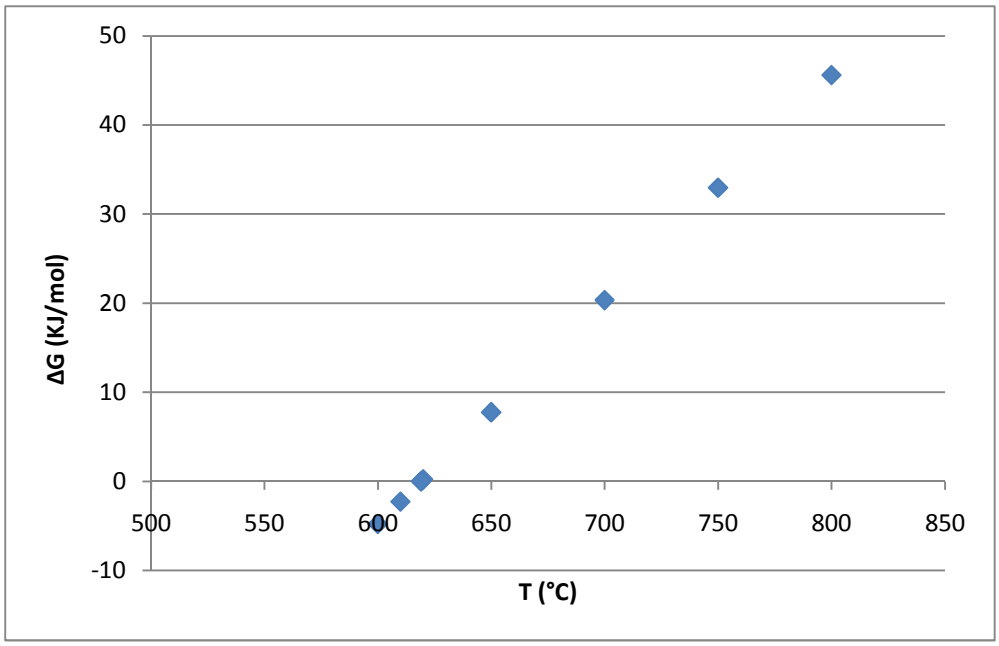

Figure 4.7. Gibbs free energy for the methanation reaction (equation 4.7).

Figure 4.8 shows the change in Gibbs free energy for the reactions that produce carbon such as the carbon formation (equation 4.4) and Boudouard reactions (equation 4.13). In general, the carbon formation reaction appears to be much more favorable, since the Gibbs free energy is much lower than that of the Boudouard reaction throughout the temperature range tested.

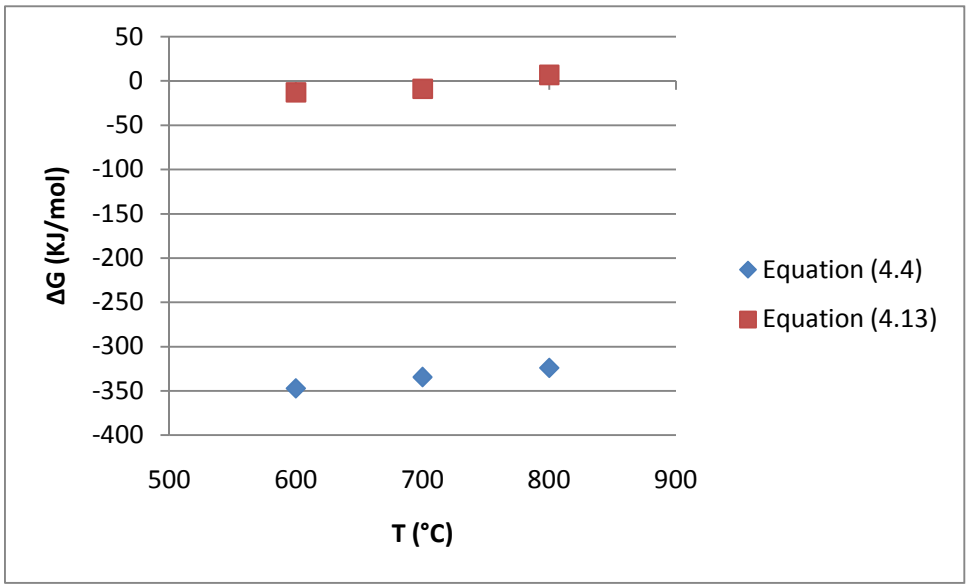

Figure 4.8 Gibbs free energy for the carbon formation reaction (equations 4.4) and the Boudouard reaction (equation4.13).

4.4 Conclusions

- The catalysts that show the larger extents of reaction for steam reforming are Reformax 250 and Hifuel R-110, indicating that these two commercial catalysts would be the best candidates for transforming toluene. This finding is consistent with the findings in chapter 3.

- In general, the extent of reaction for steam reforming increases with increasing temperature.

- The values of extent of reaction for the methanation reaction are positive at 600 ^{o}C and negative at 700 and 800 ^{o}C. This finding is consistent with the fact that the differential Gibbs free energy becomes positive for this reaction at temperatures slightly above 620 ^{o}C.

- Extent of reaction values for the carbon formation reactions are very small, and show virtually no dependence on temperature. Values for biochar were much larger than those for the commercial catalysts.

- Based on the extent of reaction values calculated for the steam reforming and carbon formation reactions at these conditions, 0.0113 mol/hr of toluene reacts through the steam reforming reaction, which represents 99.23% of the toluene conversion, while only 0.000088 mol/hr of toluene reacts through the carbon formation reaction, representing only 0.77% of the toluene conversion.

- For the three commercial catalysts, the extent of reaction model worked well for determining the distribution of products. The difference in terms of mass balance between the model and experimental results was 25% or less in 60% of the cases.

- Unlike the commercial catalysts, the prediction of the extent of reaction for the biochar seemed erratic, and failed to accurately predict product distributions. In particular, the effect of temperature on biochar was often inconsistent, especially at 600 ^{o}C. One option for this disparity is that char may have residual components which interact with the reactants and/or products of the reactions.

- Of the three reactions discussed for the reforming of toluene, the steam reforming defined by reaction 4.2 is thermodynamically more favorable under the operating temperatures tested.

REFERENCES

Abu El-Rub, Z. Y., Bramer, E. A., Brem, G. 2004. Review of catalysts for tar elimination in biomass gasification processes. Industrial & Engineering Chemistry Research 43, 6911–6919.

Abu El-Rub, Z. Y., Bramer E. A., Brem, G. 2008. Experimental comparison of biomass chars with other catalysts for tar reduction. Fuel 87, 2243–2252.

Ahmed, A., Cateni, B. G., Huhnke, R. L., Lewis, R. L. 2006. Effects of biomass-generated producer gas constituents on cell growth, product distribution and hydrogenase activity of Clostridium carboxidivorans $P7^T$. Biomass & Bioenergy 30, 665-672.

Ankita, J., Sudhagar, M., Kaster, J. 2010. Catalytic Cracking of Tar using Biochar as a Catalyst. ASABE Annual International Meeting.

Arauzo, J., Radlein, D., Piskorz, J.,Scott, D. S. 1994. A New Catalyst for the Catalytic Gasification of Biomass. Energy & Fuels 8, 1192-1196.

Asadullah, M., Fujimoto, K., Tomishige, K. 2001. Catalytic performance of rhodium/cerium dioxide in the gasification of cellulose to synthesis gas at low temperature. Industrial & Engineering Chemistry Research 40, 5894-5900.

Asadullah, M., Ito, S., Kunimori, K., Yamada, M., Tomishige, K. 2002. Energy efficient production of hydrogen and syngas from biomass: development of low temperature catalytic process for cellulose gasification. Environmental Science Technology 36, 4476-4481.

Aznar, M. P., Caballero, M. A., Gil, J., Martin, J. A., Corella, J. 1998. Commercial steam reforming catalysts to improve biomass gasification with steam-oxygen mixtures for catalytic tar removal. Industrial & Engineering Chemistry Research 37, 2668–2680.

Bain, R., Dayton, D., Carpenter, D. Czernik, S., Feik, C., French, R., Magrini-Bair, K., Phillips, S. 2005. Evaluation of Catalyst Deactivation during Catalytic Steam Reforming of Biomass-Derived Syngas. Industrial & Engineering Chemistry Research 44, 7945-7956.

Basu P. 1996. Combustion and Gasification in Fluidized Beds. Taylor and Francis.

Beccat P., Da Silva, P., Huiban, Y., Kasztela, S. 1999. Quantitative Surface Analysis by XPS: Application to Hydrotreating Catalysts. Oil & Gas Science and Technology 54, 487-496.

Biomass Technology Group (BTG) Report 9910. 1999. University of Twente.

BP Statistical review of world energy. 2009. BP Distribution Services

BP Statistical review of world energy. 2010. BP Distribution Services.

Brandt, P., Larsen, E., Henriksen, U. 2000. High Tar Reduction in a Two-Stage Gasifier. Energy & Fuels 14, 816-819.

Caballero, M. A., Corella, J., Aznar, M.P., Gil, J. 2000. Biomass Gasification with Air in Fluidized Bed. Hot Gas Cleanup with Selected Commercial and Full-Size Nickel-Based Catalysts. Industrial & Engineering Chemistry Research 39, 1143-1154.

Canagaratna S. 2000. The use of Extent of Reaction in Introductory Courses. Journal of Chemical Education 77, 52-54

Coll, R., Salvado, J., Farriol,.X., Montane, D. 2001. Steam reforming model compounds of biomass gasification tars: conversion at different operating conditions and tendency towards coke formation. Fuel Processing Technology 74, 19–31.

Corella, J., Orio, A., Toledo, J. M. 1999. Biomass gasification with air in a fluidized bed: exhaustive tar elimination with commercial steam reforming catalysts. Energy & Fuels 13, 702–709.

Courson, C., Makaga, E., Petit, C., Kiennemann, A. 2000. Development of nickel catalysts for gas production from biomass gasification. reactivity in steam and dry-reforming. Catalysis Today 63, 427–437.

Dayton, D. 2002. Review of the literature on catalytic biomass tar destruction: Milestone completion report. National Renewable Energy Laboratory.

Delgado, J., Aznar, P.M., Corella, J. 1999. Calcined Dolomite, Magnesite, and Calcite for Cleaning Hot gas from a Fluidized Bed with Steam: Life and Usefulness. . Industrial & Engineering Chemistry Research 35, 3637-3643.

Demirbas, A. 2002. Sustainable cofiring of biomass with coal. Energy Conversion and Management 44, 1465–1479.

Depner, H., Jess, A. 1998. Kinetics of nickel-catalyzed purification of tarry fuel gases from gasification and pyrolysis of solid fuels. Fuel 78, 1369-1377.

Djaidja, A., Libs, S., Kiennemann, A., Barama, A. 2006. Characterization and activity in dry reforming of methane in NiMg/Al and Ni/MgO catalysts. Catalysis Today 113, 194-200.

Devi, L., Ptasinski, K., Janssen, F. J. 2002. A review of the primary measures for tar elimination in biomass gasification processes. Biomass and Bioenergy 24, 125–140.

Devi, L., Ptasinski, K., Janssen, F. J. 2005. Decomposition of naphthalene as a biomass tar over pretreated olivine: Effect of gas composition, kinetic approach, and reaction scheme. Industrial & Engineering Chemistry Research 44, 9096–9104.

Dogru, M., Howarth, C. R., Akay, G., Keskinler, B., Malik, A. 2002. Gasification of Hazelnut Hhells in a Downdraft Gasifier. Energy 27, 415-427.

Doraiswamy, L. K. 2001. Organic Synthesis Engineering, Oxford University Press.

Dou B., Jinsheng G., Xingzhong S., Seung, W. 2003. Catalytic Cracking of Tar Component from High-temperature Fuel Gas. Applied Thermal Engineering 23, 2229-2239.

Draelants, D. J., Zhao, H.B., Baron, G. V. 2000. Catalytic conversion of tars in biomass gasification fuel gases with nickel-activated ceramic filters. Studies in Surface Science and Catalysis,; 130B International Congress on Catalysis, Pt. B, 1595-1600.

Elliot. D. C. 1988. Relation of reaction time and temperature to chemical composition of pyrolisis oil. ACS Symposium Series 376.

Ibarra, J. V., Royo, C., Monzon, A., Santamaria, J. 1995. Fourier transform infrared spectroscopy study of coke deposits on a $Cr_2O_3 – Al_2O_3$ catalyst. Vibrational Spectroscopy 9, 191-196.

International-Energy-Annual. 2008. U. S. Energy Administration. International Energy Agency. DOE.

Felder, R. 1999. Elementary Principles of Chemical Processes. 3er edition Wiley.

Friedly, J. 1991. Extent of Reaction in Open Systems with Multiple Heterogeneous Reactions. AICHE Journal 37, 687-693

Froment, G. and Bischoff, K.1979. Chemical Reactor Analysis and Design. John Wiley & Sons

Foutch, G. and Johannes, A. 2007. CHE 5123 Lecture Notes. Stillwater, Oklahoma, Oklahoma State University.

Garcia, L., French, R., Czernik, S., Chornet, E. 2000. Catalytic steam reforming of bio-oils for the production of hydrogen: effect of catalyst composition. Applied Catalysis A: General 201, 225-239.

Gardner, D., Bartholomew C. 1981. Kinetics of Carbon Deposition during Methanation of CO. Industrial & Engineering Chemistry Research. 20, 80-87.

Gebhard, S. C., Wang, D., Overend, R. P., Paisley, M. A. 1994. Catalytic conditioning of synthesis gas produced by biomass gasification. Biomass and Bioenergy 7, 307-313.

Graham R., G., Bain R. 1993. Biomass gasification: Hot gas clean-up. NREL.

Han, J., Kim, H. 2008. The reduction and control technology of tar during biomass gasification/pyrolysis: An overview. Renewable and Sustainable Energy Reviews 12, 397–416.

Herz, R. 1999. Multiple Reaction Stoiquiometry. Last retrieved April 2011 from http//reactorlab.net/dir/stoichnotes.html.

Huber, G., Iborra, S., and Corma, A. 2006. Synthesis of transportation fuels from biomass: chemistry, catalysts, and engineering. Chem. Rev. 106, 4044–4098.

Konya, Z., Vesselenyi, I., Kiss, J., Farkas, A., Oszko, A., Kiricsi, I. 2004. XPS study of multiwall carbon nanotube synthesis on Ni, V and Ni, V ZMs-5 catalysts. Applied Catalysts. 260, 55-61.

Kumar, A., Jones, D. D. ,Hanna, M. A. 2009. Thermochemical Biomass Gasification : A Review of the Current Status of the Technology Energies 2, 556–581.

Lei, H., Song, Z., Tan, D., Bao, X., Mu, X., Zong, B., Min, E. 2001. Preparation of novel Raney-Ni catalysts and characterization by XRD, SEM and XPS. Applied Catalysts 214, 69-76.

Mann, U. 2009. Chemical Reactor Analysis and Design. New Tools for Industrial Chemical Reactor Operations. 2nd edition. John Wiley & Sons.

Milne, T. A., Evans, R. J., Abatzaglou, N. 1998. Biomass gasifier ”tars”: Their nature, formation, and conversion. National Renewable Energy Laboratory.

Minowa, T., Ogi, T. 1998. Hydrogen production from cellulose using a reduced nickel catalyst. Catalysis Today. 45, 411-416.

Mudge, L.K., Baker, E.G., Mitchell, D.H., Brown, M.D. 1985. Catalytic steam gasification of biomass for methanol and methane production. Journal of Solar Energy Engineering 107, 88–92.

Mudinoor, A.R. 2010. Conversion of toluene (model tar) in the presence of syngas using selected steam reforming catalyst. Oklahoma State University. Master thesis.

Narvaez, I., Orio, A., Aznar, M.P., Corella, J. 1996. Biomass gasification with air in an atmospheric bubbling fluidized bed. effect of six operational variables on the quality of the produced raw gas. Industrial & Engineering Chemistry Research 35, 2110–2120.

Neeft, J. P. 1996. Diesel particulate emission control. Fuel Processing Technology 47, 1-69.

O'Rear, G. B. 1989.Determination of reaction kinetics from measurements at constant extent of reaction. American Chemical Society 34, 644.

Orio, A., Corella, J., Narvaez, I. 1997. Performance of different dolomites on hot raw gas cleaning from biomass gasification with air. Industrial & Engineering Chemistry Research 36, 3800–3808.

Ozcimen, D., Mericboyu, A. 2010. Characterization of biochar and bio oil samples obtained from carbonization of various biomass materials. Renewable Energy 35, 1319-1324.

Pieck, C., Jablonski, E. L., Parera, J. M., Frety, R., Lefebvre, F. 1992. Characterization of Residual Coke during Burning. Industrial & Engineering Chemistry Research 31, 1017-1021.

Pfeifer, C., Hofbauer, H. 2008. Development of catalytic tar decomposition downstream from a dual fluidized bed biomass steam gasifier. Powder Technology 180, 9–16.

Pleths, N. L., Schonning, M., Christensen, S. V., Hoffmann, S.V., Li, Z., Hofmann, P., Besenbacher, F., Clausen, B. S. 2001. Combined TPS,XPS, EXAFS, and NO-TPD study of the sulfiding of Mo/Al_2O_3. Catalysis Letters. 73, 85-90

Poncelet, G., Centeno, M. A., Molina, R. 2005. Characterization of α alumina-supported nickel catalysts y spectroscopies and chemisorptions measuraments. Applied Catalysis 288, 232-242.

Rapagna, S., Jand, N., Foscolo, P. U. 1998. Catalytic gasification of biomass to produce hydrogen rich gas. International Journal of Hydrogen Energy 23, 551–557.

Reformax brochure, 2001. SudChemie Inc.

Renewable Biomass Global Status Report. 2010. REN21.

Satterfield C. 1991. Heterogeneous Catalysis in Industrial Practice. 2nd edition. Mc Graw Hill Inc.

Seshardi, K.S.,Shamsi, A. 1998. Effect of Temperature, Pressure, and Carrier gas on the Cracking of Coal Tar over a Char-Dolomite Mixture and Calcined Dolomite in a Fixed Bed Reactor. Industrial & Engineering Chemistry Research 37, 3830- 3837.

Sehested, J. 2006. Four challenges for nickel steam-reforming catalysts. Catalyst Today 111, 103–110.

Simell, P. A., Kurkela, E. A., Stahlberg, P., Hepola J. O. 1996. Catalytic hot gas cleaning of gasification gas. Catalysis Today 27, 55-62.

Simell, P. A., Hakala, N., Haario, H.E. 1997. Catalytic decomposition of gasification gas tar with benzene as the model compound. Industrial & Engineering Chemistry Research 36, 42-51.

Simell, P. A., Hirvensalo, E.K., Smolander, V. T.,. Krause, A.O. 1999. Steam reforming of gasification gas tar over dolomite with benzene as a model compound. Industrial & Engineering Chemistry Research 38, 1250–1257.

Smith J, Van Ness H., Abbott M. M. 1996. Introduction to Chemical Engineering Thermodynamics. 5th edition. Mc. Graw Hill.

Smulders, H.W. 1998.Pulsed power corona discharges for air pollution control. Transactions on Plasma Science 26,1476-1484.

Sutton, D., Kelleher, B., Ross, J. R. 2001. Review of literature on catalysts for biomass gasification. Fuel Processing Technology 73, 155–173.

Swartz, S., Azad, A., Seabaugh, M. 2003.Ceria based water gas shift catalyst. AICHE Spring National Meeting.

Swierczynski, D., Courson, C., Kiennemann, A. 2008. Study of steam reforming of toluene used as model compound of tar produced by biomass gasification. Chemical Engineering and Processing: Process Intensification 47, 508–513.

Swierczynski, D., Libs, S., Courson, C., Kiennemann, A. 2007. Steam reforming of tar from a biomass gasification process over ni/olivine catalyst using toluene as a model compound. Applied Catalysis B: Environmental 74, 211–222.

Taralas, G. 1991. Thermal and catalytic cracking of n-heptane in presence of CaO, MgO and calcined dolomites. Canadian Journal of Chemical Engineering. 69, 1413-1419.

Torres W., Pansare, J., Goodwin J. 2007. Hot Gas Removal of Tars, Amonia, and Hydrogen Sulfide from Biomass Gasification Gas. Catalysis Reviews 49, 407-439.

Twigg M. 1996. Catalyst Handbook. 2nd edition. Manson Publishing.

Tsujii, T., Okajima, S., Sasaki, A., Madusa, T. 2005. Steam Reforming of Oils Produced from Waste Plastics. Journal of Chemical Engineering of Japan 38, 859 864.

Wang, T.,Chang, J.,Lv, P. 2005. Novel Catalyst for Cracking of Biomass Tar. Energy & Fuels 19, 22-27.

Wen, Y.W., Cain, E. 1984. Catalytic pyrolysis of a coal tar in a fixed-bed reactor. Industrial and Engineering Chemistry Process Design and Development 23, 627-637.

Yung, M., Jablonski, W., Magrini-Bair, K. 2009. Review of Catalytic Conditioning of Biomass-Derived Syngas. Energy & Fuels 23, 1874-1887.

Zanzi, R., K., Sjostrom, K., Bjornbom, E. 1996. Rapid High-Temperature Pyrolysis of Biomass in a Free-Fall Reactor. Fuel 75, 545-550.

Zhang, R., Brown, R.C., Suby, A., Cummer, K. 2004 Catalytic destruction of tar in biomass derived producer gas. Energy Conversion and Management 45, 995–1014.

APPPENDICES

A.1 EXPERIMENTAL PROTOCOL FOR CATALYST TESTING

Table A.1.1 Summary of valves

VALVE NUMBER	DESCRIPTION
1	Located on rotameters, allows hydrogen or nitrogen to pass through the reactor depending on gas needed
2	Located on rotameters, allows the gas mixture to pass through the reactor
3	Located on front panel, port to check temperature of the exiting gases
3 way valve (3WV)	Located on front panel, defines whether reactor mode is down flow or up flow
4	Located on front panel, defines gas flow path, open for down flow, closed for up flow
5	Located on front panel, defines gas flow path, closed for down flow, open for up flow
6	Located on top of GC, sample gas going to the GC
7	Located on top of GC, gas exit for GC (vent)
8	Located on back of GC, regulates gas flow to GC, and helps regulate the system pressure

Table A.2.2 Summary of Gas Cylinders

Cylinder Number	**Description**	**Set point for pressure (psi)**	**Location**	**Purpose**
1	Gas Mixture for experiments		Outside	Experimental gas
2	Argon (Ultra High Purity)	30	Outside	Used by the FID
3	Air		Inside	Used by the FID
4	H_2 (Hydrogen compressed)		Outside	For reducing the catalyst
5	N_2 (Ultra High Purity)		Inside	Carrier gas
6	Argon (Ultra High Purity)	30	Inside	Purging system
7	Helium		Inside	Checking for leaks on GC

Preliminary Activities

Powder the catalysts according to the following guidelines:

1) Select the catalyst (pellets, granular, powdered).
2) Weigh an amount of the catalyst in a weigh boat and place it in the mortar.
3) Using a pestle grind the catalyst to a very small particle size.

For Active catalyst: Using the sieve with mesh size 270 (particle size 53um), sieve the powdered catalyst onto a clean piece of paper. Pour out the right mesh sized catalyst into a clean glass bottle which has the label indicating the name of the catalyst, particle size and date of powdering it along with the weight (if possible).

For Support: Using the sieve with mesh size 70 (particle size 212 um), sieve the powdered catalyst onto a clean piece of paper. Pour out the right mesh sized catalyst into a clean glass bottle which has the label indicating the name of the catalyst, particle size and date of powdering it along with the weight (if possible).

Set mode of operation for reactor as down flow, or up flow based on valve positions as below:

Reactor Mode	**Valve Position**
Down Flow	3 WV: up 3: closed 4: open 5: closed
Up Flow	3WV: down 3: closed 4: closed 5: open

Experimental set up

To set experimental set up follow these steps:

1) Plug the reactor with quartz wool such that there is a tight fit.
2) Sprinkle powdered support and sprinkle on the quartz wool from the top of the reactor using a weigh boat.
3) Sprinkle powdered catalyst and place over the support using a weigh boat.
4) Plug another quartz wool , this one goes over the catalyst (around 1 inch over catalyst bed)
5) Check the fittings for leaks. Place the K-type thermocouple at the bottom of the reactor in such a way that the tip of the thermocouple touches the bed of the catalyst and check for leaks.
6) To place the tube in the tube reactor use one ultratorr + 2 gaskets + 1 ferrul in each end , tighten properly, and check for leaks.
7) Set the syringe pumps following these adjustments:
   Turn the syringe pump on.
   Press the select key for a few seconds in order to go to the main menu
   Select the table option in the syringe pump by using the arrow key.
   The syringe pump has a few set syringe dimensions which we need to select. If the company of the syringe we are using is not in the options of the syringe pump, we then manually enter the diameter of the syringe pump.
   Go to the main menu again by holding the select key for a few seconds.

Select the other parameter you want to choose by using the arrow key.
We next set the volume we are filling into our syringe. This is done so that the syringe stops the flow of the fluid we are injecting automatically once the desired volume is reached.
We next set the rate at which we want our liquid to be injected.
Turn the syringe pump on when the entire setup is ready by pressing the run button.
Fill in the syringe pump with water and set the flow rate
Fill in the syringe pump with toluene and set the flow rate Repeat previous step for the syringe containing toluene as well.

8) Be sure the T is covered with a heat tape and heat the T to 250 degrees Celsius.
9) Insert the two needles into the proper T and when the entire set up is ready press start.

Preparing the GC

Follow these steps to prepare the gas analysis system:

1) Open bottles 6, 3 and 2
2) Set the flow rate of the carrier gas to be 5 mL/min.
3) Set the flow through the split vent to be 50 mL/min. (in order to get a 10:1 split.
4) Set the flow of the reference gas to the TCD at 20 mL/min.
5) Set the flow of the gases to the FID -Air and hydrogen to be 300 and 50 mL/min respectively.
6) Check the flow of the gas through column one only and set it at 5 mL/min using the restriction Valve.
7) Load the right method.
8) Check the method once to check if the valve 2 is opening and closing at the right time and if the pressure to the EPC is right. Also check the temperature profile.
9) Check if the positions of the valves leading the sample in and out of the loop are completely open and the valve in between is open enough to give pressure for the flow to be possible.
10) Turn on the detectors.
11) Light the FID by pressing the ignite button and check if signal 2 value stabilizes at a particular value. Also check if there is condensation on any smooth shiny surface to double check that the flame is burning
12) Open valves 6 and 7

Catalyst Deactivation Testing

Follow these steps to perform catalyst deactivation experiments:

1) Open Valve 2
2) Open Bottle 1 and set the flow rate
3) Check if the T at the top of the reactor has reached 250 degrees Celsius.
4) Turn the syringe pumps on.
5) Every 30minutes check on the following values: temperature, pressure indicator, and values reported on the GC : H_2,N_2,CH_4,CO,CO_2,C_7H_8 and record values.

A.2 EXAMPLE OF MASS BALANCE

The following is an example of a mass balance for Hifuel R-110 at 800^{o}C.

Table A.2.1 Composition of experimental gas

Compound	Molecula weight	molar concentration	molar comp.
H2	2.016	5.108	0.05108
N2	28.02	51.274	0.51274
CO	28.01	19.3	0.193
CH4	16.04	7.518	0.07518
CO2	44.01	16.8	0.168

P (Pa)	101325
T (K)	296.15
R (J/molK)	8.3144
V (m3/h)	0.0283168
n (mol/h)	**1.1652493**

Mol/h of each compound entering the reactor (dry basis) applying equation 3.2:

Moles per compound entering the system per hour	**H2**	**0.059520934**
	N2	0.597469924
	CO	**0.224893114**
	CH4	**0.087603442**
	CO2	**0.195761882**
	total mol	**1.165249296**

grams per compound entering the system	**H2**	**0.119994203**
	N2	**16.74110727**
	CO	**6.299256126**
	CH4	**1.405159211**
	CO2	**8.615480414**
total g/h		**33.18099722**

Table A.2.2 GC results per compound per run in g/L.

			g/L				
Run	time (min)	CH4	C7H8	CO2	H2	N2	CO
101	21	0.00302	0.000188347	0.181822	0.0133696	0.188974	0.0672
102	42	0.002753	0.0002722	0.171977	0.0135347	0.198505	0.0907
103	63	0.003018	0.000198814	0.176492	0.0132126	0.200237	0.0825
104	84	0.003223	0.000328162	0.178626	0.0134872	0.195586	0.0834
105	105	0.003351	0.000265265	0.168528	0.013038	0.184782	0.0835
106	126	0.003736	0.000237549	0.181691	0.013913	0.213933	0.0969
107	147	0.003665	0.000287454	0.206543	0.0138389	0.200579	0.0883
108	168	0.003956	0.000301476	0.205512	0.0134301	0.214391	0.0981
109	189	0.004552	0.000300351	0.186287	0.0131787	0.205326	0.0942
110	210	0.004542	0.000510346	0.202343	0.0133311	0.207252	0.0909
111	231	0.007026	0.000970279	0.186979	0.0132425	0.205777	0.0957
112	252	0.006799	0.0008404	0.201134	0.0110564	0.191184	0.0647

Table A.2.3 Mol% per compound per run.

			mol%				
Run	time (h)	CH4	C7H8	CO2	H2	N2	CO
101	21	0.936851	0.010171839	20.5559191	32.99664042	33.55643092	11.944
102	42	0.812734	0.013990052	18.5033891	31.78998965	33.54560275	15.334
103	63	0.902749	0.010352459	19.2385028	31.44092934	34.28260494	14.125
104	84	0.960974	0.017033332	19.409113	31.9921666	33.37966831	14.241
105	105	1.040198	0.01433556	19.0658637	32.20002687	32.83426641	14.845
106	126	1.041757	0.011531959	18.464307	30.86606197	34.14763392	15.469
107	147	1.033884	0.014116915	21.2339907	31.05872003	32.38842589	14.271
108	168	1.084748	0.014392471	20.5385368	29.30032257	33.65286954	15.409
109	189	1.304719	0.014989567	19.4622144	30.056826	33.69278331	15.468
110	210	1.278881	0.025019338	20.7658151	29.86672654	33.40740687	14.656
111	231	1.988646	0.047812945	19.2881866	29.82149349	33.34100113	15.513
112	252	2.160269	0.046488592	23.2913972	27.95018157	34.77321388	11.778

Initial moles/h of N2	0.59746992

Considering that nitrogen is an inert we can determine total number of moles exiting the system for each run		
total number of moles moles/h exiting (run 1)	1.78049306	
Total experiment length (h)		4.2

Table A.2.4 Mol/h/compound exiting the system at each run.

								Total
			moles/h/compound exiting					mol/h
Run	time (h)	CH4	C7H8	CO2	H2	N2	CO	exiting
101	21	0.016681	0.000181109	0.36599671	0.587502893	0.597469924	0.2127	1.78
102	42	0.014475	0.000249172	0.3295579	0.566201265	0.597469924	0.2731	1.781
103	63	0.015733	0.00018042	0.33528452	0.547945808	0.597469924	0.2462	1.743
104	84	0.017201	0.000304883	0.34740792	0.57263473	0.597469924	0.2549	1.79
105	105	0.018928	0.000260858	0.34693268	0.585928961	0.597469924	0.2701	1.82
106	126	0.018227	0.000201771	0.32306391	0.540053339	0.597469924	0.2707	1.75
107	147	0.019072	0.000260415	0.39170384	0.572940814	0.597469924	0.2633	1.845
108	168	0.019259	0.000255523	0.36463928	0.520195209	0.597469924	0.2736	1.775
109	189	0.023136	0.000265808	0.34512102	0.532993947	0.597469924	0.2743	1.773
110	210	0.022872	0.000447455	0.37138321	0.53414714	0.597469924	0.2621	1.788
111	231	0.035636	0.000856807	0.34564383	0.534400433	0.597469924	0.278	1.792
112	252	0.037118	0.000798762	0.40019048	0.480237257	0.597469924	0.2024	1.718

		Adding water and carbon to mass balance							
	Water								
	a) Water in gas phase at 23 C								
		$w = \frac{\text{Pv(Mpa)}}{\text{Pdg(Mpa)}} \cdot \text{mgas (g/h)} = \frac{\text{mvapor (g/h}}{\text{MWdg}}$							
	Pv(Mpa)	0.00231		w	0.030850827				
	Pdg(Mpa)	0.09869		mgas (g/h)	24.32408512				
	Mwwater	18.015		mvapor (g/h	0.750418152				
	MWdg	13.668							
	b) water in liquid phase collected at the end of experiment								
		we assume that the mol/hr of water and C are the same in each run.							
				mL/h					
	Water collected		80	19.047619		Carbon (g)	0.048		
	per exp. (ml)					C (g/h)	0.0114		
		Water pe	19.75994196	Water per	1.096860503				
		run (g/h)		run (mol/h)					
						C (mol/h)	0.001		
						per run			

Table A.2.5 Mol/h/compound exiting the system at each run including water and carbon.

				Mol/h					
Run	t (min)	CH4	C7H8	CO2	H2	N2	CO	H2O	C
101	21	0.016681	0.000181109	0.36599671	0.587502893	0.597469924	0.2127	1.097	0.000952381
102	42	0.014475	0.000249172	0.3295579	0.566201265	0.597469924	0.2731	1.097	0.000952381
103	63	0.015733	0.00018042	0.33528452	0.547945808	0.597469924	0.2462	1.097	0.000952381
104	84	0.017201	0.000304883	0.34740792	0.57263473	0.597469924	0.2549	1.097	0.000952381
105	105	0.018928	0.000260858	0.34693268	0.585928961	0.597469924	0.2701	1.097	0.000952381
106	126	0.018227	0.000201771	0.32306391	0.540053339	0.597469924	0.2707	1.097	0.000952381
107	147	0.019072	0.000260415	0.39170384	0.572940814	0.597469924	0.2633	1.097	0.000952381
108	168	0.019259	0.000255523	0.36463928	0.520195209	0.597469924	0.2736	1.097	0.000952381
109	189	0.023136	0.000265808	0.34512102	0.532993947	0.597469924	0.2743	1.097	0.000952381
110	210	0.022872	0.000447455	0.37138321	0.53414714	0.597469924	0.2621	1.097	0.000952381
111	231	0.035636	0.000856807	0.34564383	0.534400433	0.597469924	0.278	1.097	0.000952381
112	252	0.037118	0.000798762	0.40019048	0.480237257	0.597469924	0.2024	1.097	0.000952381
		CH4	C7H8	CO2	H2	N2	CO	H2O	
gr exiting		1.450308	0.137462019	65.7255841	4.639448274	70.31265053	30.207	82.99	
gr entering		5.901669	7.2408	36.1850177	0.503975653	70.31265053	26.457	100.6	

Table A.2.6 Carbon balance results.

	CARBON BALANCE							
				entrance			exit	
	Moles per	Compounds	Moles per/h/	number of	g/hC	g total	moles	grs
	compound	containing C	compound	atoms of C		entrance	totales	total
	of C entering	CO	0.224893114	1	2.698717369	11.33461295	1.0784	12.94
	the system	CH4	0.087603442	1	1.051241305	4.41521348	0.0904	1.085
	per hour	CO2	0.195761882	1	2.34914258	9.866398838	1.4934	17.92
		toluene	0.018712689	7	1.571865842	6.601836535	0.0015	0.125
					7.670967096	32.2180618		32.07
						C diff theo	0.1454	

Table A.2.7 Data for the method of extent of reaction using Hifuel R110 at 800°C.

		run 4		run8		run 12	
Compoun	**Nao (mol/h)**	Na (mol/h)	Na-Nao	Na	Na-Nao	Na	Na-Nao
CO2	0.195761882	0.34740792	0.151646041	0.364639277	0.1689	0.4	0.204428602
CO	0.224893114	0.25490356	0.030010444	0.273572269	0.0487	0.202	-0.02251695
C7H8	0.018712689	0.00030488	-0.018407805	0.000255523	-0.018	8E-04	-0.01791393
H2	0.059520934	0.57263473	0.513113796	0.520195209	0.4607	0.48	0.420716323
CH4	0.087603442	0.01720067	-0.070402768	0.019258522	-0.068	0.037	-0.05048591
H20	1.329558701	1.0968605	-0.232698198	1.096860503	-0.233	1.097	-0.2326982
C	0	0.00095238	0.000952381	0.000952381	0.001	1E-03	0.000952381

A.3 RESIDENCE TIME CALCULATIONS AND ACTIVATION ENERGY PLOTS FOR TESTED CATALYSTS

Residence Time Calculations

RESIDENCE TIME CALCULATIONS		
Gas flow rate at inlet (m3/h)		0.028317
Gas	Moles of gas at inlet (23 C)	
	(1 atm) without water	
	and toluene (mol/h)	1.165249
	Flow rate of water (ml/h)	24
	Density of water (g/cm3)	0.997
Water	Mass of water (g/h)	23.928
	Molecular weight of water (g/mol)	18.015
	moles of water (mol/h)	1.328226
	Flow rate of toluene (ml/h)	2
	Density of toluene (g/cm3)	0.862
Toluene	Mass of water (g/h)	1.724
	Molecular weight of toluene (g/mol)	92.13
	moles of toluene (mol/h)	0.018713
Mix	Total number of moles entering	
	the system (mol/h)	2.512188

	T .(C)	vo (m3/h)
Gas flow rate	600	0.17996198
(m3/h)	700	0.200576181
	800	0.221190383

		HIFUEL R-110	REFORMAX 250	2% PT CATALYST	CHAR
	mass of cat (g)	0.15	0.15	0.15	0.3
	mass of cat (Kg)	0.00015	0.00015	0.00015	0.0003
	catalyst density (g/cm3)	0.951	0.95	6.6	0.194
	Vr (cm3)	0.157728707	0.157894737	0.022727	1.546392
	Vr (m3)	1.57729E-07	1.57895E-07	2.27E-08	1.55E-06
residence	600 C	0.000833509	0.000833509	0.000834	0.001667
time	700 C	0.000747846	0.000747846	0.000748	0.001496
kg/(m3/h)	800 C	0.000678149	0.000678149	0.000678	0.001356

Activation Energy Plots

Reformax 250

T (K)	1/T	lnkaap
873.15	0.001145	6.163576
973.15	0.001028	6.95912
1073.15	0.000932	7.447933

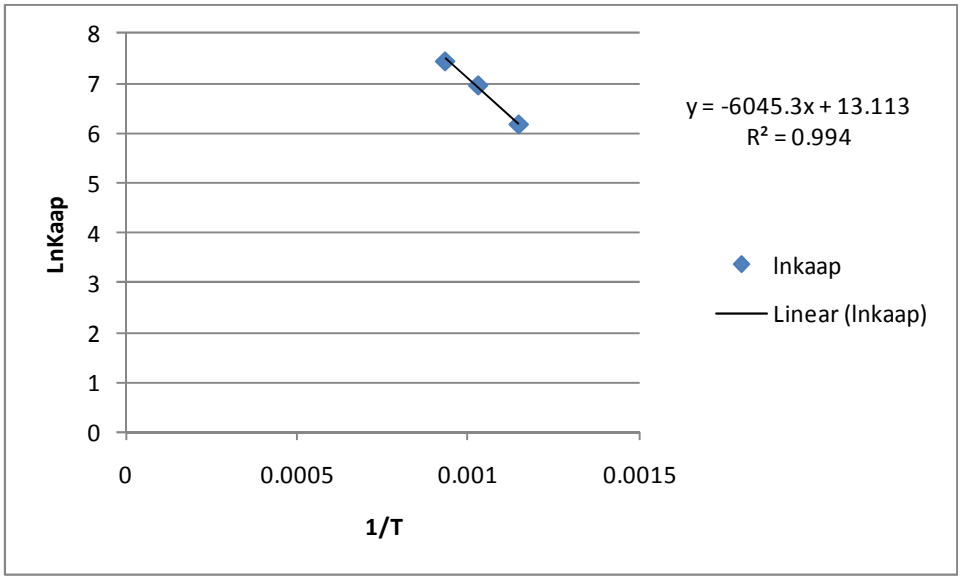

Hifuel R-110

T (K)	1/T	lnkaap
873.15	0.001145	7.458496
973.15	0.001028	7.891726
1073.15	0.000932	8.793088

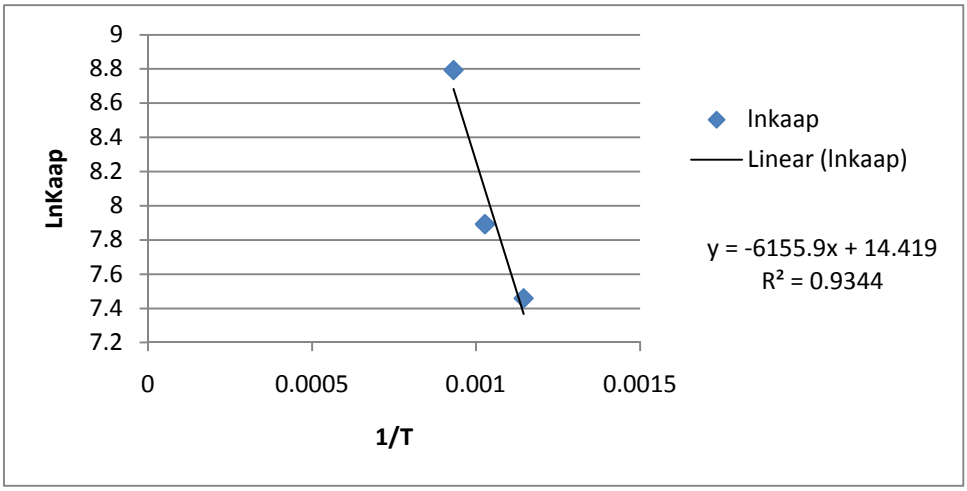

NextechA

T (K)	1/T	lnkaap
873.15	0.001145	6.25689
973.15	0.001028	6.95912
1073.15	0.000932	7.792619

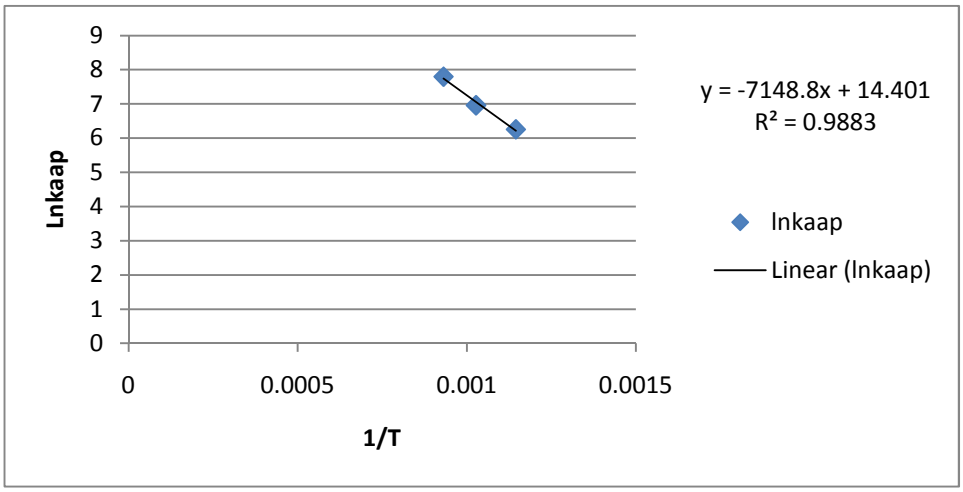

BioChar

T (K)	1/T	ln (kaap)
873.15	0.001145	5.5137637
973.15	0.001028	6.1228693
1073.15	0.000932	7.1136271

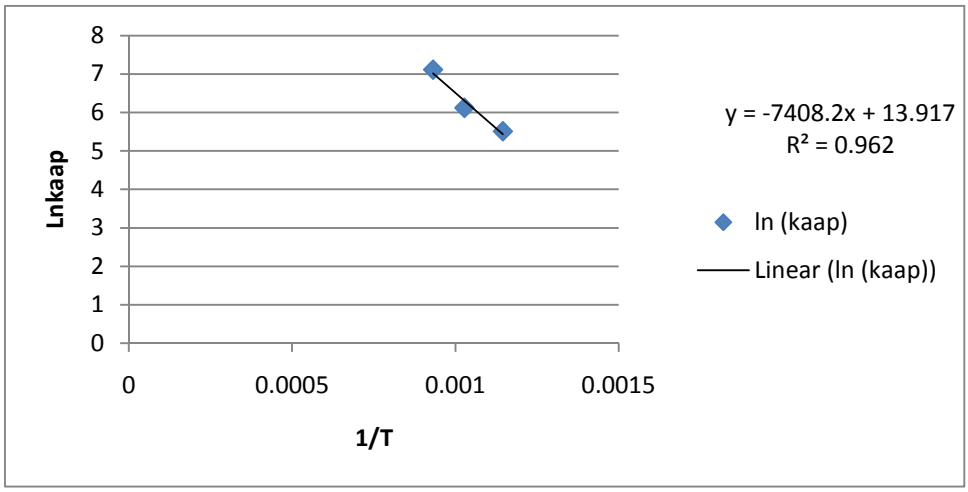

A.4 INTERFEROGRAM FOR COMMERCIAL CATALYSTS

Hifuel R-110

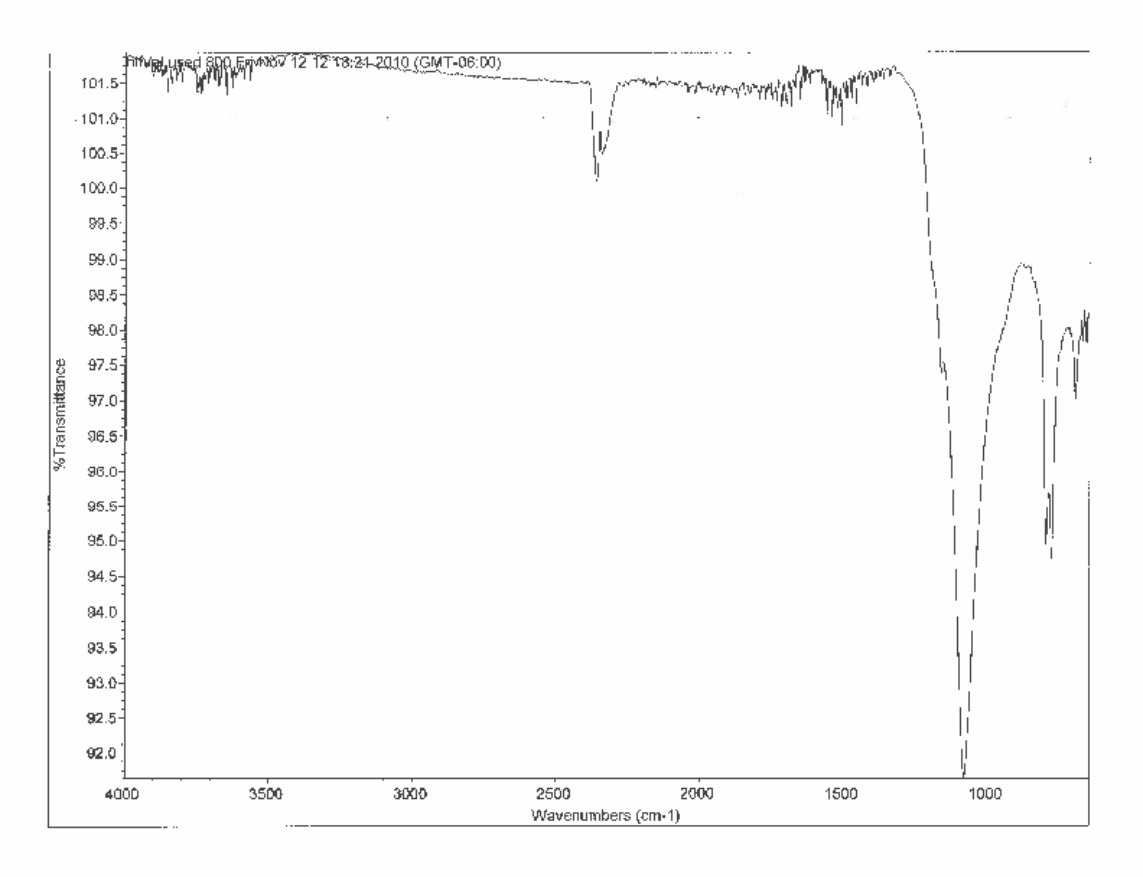

Figure A.4.1 Interferogram for Hifuel R 110

NextechA

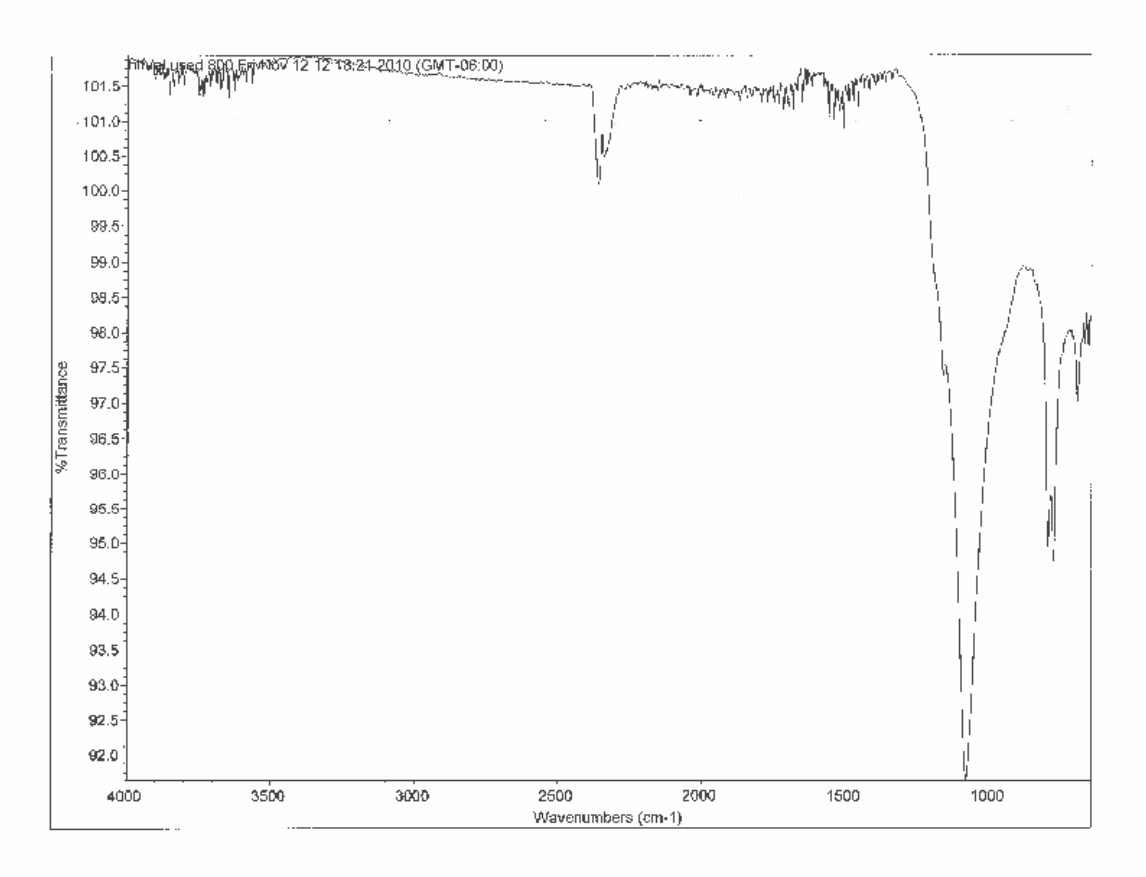

Figure A.4.2 Interferogram for NextechA

Reformax 250

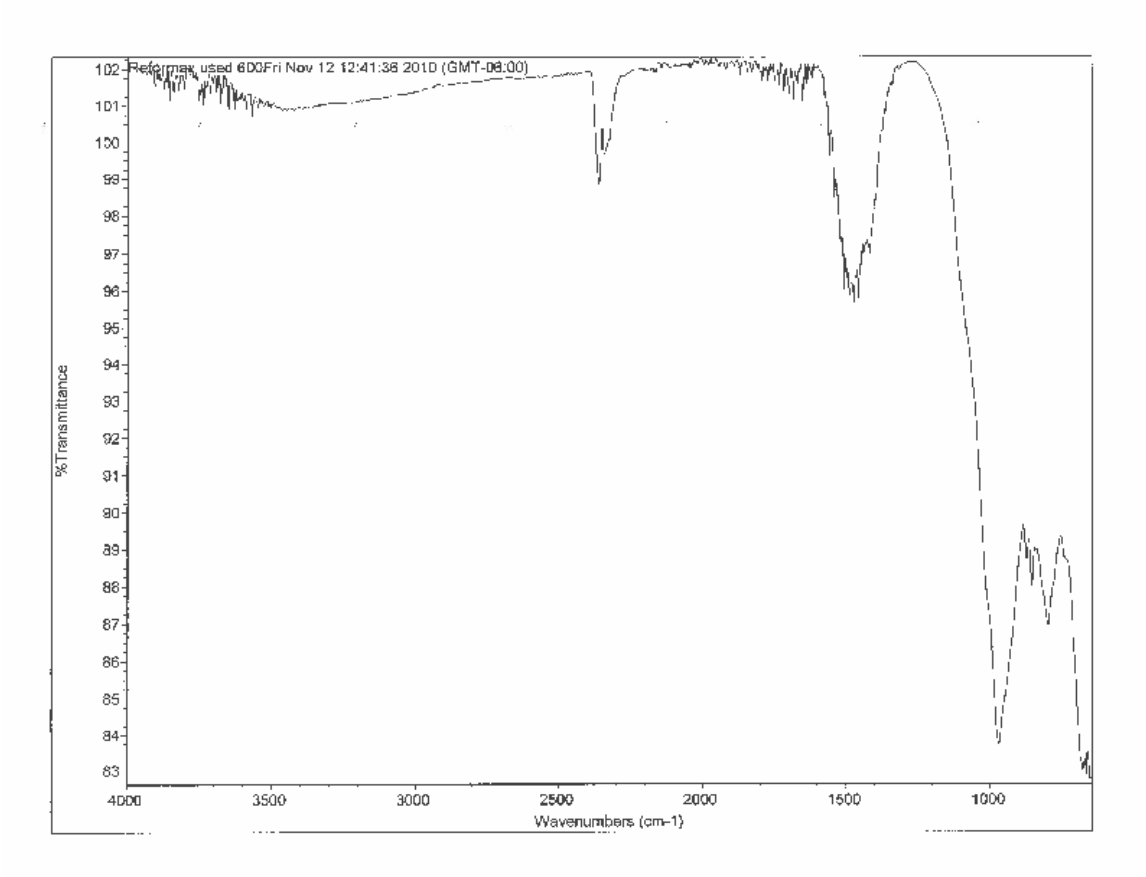

Figure A.4.3 Interferogram for Reformax 250

A.5 MASS BALANCE VERIFICATION RESULTS

Table A.5.1 Mass balance verification showing model calculated results (Cal), experimental results (Exp) and the percent difference (% Diff) for reaction set two for tested catalysts at three different temperatures.

		600 °C			700 °C			800 °C		
Catalyst	**Compound**	**Cal**	**Exp**	**% Diff**	**Cal**	**Exp**	**% Diff**	**Cal**	**Exp**	**% Diff**
Reformax 250	**H_2O**	-0.14	-0.24	43.68	-0.18	-0.28	36.43	-0.16	-0.21	24.68
	CO_2	0.07	0.10	29.38	0.06	0.12	48.36	0.04	0.20	78.55
	H_2	0.15	0.17	12.51	0.26	0.17	51.62	0.22	0.30	27.65
Hifuel R110	**H_2O**	-0.20	-0.24	16.42	-0.22	-0.30	27.70	-0.24	-0.23	0.86
	CO_2	0.12	0.22	45.88	0.07	0.18	59.31	0.05	0.06	10.30
	H_2	0.25	0.38	33.21	0.37	0.39	5.81	0.43	0.16	165.39
NextechA	**H_2O**	-0.20	-0.19	8.75	-0.21	-0.23	8.39	-0.18	-0.21	14.18
	CO_2	0.16	0.22	28.33	0.12	0.20	38.52	0.09	0.19	53.46
	H_2	0.22	0.22	2.38	0.27	0.26	2.80	0.26	0.30	12.85
Biochar	**H_2O**	-0.15	-0.26	41.88	-0.18	-0.30	41.23	-0.07	-0.30	77.20
	CO_2	0.04	0.01	347.00	0.06	0.17	65.61	0.01	0.15	93.28
	H_2	0.29	-0.01	5918.40	0.31	0.37	16.39	0.18	0.49	63.22

Table A.5.2 Mass balance verification showing model calculated results (Cal), experimental results (Exp) and the percent difference (% Diff) for reaction set three for tested catalysts at three different temperatures.

		600 °C			700 °C			800 °C		
Catalyst	**Compound**	**Cal**	**Exp**	**% Diff**	**Cal**	**Exp**	**% Diff**	**Cal**	**Exp**	**% Diff**
Reformax 250	**H_2O**	-0.21	-0.24	10.81	-0.28	-0.28	0.72	-0.28	-0.21	32.90
	CO_2	0.15	0.10	47.65	0.17	0.12	39.48	0.16	0.20	16.58
	H_2	0.23	0.17	33.96	0.37	0.17	111.5	0.34	0.30	12.39
Hifuel R110	**H_2O**	-0.27	-0.24	15.16	-0.31	-0.30	4.28	-0.36	-0.23	52.30
	CO_2	0.19	0.22	11.37	0.17	0.18	6.69	0.17	0.06	190.4
	H_2	0.33	0.38	13.45	0.46	0.39	18.89	0.55	0.16	239.8
NextechA	**H_2O**	-0.25	-0.19	34.55	-0.28	-0.23	25.89	-0.25	-0.21	19.03
	CO_2	0.21	0.22	6.59	0.20	0.20	0.48	0.16	0.19	17.00
	H_2	0.27	0.22	24.49	0.34	0.26	32.66	0.33	0.30	10.20
Biochar	**H_2O**	-0.20	-0.26	21.91	-0.25	-0.30	16.61	-0.07	-0.30	75.82
	CO_2	0.10	0.01	866.2	0.13	0.17	22.57	0.01	0.15	90.52
	H_2	0.34	-0.01	6956	0.38	0.37	3.75	0.18	0.49	62.37

Table A.5.3 Mass balance verification showing model calculated results (Cal), experimental results (Exp) and the percent difference (% Diff) for reaction set four for tested catalysts at three different temperatures.

		600 °C			700 °C			800 °C		
Catalyst	**Compound**	**Cal**	**Exp**	**% Diff**	**Cal**	**Exp**	**% Diff**	**Cal**	**Exp**	**% Diff**
Reformax 250	**H_2O**	-0.21	-0.24	10.81	-0.28	-0.28	0.72	-0.28	-0.21	32.90
	CO_2	0.15	0.10	47.05	0.16	0.12	38.86	0.16	0.20	16.97
	H_2	0.23	0.17	33.96	0.37	0.17	111.51	0.34	0.30	12.39
Hifuel R110	**H_2O**	-0.27	-0.24	15.16	-0.31	-0.30	4.28	-0.36	-0.23	52.30
	CO_2	0.19	0.22	11.83	0.17	0.18	7.21	0.17	0.06	188.80
	H_2	0.33	0.38	13.45	0.46	0.39	18.89	0.55	0.16	239.84
NextechA	**H_2O**	-0.25	-0.19	34.55	-0.28	-0.23	25.89	-0.25	-0.21	19.03
	CO_2	0.21	0.22	6.85	0.20	0.20	0.00	0.16	0.19	17.51
	H_2	0.27	0.22	24.49	0.34	0.26	32.66	0.33	0.30	10.20
Biochar	**H_2O**	-0.20	-0.26	21.91	-0.25	-0.30	16.61	-0.07	-0.30	75.82
	CO_2	0.09	0.01	846.40	0.13	0.17	23.72	0.01	0.15	91.98
	H_2	0.34	-0.01	6956.80	0.13	0.37	64.29	0.18	0.49	62.37

Table A.5.4 Mass balance verification showing model calculated results (Cal), experimental results (Exp) and the percent difference (% Diff) for reaction set five for tested catalysts at three different temperatures.

		600 °C			700 °C			800 °C		
Catalyst	**Compound**	**Cal**	**Exp**	**% Diff**	**Cal**	**Exp**	**% Diff**	**Cal**	**Exp**	**% Diff**
Reformax 250	**H_2O**	-0.21	-0.24	10.81	-0.28	-0.28	0.72	-0.28	-0.21	32.90
	CO_2	0.15	0.10	47.65	0.17	0.12	39.48	0.16	0.20	16.58
	H_2	0.23	0.17	33.96	0.37	0.17	111.5	0.34	0.30	12.39
Hifuel R110	**H_2O**	-0.27	-0.24	15.16	-0.31	-0.30	4.28	-0.36	-0.23	52.30
	CO_2	0.19	0.22	11.37	0.17	0.18	6.69	0.17	0.06	190.4
	H_2	0.33	0.38	13.45	0.46	0.39	18.89	0.55	0.16	239.8
NextechA	**H_2O**	-0.25	-0.19	34.55	-0.28	-0.23	25.89	-0.25	-0.21	19.03
	CO_2	0.21	0.22	6.59	0.20	0.20	0.48	0.16	0.19	17.00
	H_2	0.27	0.22	24.49	0.34	0.26	32.66	0.33	0.30	10.20
Biochar	**H_2O**	-0.20	-0.26	21.91	-0.25	-0.30	16.61	-0.07	-0.30	75.82
	CO_2	0.10	0.01	866.2	0.13	0.17	22.57	0.01	0.15	90.52
	H_2	0.34	-0.01	6956	0.38	0.37	3.75	0.18	0.49	62.37

A.6 GIBBS FREE ENERGY CALCULATIONS

Table A.6.1 Gibbs Free Energy calculations for integral 1.

Gibbs Free Energy							
Integral 1							
	Delta A	Delta B	Delta C	Delta D	T(K)	Integral 1	
Steam Reforming (1)	34.791	-0.04866	0.000015716	-15100	873	6935.97	
	34.791	-0.04866	0.000015716	-15100	973	7262.083	
	34.791	-0.04866	0.000015716	-15100	1073	7407.751	
Steam Reforming (2)	47.811	-0.05244	0.000015716	-829900	873	11348.99	
	47.811	-0.05244	0.000015716	-829900	973	12532.29	
	47.811	-0.05244	0.000015716	-829900	1073	13515.22	
Dry Reforming	21.771	-0.04488	0.000015716	799700	873	2522.949	
	21.771	-0.04488	0.000015716	799700	973	1991.88	
	21.771	-0.04488	0.000015716	799700	1073	1300.285	
Carbon Formation	11.624	0.016515	0.000000568	0	873	12364.74	
	11.624	0.016515	0.000000568	0	973	15099.91	
	11.624	0.016515	0.000000568	0	1073	18011.29	
Bourdan	-1.295	-6.9E-05	0	-109500	873	-1009.87	
	1.295	6.9E-05	0	109500	973	1158.635	
	1.295	6.9E-05	0	109500	1073	1305.681	
WGS	1.86	-0.00054	0	-116400	873	630.4316	
	1.86	-0.00054	0	-116400	973	752.8862	
	1.86	-0.00054	0	-116400	1073	872.4951	
	1.86	-0.00054	0	-116400	1101	905.3809	
	1.86	-0.00054	0	-116400	1173	988.605	
Methanation	-7.951	0.008708	-0.000002164	-9700	873	-2122.45	
	-7.951	0.008708	-0.000002164	-9700	973	-2299.48	
	-7.951	0.008708	-0.000002164	-9700	1073	-2431.33	
	-7.951	0.008708	-0.000002164	-9700	923	-2216.89	
	-7.951	0.008708	-0.000002164	-9700	1023	-2370.78	
	-7.951	0.008708	-0.000002164	-9700	883	-2142.31	
	-7.951	0.008708	-0.000002164	-9700	893	-2161.68	
	-7.951	0.008708	-0.000002164	-9700	892.1	-2159.96	

Table A.6.2 Gibbs Free Energy calculations for integral 2.

Integral 2							
	Delta A	Delta B	Delta C	Delta D	T(K)	Integral 2	
Steam	34.791	-0.04866	0.000015716	-15100	873	14.63063	
Reforming (1)	34.791	-0.04866	0.000015716	-15100	973	14.98622	
	34.791	-0.04866	0.000015716	-15100	1073	15.13004	
Steam Reforming(2)	47.811	-0.05244	0.000015716	-829900	873	22.3985	
	47.811	-0.05244	0.000015716	-829900	973	23.68386	
	47.811	-0.05244	0.000015716	-829900	1073	24.64695	
Dry Reforming	21.771	-0.04488	0.000015716	799700	873	6.862763	
	21.771	-0.04488	0.000015716	799700	973	6.288583	
	21.771	-0.04488	0.000015716	799700	1073	5.613134	
Carbon Formation	11.624	0.016515	0.000000568	0	873	22.18131	
	11.624	0.016515	0.000000568	0	973	25.14585	
	11.624	0.016515	0.000000568	0	1073	27.99262	
Bourdan	-1.295	-6.9E-05	0	-109500	873	-1.97628	
	1.295	6.9E-05	0	109500	973	2.137632	
	1.295	6.9E-05	0	109500	1073	2.281498	
WGS	1.86	-0.00054	0	-116400	873	1.109695	
	1.86	-0.00054	0	-116400	973	1.242519	
	1.86	-0.00054	0	-116400	1073	1.359558	
	1.86	-0.00054	0	-116400	1101	1.389814	
	1.86	-0.00054	0	-116400	1173	1.463044	
Methanation	-7.951	0.008708	-0.000002164	-9700	873	-4.31576	
	-7.951	0.008708	-0.000002164	-9700	973	-4.50821	
	-7.951	0.008708	-0.000002164	-9700	1073	-4.63754	
	-7.951	0.008708	-0.000002164	-9700	923	-4.42101	
	-7.951	0.008708	-0.000002164	-9700	1023	-4.57971	
	-7.951	0.008708	-0.000002164	-9700	883	-4.33838	
	-7.951	0.008708	-0.000002164	-9700	893	-4.36019	
	-7.951	0.008708	-0.000002164	-9700	892.1	-4.35826	

Free Energy of Gibbs									
	G00	H00	R	1/T*Integral1	Integral2	T	Ln(K)	G Formation	K
Steam Reforming(1)	517771	868881	8.314	7.94498273	14.63063	873	28.69	-208231.6	2.88E+12
	517771	868881	8.314	7.46360045	14.98622	973	41.83	-338382.9	1.47E+18
	517771	868881	8.314	6.90377564	15.13004	1073	52.54	-468736.5	6.60E+22
Steam Reforming(2)	317445	580719	8.314	12.9999895	22.3985	873	35.65	-258765.7	3.04E+15
	317445	580719	8.314	12.8800482	23.68386	973	45.28	-366294.7	4.62E+19
	317445	580719	8.314	12.5957289	24.64695	1073	53.22	-474752.1	1.29E+23
Dry Reforming	718097	1157043	8.314	2.88997598	6.862763	873	21.73	-157697.5	2.73E+09
	718097	1157043	8.314	2.04715273	6.288583	973	38.38	-310471.0	4.66E+16
	718097	1157043	8.314	1.2118224	5.613134	1073	51.87	-462720.9	3.36E+22
Carbon Formation	-475270	-571810	8.314	14.1635069	22.18131	873	47.83	-347187.4	5.95E+20
	-475270	-571810	8.314	15.5189239	25.14585	973	41.35	-334474.4	9.05E+17
	-475270	-571810	8.314	16.7859158	27.99262	1073	36.34	-324175.4	6.05E+15
Bourdan	-120021	-172459	8.314	-1.15678674	-1.97628	873	1.78	-12892.3	5.91E+00
	-120021	-172459	8.314	1.19078575	2.137632	973	1.10	-8903.2	3.01E+00
	-120021	-172459	8.314	1.21685131	2.281498	1073	-0.77	6855.4	4.64E-01
WGS	-28618	-41166	8.314	0.72214382	1.109695	873	0.99	-7219.2	2.70E+00
	-28618	-41166	8.314	0.77377825	1.242519	973	0.49	-3987.4	1.64E+00
	-28618	-41166	8.314	0.81313618	1.359558	1073	0.10	-859.4	1.10E+00
	-28618	-41166	8.314	0.82232593	1.389814	1101	0.00	-0.4	1.00E+00
	-28618	-41166	8.314	0.84280048	1.463044	1173	-0.22	2177.1	8.00E-01
Methanation	-141863	-205813	8.314	-2.43121309	-4.31576	873	0.66	-4791.3	1.94E+00
	-141863	-205813	8.314	-2.36328915	-4.50821	973	-2.51	20341.6	8.09E-02
	-141863	-205813	8.314	-2.26591821	-4.63754	1073	-5.11	45607.0	6.02E-03
	-141863	-205813	8.314	-2.40182793	-4.42101	923	-1.01	7755.2	3.64E-01
	-141863	-205813	8.314	-2.3174766	-4.57971	1023	-3.88	32960.9	2.07E-02
	-141863	-205813	8.314	-2.42617297	-4.33838	883	0.31	-2285.6	1.37E+00
	-141863	-205813	8.314	-2.42069538	-4.36019	893	-0.03	222.0	9.71E-01
	-141863	-205813	8.314	-2.42120577	-4.35826	892.1	0.00	-3.7	1.00E+00

VITA

Luz Stella Marin

Candidate for the Degree of

Doctor of Philosophy

Thesis: TREATMENT OF BIOMASS-DERIVED SYNTHESIS GAS USING COMMERCIAL STEAM REFORMING CATALYSTS AND BIOCHAR

Major Field: Biosystems Agricultural Engineering

Biographical:

Personal Data: Born in Merida, Venezuela on April 4, 1969

Education:

Completed the requirements for the Doctor of Philosophy Biosystems Agricultural Engineering at Oklahoma State University, Stillwater, Oklahoma in July, 2011.

Completed the requirements for the Master of Science in Chemical Engineering. Universidad Simón Bolívar. Caracas Venezuela, 1992

Completed the requirements for the Bachelor of Science in Chemical Engineering. Universidad Simón Bolívar. Caracas Venezuela, 1991

Experience:

Graduate Research Associate, Oklahoma State University August 2005- May 2011
Stillwater, Oklahoma
Student Intern assigned in NREL's National Bioenergy Center., June-August))/2006
Golden CO
Technological Institute Jose Antonio Anzoategui, Venezuela October 1995-August 2003
Project Leader, Asfapetrol Caracas, Venezuela February 1991-July 1995
Instructor, Universidad Simon Bolivar January/1991 – July1992

Professional Memberships:

- American Institute of Chemical Engineers (AICHE) 2004-Present
- American Chemical Society (ACS) 2006-Present

American Society of Agricultural and Biological Engineers (ASABE) 2005-Present

Name: Luz Stella Marin Date of Degree: December, 2011

Institution: Oklahoma State University Location: Stillwater, Oklahoma

Title of Study: TREATMENT OF BIOMASS-DERIVED SYNTHESIS GAS USING COMMERCIAL STEAM REFORMING CATALYSTS AND BIOCHAR

Pages in Study: 155 Candidate for the Degree of Doctor of Philosophy

Major Field: Biosystems and Agricultural Engineering

Scope and Method of Study: The destruction of tars is a crucial technological barrier for the development and further commercialization of biomass gasification. The decomposition of tar compounds using catalysts is a suitable solution to this problem. Biochar, which is generated during gasification, is also a potential catalyst for tar destruction. Biochar along with three commercial steam reforming catalysts were evaluated for tar removal using toluene as a model tar compound. Two of the commercial catalysts were nickel based (Reformax 250 and Hifuel R-110) and one was platinum based (Nextech-A). The biochar was generated during switchgrass gasification in a down draft gasifier at the OSU thermochemical conversion facility. Tar destruction experiments were performed in a bench scale fixed bed reactor between 600 and 800^{o}C under atmospheric pressure using a synthetic gas mixture with similar composition to the syngas generated from switchgrass gasification. The reaction coordinate or molar extent of reaction method was used in order to determine the importance of different reactions in the reaction network involved in the steam reforming of toluene.

Findings and Conclusions: Toluene conversion results showed that the biochar performance was comparable to the commercial catalysts and Reformax was the most active of the tested catalysts. The activation energy of toluene steam reforming over these catalytic materials was found to be 50.26 KJ/mol for Reformax 250; 51.18 for Hifuel R-110 KJ/mol; 59.44 KJ/mol for Nextech-A and 61.59 KJ/mol for biochar. Catalyst characterization by SEM, XPS, TGA, and FTIR was also conducted on the used catalysts and according to the XPS spectra graphitic carbon was found on all catalysts. Reformax and NextechA have a medium tendency to coke formation while Hifuel has the highest tendency toward coke formation. The extent of reaction for steam reforming increased with temperature. The catalysts that showed the larger extent of reaction during steam reforming were Reformax 250 and Hifuel R-110.

ADVISER'S APPROVAL: Dr. Danielle Bellmer